W-Pos246

PHYSICOCHEMICAL CHARACTERIZATION BY ^2H AND ^1H NMR OF AQUEOUS LIPID DISPERSIONS RESEMBLING BILE. ((P. W. Westerman*†, R. Jacquet*, B. Quinn*, P. Rinaldi§ and Y. Sun§)) *Northeastern Ohio Universities College of Medicine, Rootstown, Ohio 44272; †Kent State University, Kent, Ohio 44242 and §University of Akron, Akron, Ohio 44325.

The phase properties of aqueous dispersions of model bile mixtures containing cholesterol, lecithin and bile salts have been characterized by ^2H NMR. We have chemically incorporated a deuteriomethyl (CD_3) group into one lipid component, and utilized the differences in magnitude of the motionally-averaged quadrupole splitting ($\delta\nu$) to determine by spectral integration, the distribution of that lipid between solid, multilamellar and micellar phases. By ^2H-labelling both cholesterol and lecithin in a system of a given overall composition we have used the different CD_3 chemical shifts and $\delta\nu$ values, to determine directly the chemical composition of the micellar and multilamellar phases. ^2H relaxation times of C^2H_2 sites in the lecithin component have been measured for the micellar phases in these same mixtures. Differences between T_1 and T_2 values were employed to estimate particle size, assuming either a spherical or ellipsoidal shape. The structure of the micellar particles in model bile systems were investigated by ^1H NMR. 600 MHz 1D and 2D ^1H NMR spectra of cholesterol/lecithin/taurocholate (NaTC) dispersions in D_2O were recorded at 37°C. On the basis of cross-peaks in 2D homonuclear NOESY experiments a "golf-ball" like spherical structure for the mixed micelles is proposed.

LIPID-PROTEIN INTERACTIONS

W-Pos247

STUDY OF THE INTERACTION BETWEEN ACTIN AND LIPID BILAYERS BY FTIR AND ^{19}F NMR ((Mario Bouchard*, Chantal Paré*, Jean-Pierre Dutasta[%], Jean-Paul Chauvet[%], Claude Gicquaud[#], and Michèle Auger*)) *Département de Chimie, CERSIM, Université Laval, Québec, Canada, G1K 7P4, [%]École Normale Supérieure de Lyon, Lyon, France, [#]Département de Chimie-Biologie, UQTR, Trois-Rivières, Québec, Canada, G9A 5H7.

Actin is a ubiquitous cytosqueletal protein which is involved in cell motility and morphogenesis. Actin can exist as a monomer, G-actin, or as a polymer, F-actin. The polymerization of G-actin into F-actin can be induced by millimolar concentrations of salts. We have investigated by attenuated total reflectance (ATR) infrared spectroscopy the effect of F-actin on the acyl chains of several lipids with different chain lengths and polar head groups. The results indicate that the conformational order of the lipid acyl chains is not affected by the presence of F-actin. On the other hand, we have selectively attached a fluorinated probe, 3-bromo-1,1,1-trifluoropropanone, on the cysteines 10, 284 and 374 of the protein. By ^{19}F NMR spectroscopy, we have observed a conformational change of these cysteines in the presence of some charged lipids. More specifically, the results obtained indicate a conformational change of G-actin in the presence of DMPG, a negatively charged lipid, and in the presence of positively charged liposomes made of DMPC and stearylamine.

W-Pos248

MODEL OF INTERACTION BETWEEN A CARDIOTOXIN AND DIMYRISTOYLPHOSPHATIDIC ACID BILAYERS DETERMINED BY SOLID-STATE ^{31}P NMR SPECTROSCOPY. ((Frédéric Picard*, Michel Pézolet*, Pierre E. Bougis[%] and Michèle Auger*))*Département de Chimie, CERSIM, Université Laval, Québec, Québec, Canada, G1K 7P4, [%]Laboratoire de Biochimie, URA 1455 du CNRS, Institut Fédératif de Recherche Jean Roche, Université de la Méditerranée, Faculté de Médecine Secteur Nord, Bd. P. Dramard, 13326 Marseille Cedex 20, France.

The interaction of cardiotoxin IIa, a small basic protein extracted from *Naja mossambica mossambica* venom, with dimyristoylphosphatidic acid (DMPA) membranes has been investigated by solid-state ^{31}P nuclear magnetic resonance spectroscopy. Both the spectral lineshapes and transverse relaxation time values have been measured as a function of temperature for different lipid-to-protein molar ratios. The results indicate that the interaction of cardiototoxin with DMPA gives rise to the complete disappearance of the bilayer structure at a lipid-to-protein molar ratio of 5:1. However, a coexistence of the lamellar and isotropic phases is observed at higher lipid contents. In addition, the number of phospholipids interacting with cardiotoxin increases from about 5 at room temperature to approximately 15 at temperatures above the phase transition of the pure lipid. The isotropic structure appears to be an inverted micellar phase that can be extracted by a hydrophobic solvent.

W-Pos249

INTERACTIONS OF THE NBF-1 DOMAIN OF CFTR WITH PHOSPHOLIPID MEMBRANES.
((Shoshana BarNoy, Peter McPhie, Y. Wang, Eric Sorscher, George Lee, Ofer Eidelman, and Harvey B. Pollard)) LCBG & LBP, NIDDK, NIH, Bethesda, MD, and Departments of Physiology and Medicine, University of Alabama at Birmingham, Birmingham, AL.

The nucleotide binding fold domain (NBF-1) of CFTR is the locus of the main ΔF508 mutation in cystic fibrosis. Even though NBF-1 has been assumed to be principally cytosolic, the 20 kDa rNBF-1 was shown to form ion-conducting pathways in planar lipid bilayers. Recently, rNBF-1 has been shown to gain access to the extracellular side of the membrane. To further understand the molecular basis of lipid interactions with NBF-1 we studied the reciprocal interactions of both components. rNBF-1 induced the permeabilization of PS membranes to calcein, a large, negatively charged dye molecule, in a dose dependent manner. This process was dependent on ionic strength and on lipid composition. Permeabilization caused by rNBF-1(ΔF508) was characteristically different. rNBF-1 also drove the aggregation of PS liposomes, in a sub-milimolar Ca-dependent manner. On the other hand, addition of PS liposomes induced conformational changes in the polypeptide as evidenced by tryptophan emission, accessibility to aqueous quenchers and CD.

W-Pos250

MODELING MEMBRANE-PROTEIN INTERACTIONS: A *de novo* DESIGN FOR A PEPTIDE THAT INSERTS INTO LIPID BILAYERS. ((L. A. Chung and T. E. Thompson)) University of Virginia, Biochemistry Dept., Charlottesville, VA 22908.

The biogenesis of all membrane proteins requires the partitioing of hydrophobic sequences into a non-polar environment. This is true for *sec*-independent proteins, which do not need a fully functional translocation complex; spontaneously inserting proteins, which incorporate into membranes post-translationally; and membrane proteins that must be released from the translocon complex into the surrounding lipid. To study the partitioning of hydrophobic sequences from polar to non-polar environments, we have designed a peptide sequence, H_2N-Ala_2-Leu_3-Ala_{22}-Tyr-Lys_6-$CONH_2$, that is highly soluble in buffer and also incorporates into lipid bilayers from aqueous solutions. The solution and membrane-bound conformations of the peptide were characterized with infrared (IR) spectroscopy and confirmed with circular dichroic (CD) spectroscopy. Using Fourier Transform IR (FTIR) we analyzed both the solution and membrane-bound structures of the peptide while Attenuated Total Reflectance IR (ATR-IR) yielded an orientation for the helical peptide in a planar lipid bilayer. Recently, new information obtained from curvefitting analysis of the solution spectra gave three conformations for the peptide in solution: helix, β-sheet, and extended structures. Curvefitting analysis also gave evidence for the lipid-bound peptide in helical, unordered, and β-structures with the helical conformation oriented perpendicular to the plane of the bilayer. Here we report both the results of our curvefitting analysis and a revised model for the binding and insertion of this peptide into lipid bilayers. (This work is funded by NIH grant GM-14628.)

W-Pos251

PROTEIN-LIPID INTERACTION IN MONOLAYERS AS STUDIED BY IRRAS AT THE A/W INTERFACE. ((Carol R. Flach[1], Joseph W. Brauner[2], and Richard Mendelsohn[1])) [1]Department of Chemistry, Rutgers University, Newark, N.J. 07102 and [2]St. Peter's College, Jersey City, N.J. 07306.

Protein-lipid interaction in Langmuir films is investigated using external infrared reflection-absorption spectroscopy (IRRAS) at the air/water interface. Improved instrumentation permits the determination of peptide secondary structure from the frequency of the amide I (I') mode and the acquisition of H-D exchange information from the presence of the amide II band. Peptide-induced changes in phospholipid acyl chain conformation are monitored by measuring CH_2 asymmetric and symmetric stretching frequencies, and in particular cases, changes in chain tilt can be inferred from the measured band intensities. Investigations of melittin adsorption to 1,2-dipalmitoylphosphatidylcholine (DPPC) and 1,2-dipalmitoylphosphatidyserine (DPPS) monolayers indicate that melittin adopts a secondary structure dramatically different from that observed in bilayer and multibilayer states, while melittin-induced changes in acyl chain conformation are dependent on the lipid composition of the monolayer. Studies of binary monolayers consisting of DPPC and the lung surfactant protein, SP-C, suggest a protein-induced alteration in lipid acyl chain tilt.

W-Pos252

THERMODYNAMICAL MODEL OF THE ASSOCIATION OF PROTEIN KINASE C WITH ITS LIGANDS. ((Marian Mosior and Alexandra C. Newton)) Dept. Pharmacol., Univ. Calif., San Diego, La Jolla, CA 92093

Three classes of ligands: anionic lipids, diacylglycerols (or their functional analogs phorbol esters) and Ca^{2+} cause protein kinase C (PKC) to associate with lipid bilayers. We demonstrate that the appropriate stoichiometries and association constants characteristic of the protein:ligand equilibria can be determined by use of the linkage approach. These equilibrium parameters are obtained directly from the dependence of the apparent membrane association constants of PKC on the concentration of a given ligand. For example, protein kinase C βII binds 8 phosphatidylserine molecules with the average value of the association constant in the range of 3 to 4 M^{-1}; it binds one DG with the association constant of 200 M^{-1}, and one Ca^{2+} with the association constant of 10^6 M^{-1}. This set of experimentally determined equilibrium parameters constitutes a complete thermodynamical model describing the association of PKC with its ligands. This model can be used as an analytical tool to determine which ligand interactions have been perturbed by a specific mutation of PKC. Generality of experimental and theoretical approaches utilized here for the study of PKC can be extended for other families of amphitropic proteins. We introduce also a general method for treating the problem of site-site interactions in an amphitropic protein, like PKC, with multiple binding sites for membrane-bound ligands, like anionic lipids. In particular, we demonstrate that the apparent cooperativity seen in the association of PKC with anionic lipids arises predominantly from the first binding event that changes the dimensionality of protein/lipid interaction from 3D to 2D.

W-Pos253

THE ANCHORING OF MEMBRANE PROTEINS TO THE BILAYER; A THEORETICAL STUDY BASED ON SOLVATION FREE ENERGY. ((M. Nina, S. Bernèche, I. Gambu and B. Roux)) Department of Chemistry, University of Montreal, Montreal, Quebec, Canada H3C 3J7

Specific lipid-protein interactions are of central importance for understanding numerous fundamental biological processes since they are responsible for the anchoring and stabilization of membrane proteins. The dominant effect of the membrane-solvent interface between the hydrophobic and hydrophilic regions is usually understood as a thermodynamic driving force partitioning the amino acids according to their solubility. A microscopic approach for the evaluation of protein solvation energies using computer calculations is proposed. The electrostatic contribution to the free energy of solvation is obtained by solving numerically the Poisson-Bolzmann equation for the protein embedded in a low dielectric medium and in water. The hydrophobic effect is calculated from the solvent exposed area. Protein-membrane systems including melittin, PGHS-1 monotypic membrane anchor domain, and bacteriorhodopsin are examined. Monte-Carlo simulations on melittin and PGHS-membrane systems are performed to give energetically favourable orientations of the protein related to the membrane.

W-Pos254

WHEN BIVALENT PROTEINS MIGHT WALK ACROSS CELL SURFACES ((Willem Vanden Broek and Nancy L. Thompson)) Department of Chemistry, University of North Carolina, Chapel Hill, NC, 27599-3290

Molecular events at cell surfaces are central to signal transduction and subsequent cellular response. Although it has long been known that antibodies are bivalent for cell surface antigens, recent work has demonstrated that many other protein ligands (e.g., fibrinogen and growth factors) are also bivalent in their capacity to bind to molecular determinants on cell surfaces. In these cases, the dynamics of conversion between dissociated, monovalently bound, and bivalently bound ligand are not well understood. In addition, the possibility that these dynamics might occur in a biologically reasonable time frame suggests that bivalent or multivalent proteins might laterally move across the cell surfaces by sequential detachment and attachment of single binding sites. In this work, the conditions under which this putative mode of translational mobility, called "walking", might occur in a biologically significant manner are theoretically predicted. Both symmetric and asymmetric ligands are considered. Supported by NIH GM37145 and by NSF GER-9024028.

W-Pos255

STRUCTURE AND ORIENTATION OF THE MAMMALIAN ANTIBACTERIAL PEPTIDE CECROPIN P1 WITHIN PHOSPHOLIPID MEMBRANES - ATR-FTIR STUDY ((Ehud Gazit and Yechiel Shai)). Department of Membrane Research and Biophysics, Weizmann Institute of Science, Rehovot, 76100, ISRAEL.

Cecropins are positively charged antibacterial peptides, that act by permeating the membrane of susceptible bacteria. To gain insight into the mechanism of membrane permeation, the secondary structure and the orientation within phospholipid membranes of the mammalian Cecropin P1 (CecP) were studied using attenuated total reflectance fourier-transform infrared (ATR FTIR) spectroscopy. The frequencies of the amide I and amide II absorption peaks of CecP within acidic PE/PG multybilayers (7:3 w/w ratio, a composition of phospholipids similar to that of many bacterial membranes), indicated that the peptide is predominantly α-helical. Polarized ATR-FTIR spectroscopy was used to determine the orientation of the peptide relatively to the normal of phospholipid membranes multybilayers. The ATR dichroic ratio of the amide I band of CecP peptide reconstituted to oriented PE/PG phospholipid membranes, indicated that the peptide is preferentially oriented nearly parallel to the surface of the lipid membranes. Similar secondary structure and orientation were found when zwitterionic PC phospholipids were used. The incorporation of CecP did not significantly change the order parameters of the acyl chain of the lipids multibilayer, further suggesting that CecP do not penetrate the hydrocarbon core of the membranes. Taken together, the results further support a "carpet-like" mechanism, rather than the formation of transmembranal pores, as the mode of action of CecP. According to the suggested model, the formation of a layer of peptide monomers on the surface of the membrane, cause destabilization of the phospholipid packing of the membrane, leading to its disintegration.

W-Pos256

MEMBRANE DEFORMATION ENERGY, CURVATURE FRUSTRATION, AND RHODOPSIN FUNCTION. ((Michael F. Brown, Nicholas J. Gibson and Robin L. Thurmond)) Department of Chemistry, University of Arizona, Tucson, Arizona 85721, USA. (Spon. by J. A. Rupley)

The Standard Model of lipid/protein interactions implies that the lipid bilayer serves mainly as a permeability barrier and plays a role in the vectorial organization of membrane constituents. An alternative is that the lipid diversity of natural biomembranes yields characteristic bilayer properties which influence biomembrane functions.[1] We tested the hypothesis that the membrane bilayer governs the energetics of functionally linked conformational transitions of integral membrane proteins. The MI-MII transition of **rhodopsin** is favored by lipids having relatively small head groups, which produce a condensed bilayer surface as in the case of phosphatidylethanolamine (PE), together with bulky acyl chains such as docosahexaenoic acid (DHA; 22:6ω3), which favor a relatively large cross-sectional area. The resulting force imbalance yields a curvature elastic stress of the constituent monolayers. **Non-lamellar forming lipids** shift the MI-MII equilbrium to the right; whereas lipids forming the lamellar phase do not support native-like photochemical function of rhodopsin.[2,3] Average or material properties are formulated in terms of a **flexible surface model**. According to this new biophysical paradigm, the curvature free energy of the bilayer is frustrated in the planar lamellar state, and is relieved by protein conformational transitions linked to function, as in the case of rhodopsin. [1]Brown, M.F. (1994), *Chem. Phys. Lipids* **73**, 159-180. [2]Wiedmann, T.S., Pates, R.D., Beach, J.M., Salmon, A., and Brown, M.F. (1988), *Biochemistry* **27**, 6469-6474. [3]Gibson, N.J., and Brown, M.F. (1993), *Biochemistry* **32**, 2438-2454. [4]Deese, A.J., Dratz, E.A., and Brown, M.F. (1981), *FEBS Lett.* **124**, 93-99. Supported by NIH grants EY03754 and EY10622.

W-Pos257

A MYRISTOYL-ELECTROSTATIC SWITCH MODULATES THE MEMBRANE BINDING OF A PEPTIDE CORRESPONDING TO THE NH_2-TERMINUS OF SRC. ((C. A. Buser and S. G. Vogel)) SUNY, Stony Brook, NY 11794. (Spon. By M. Eisenberg)

Membrane association is required for cell transformation by $pp60^{v\text{-}src}$ (v-Src) and activated $pp60^{c\text{-}src}$ (c-Src). Our previous work with myristoylated peptides (amino acids 2-16 of Src), as well as c-Src and v-Src translated *in vitro* in reticulate lysates, showed that Src is anchored firmly to the membrane by the combined hydrophobic insertion of the myristate into the membrane and electrostatic binding of NH_2-terminal basic residues to acidic phospholipids. A simple model, which predicts that the hydrophobic and electrostatic energies add (or the binding constants multiply), quantitatively described our results. We now show that this model also accounts for the membrane binding of a longer Src peptide, myristate-GSSKSKPKDPSQRRRSLE-amide (denoted myr-src(2-19)). The apparent association constant (K) for the binding of myr-src(2-19) to vesicles containing 33% acidic lipids is $4 \times 10^6\ M^{-1}$. This is the product of the apparent association constant for the insertion of the acyl chain into the membrane ($K_A = 10^4\ M^{-1}$), determined from the binding of myr-src(2-19) to electrostatically-neutral membranes, and the apparent association constant for the interaction between basic residues and acidic lipids ($K_B = 300\ M^{-1}$), determined from the binding of a non-myristoylated analog of myr-src(2-19) to vesicles containing 33% acidic lipids. Phosphorylation of myr-src(2-19) by either PKC (at Ser 12) or PKA (at Ser 17) reduces the binding to vesicles containing 33% acidic phospholipids about 30-fold. Our results are consistent with a simple electrostatic-switch mechanism. The relevance of this mechanism to the membrane binding of Src *in vivo* will be discussed. C.A.B. is supported by the Damon Runyon-Walter Winchell Foundation Fellowship, DRG-1267.

W-Pos258

DIFFERENTIAL DEPENDENCE OF BINDING OF PHOSPHOLIPASE Cβ1, β2 AND TRUNCATED MUTANTS TO PIP_2-CONTAINING MEMBRANES ((L. Runnels, J. Jenco, A. Morris and S. Scarlata)) Depts. Physiol. & Biophysics and Pharm., S.U.N.Y. Stony Brook, Stony Brook, NY 11794. (Spon. by NIH GM53132)

Phopholipase C (PLC) is a soluble enzyme that catalyzes the hydrolysis of the membrane lipid phosphatidylinositol 4,5 bisphosphate (PIP_2) to yield the two second messengers IP_3 and diacylglycerol. The β family of PLCs are activated by G proteins. PLCβs contain a pleckstrin-homology (PH) domain and PH domains from other proteins have been shown to bind strongly to PIP_2. It has also been found that PLCβ is cleaved by calpain, a Ca^{2+} -activated protein, to yield a C-terminal truncated form whose activation properties are altered. To determine whether PH domains may mediate PLC activation by directing or anchoring the protein to the membrane surface, and whether the C-terminal arm of the proteins alter activation via membrane binding, we have studied the membrane association of two closely related isoforms, PLCβ1 and β2 to model membranes containing PIP_2. Using fluorescence spectroscopy and sedimentation, we find that the binding affinity of the β1 isoform increases in the presence of negatively charged lipids and in the presence of PIP_2. Alternately, the binding affinty of the β2 isoform increased only in the presence of anionic lipids, but not PIP_2. Similar results were obtained using C-terminal truncated forms of the two proteins allowing us to conclude that the binding affinities of these proteins is not mediated by their C-terminal arms. The differences in the binding dependence on PIP_2 for the two proteins will be discussed in terms of differences in their PH domains.

W-Pos259

CONFORMATION OF ANTIMICROBIAL PEPTIDES IN FLUORINATED LIPID BILAYERS. ((Nancy Lazaro-LLanos,* Amy E. Kearns,* W. Lee Maloy† and Jack Blazyk*)) Chemistry Department, College of Osteopathic Medicine, Ohio University, Athens, Ohio 45701 and †Magainin Pharmaceuticals, Inc., Plymouth Meeting, PA 19462. (Spon. by C. Brittain)

Magainins, small cationic peptides found in frog skin, possess potent antimicrobial activity but are nonhemolytic. These peptides can form amphiphilic α-helices in the presence of lipid bilayers and interact strongly with acidic phospholipids. Although the role of magainins as membrane active peptides is widely established, their mechanism of action has not yet been fully elucidated. 16-Fluoropalmitic acid was synthesized and incorporated into 1-palmitoyl-2-[16-fluoropalmitoyl]-phosphatidylcholine and 1-palmitoyl-2-[16-fluoropalmitoyl]-phosphatidylglycerol. These fluorinated lipids will be used in solid-state NMR studies to measure distances between the fluorine atoms and ^{13}C-labeled peptides. The phase transition temperature of the fluorinated lipids is ~10°C higher than their non-fluorinated counterparts. Here, we use FT-IR spectroscopy to monitor the interactions of three magainin analogs, $(KIAGKIA)_3\text{-}NH_2$, $(KIAKKIA)_3\text{-}NH_2$, and $(KLAGLAK)_3\text{-}NH_2$ with the fluorinated lipids. Lipid fluidity is determined by measuring the temperature dependence of the position of the methylene C–H stretching band. Peptide conformation is evaluated by analysis of the amide I′ band of the peptide in the different lipid environments, using resolution enhancement techniques in order to separate overlapping components. The effects of peptide binding on lipid fluidity, as well as peptide conformation, are compared with previous results using non-fluorinated lipids.

W-Pos260

POLARIZED ATTENUATED TOTAL REFLECTANCE INFRARED SPECTROSCOPY OF ANTIMICROBIAL PEPTIDES IN LIPID BILAYERS. ((Amy E. Kearns,* W. Lee Maloy† and Jack Blazyk*)) *Chemistry Department, College of Osteopathic Medicine, Ohio University, Athens, Ohio 45701 and †Magainin Pharmaceuticals, Inc., Plymouth Meeting, PA 19462.

Magainins, natural cationic antimicrobial peptides which are capable of forming an amphipathic α-helix, selectively permeabilize bacterial membranes either by functioning like detergents or by forming ion channels. These models may be discriminated on the basis of how the peptide associates with the membrane. Detergent-like behavior may result from the peptide accumulating on the surface of the membrane with the nonpolar face of the amphipathic α-helix in contact with the lipid acyl chains (i.e., the helical axis is parallel to the membrane). If the peptide forms ion channels, the helical axis is most likely perpendicular to the plane of the membrane. We are using polarized attenuated total reflectance infrared spectroscopy to assess the angle of orientation of antimicrobial peptides with respect to the lipid bilayer. The orientation of hydrated lipid multilayers aligned on a Zn-Se crystal is determined from the C–H stretching band at 2850 cm^{-1} and the C=O band at 1740 cm^{-1} for DPPG and 1:1 DPPC/DPPG. $Ac\text{-}K_2\text{-}L_{24}\text{-}K_2\text{-}NH_2$, a peptide known to form a transmembrane α-helix perpendicular to the bilayer, is used to validate the method. We examine three different peptides in this study: $(KIAGKIA)_3\text{-}NH_2$; $(KIAKKIA)_3\text{-}NH_2$; and $(KLAGLAK)_3\text{-}NH_2$. The orientation of these three synthetic peptides is compared and related to the mechanism by which they may interact with lipid bilayers and biological membranes.

W-Pos261

CUBIC PHASE ENTRAPPED HEMOGLOBIN: AN FTIR INVESTIGATION. ((S.B. Leslie, S. Puvvada, B.R. Ratna, and A.S. Rudolph))
Center for BioMolecular Science and Engineering, Code 6900
Naval Research Laboratory, Washington, D.C. 20375-5000.

Monoolein is a naturally occurring lipid which exhibits a variety of phases depending upon its level of hydration. At hydration levels above 20 weight percent the lipid forms a thermodynamically stable, bicontinuous, cubic phase, even in the presence of excess water. This ability to exist in a stable state in excess water makes monoolein an ideal candidate for encapsulation of bioactive materials such as drugs and proteins. In the present work we investigate the interactions between bovine hemoglobin (BHb) and a monoolein cubic phase. Monoolein can form cubic phase even with as much as 20 weight percent protein, although the lattice changes from *Pn3m* to *Ia3d* at the highest BHb concentrations. The frequency of the $\upsilon\text{-}C\text{-}OH_{in\text{-}3}$ and $\upsilon\text{-}CO\text{-}O\text{-}C$ peaks shifted from 1052 and 1183 cm^{-1}, respectively, in phosphate buffered saline, to 1054 and 1182 cm^{-1}, when BHb was present. Incubating the BHb-cubic samples at 4°C, that is forcing them into lamellar liquid crystal phase, for 24 h and then rewarming them to 37°C resulted in a broadening of the $\upsilon_{as}\text{-}CH2$ band at 2925 cm^{-1} compared to samples incubated at 25°C before warming to 37°C. The correlation coefficient of the amide I band changed from 0.95 to 0.92 after 24 h at 25°C and 0.91 at 4°C. The small change in the correlation coefficients indicates that the BHb secondary structure is not substantially changed as a result of entrapment. Additionally, the rate of met-hemoglobin formation is not substantially increased in the presence of cubic phase, further indicating minimal effects of cubic phase on hemoglobin structure.

W-Pos262

EPR ANALYSIS OF ROTATIONAL DYNAMICS, LIPID-PROTEIN INTERACTIONS, AND SELF-ASSOCIATION OF A SPIN-LABELED MODEL MEMBRANE PROTEIN, L24-CYS. ((John D. Stamm, Ruthven N.A.H. Lewis†, Ronald N. McElhaney†, Robert S. Hodges † and David D. Thomas)) Dept. of Biochemistry, University of Minnesota Medical School, Minneapolis, MN 55455, and †Dept. of Biochemistry, University of Alberta, Edmonton Canada T6G 2H7.

We have used EPR spectroscopy to investigate the molecular interactions of a model hydrophobic, helical, transmembrane peptide in lipid bilayers. The peptide, L_{24}-Cys (N-Acetyl-Cys-Lys2-Leu24-Lys2-Amide), was labeled in methanol stoichiometrically at Cys 1 with methanethiosulfonate spin label (MTSSL) and incorporated into phospholipid vesicles. Under many conditions, EPR spectra of this peptide are a superposition of mobile and motionally restricted components, suggesting that peptide self-association occurs. Probe mobility depends strongly upon temperature, lipid/protein ratio, and lipid chain length. In DOPC at 30° and 50 lipids per peptide, the probes were highly mobile, but when the temperature or lipid/protein ratio decreased, the restricted fraction increased. In DMPC, the probes were only slightly restricted at 30°, but became strongly restricted below the T_m of 23°, suggesting peptide aggregation in the gel phase. We conclude that although this peptide was designed to minimize the probability of lateral aggregation in lipid bilayers, such aggregation does occur under certain circumstances and should be considered in the interpretation of physical studies on its interaction with lipids.

W-Pos263

SPECTRIN AND PROTEIN 4.1 BINDING KINETICS TO PLANAR PHOSPHOLIPID MEMBRANES STUDIED BY TIR/FRAP. ((A. E. Mc Kiernan[1], R.C. MacDonald[3], R.I. MacDonald[3],and D. Axelrod[2])) Biophys. Res. Div.[1,2] & Dept. Physics[2], U. of Michigan, Ann Arbor, MI 48109 & Dept. Biochem, Mol & Cell Biol, Northwestern U., Evanston, IL 60208.

Possible nonspecific reversible binding of cytoskeletal proteins to lipids in living cells may guide their binding to integral membrane anchor proteins. In a model system, we measured desorption rates of the erythrocyte cytoskeletal proteins, spectrin and protein 4.1, at two different compositions of planar phospholipid membranes (supported on glass) using the Total Internal Reflection/Fluorescence Recovery After Photobleaching (TIR/FRAP) technique. The lipid membranes consisted of either 100 mol% egg-PC, or 75 mol% PC + 25 mol% PS. The following average desorption rates $\langle k_{off} \rangle$ (with the average including irreversible fractions) were measured for carboxy-fluorescein (CF)-labeled spectrin and protein 4.1. For CF-spectrin, $\langle k_{off} \rangle$ = 3.7 /s and 3.5 /s for PC+PS and PC membranes, respectively. For CF-4.1, $\langle k_{off} \rangle$ = 0.008 /s and 1.7 /s for PC+PS and PC membranes, respectively. From the desorption rates and TIRF measurements of equilibrium binding strength on the same systems, the average adsorption rate to the surface $\langle k_{on}^* \rangle$ can be calculated. For CF-spectrin, $\langle k_{on}^* \rangle$ = 21 x 10^{-6} cm/s and 18 x 10^{-6} cm/s for PC+PS and PC membranes, respectively. For CF-4.1, $\langle k_{on}^* \rangle$ = 0.7 x 10^{-6} cm/s and 27 x 10^{-6} cm/s for PC+PS and PC membranes, respectively. Clearly, for both adsorption and desorption rates, 4.1 is more sensitive to lipid type than spectrin. The two proteins affect each other's binding: CF-spectrin equilibrium binding to PC/PS membrane is enhanced by a factor of two in the presence of 4.1, and its $\langle k_{off} \rangle$ rate drops by a factor of 100 to .038 /s. CF-4.1 equilibrium binding to PC/PS membrane decreases by a factor of four in the presence of spectrin, but with no change in $\langle k_{off} \rangle$. Both CF-spectrin and CF-4.1 binding drop by a factor of 2 and 3.5, respectively to PC membrane when in the presence of the other protein, but the $\langle k_{off} \rangle$ rates are not strongly affected. Therefore, these competitive effects involve primarily changes in the adsorption rates. NSF (DA) & NIH (RM).

W-Pos264

THE BINDING OF NATIVE AND MUTANT CYTOCHROME B5 TO VESICLES CONTAINING UNSATURATED LIPIDS. ((Nilay Başaran, A. W. Steggles*, and Peter W. Holloway)) Dept. of Biochemistry, Univ. of Virginia Sch. Med., Charlottesville, VA. *Dept. of Biochemistry, Northeastern Ohio Univ. Coll. Med., Rootstown, OH.

The interaction of native cytochrome b_5 and a mutant form, where Trp 108 and 109 have been replaced by Leu, with lipid vesicles made from a variety of saturated and unsaturated phosphatidylcholines (PC) has been investigated. The affinities of the two proteins for each vesicle preparation were determined by monitoring the exchange of the protein from the donor vesicle to vesicles made from brominated lipids, by fluorescence. In this assay, both the equilibrium partitioning (K) and the rate of exchange (k) are a measure of the relative affinities of each protein for the series of vesicles and gave similar results. The highest affinity of both proteins was for dimyristoylPC and the lowest was for 1-stearoyl-2-linoleoylPC. The relative binding affinities of the native (N) and mutant (M) forms of the protein to the respective vesicles is given by k_N/k_M and, although this has a value of over 20, it was found to vary only slightly with the type of lipid. This suggests that the overall binding is influenced by the level of unsaturation and that differences seen are inherent in the lipid, irrespective of the protein. Although both proteins have identical charged polar domains, it was found that an increase in ionic strength decreased the affinity of the native protein for the vesicles but increased that of the mutant. This differential effect of ionic strength may reflect changes in the packing of the lipid molecules around the membrane binding regions of the two proteins. These changes in affinity are being correlated with lipid packing as monitored by FTIR analysis of the C=O and C-H stretching regions.

W-Pos265

INTERACTION OF A MUTANT FORM OF CYTOCHROME B5 WITH PHOSPHATIDYLSERINE-CONTAINING VESICLES ((Harold M. Goldston, Jr., A.W. Steggles*, and Peter W. Holloway)) Dept. of Biochemistry, Univ. of Virginia Sch. Med., Charlottesville, VA. *Dept. of Biochemistry, Northeastern Ohio Univ. Coll. Med., Rootstown, OH.

Cytochrome b_5 (b_5) is an amphipathic integral membrane protein which binds to lipid bilayers through its nonpolar C-terminal domain. It has been previously shown that b_5 does not bind to pure phosphatidylserine vesicles and this is likely to be due to charge repulsions from the negatively-charged, hydrophilic N-terminal domain of the protein. Cytochrome b_5 does bind under certain conditions, however, to mixed-lipid vesicles containing phosphatidylserine. The present study examines the interaction of a mutant form of b_5 with a single Trp in the membrane-binding domain with two binary mixed-lipid systems, containing POPS and either POPE or DMPC. Through the use of both calorimetry and fluorescence studies, binding of b_5 is seen in both DMPC/POPS and POPE/POPS SUV's at fluid-phase temperatures but is not observed in the same lipid mixtures in LUV's. Upon incubation at lower, gel-phase temperatures in both binary systems, binding occurs to LUV's. In addition, protein denaturation occurs upon b_5 binding to POPS-containing SUV's but not in LUV's. The differences in binding phenomena in the SUV and LUV systems are rationalized in terms of the likely effects of surface charge and vesicle defects on protein-lipid interactions in the b_5 model system.

W-Pos266

THE ROLE OF TRYPTOPHANS WITHIN THE NONPOLAR DOMAIN OF CYTOCHROME B5 IN STABLE SELF-ASSOCIATION AND LIPID BINDING. ((Robert W. Doebler, Nilay Başaran, A. W. Steggles*, and Peter W. Holloway)) Dept. of Biochemistry, Univ. of Virginia Sch. Med., Charlottesville, VA. *Dept. of Biochemistry, Northeastern Ohio Univ. Coll. Med., Rootstown, OH.

Cytochrome b_5 (b_5) is known to self-associate to form octameric micelles as well as bind spontaneously to lipid vesicles via a 43 amino acid nonpolar domain. A mutant form of cytochrome b_5, where Trp 108 and 112 in this domain are replaced by Leu, is used to examine the effect that the loss of the Trps has on self-association and lipid binding. Since the polar head of b_5 is negatively charged, changes in ionic strength are expected to influence the octamer to monomer equilibrium as measured by gel-filtration. However, the unexpected result is that changes in ionic strength show a greater effect on the 108,112 mutant than on native b_5. A decrease in conductivity indeed creates a slight increase in the critical micelle concentration (cmc) for native b_5, whereas the cmc of the 108,112 mutant increases dramatically. The relative self-association of native b_5 is twice that of the mutant at a conductivity of 2000μS, but is 25 times that of the mutant at 500μS. A similar trend is seen in membrane affinity versus temperature for native and mutant b_5, as measured by inter-vesicle exchange. The off-rate for native b_5 from POPC LUVs increases slightly as temperature rises, whereas the off-rate for the 108,112 mutant increases dramatically as temperature is raised. Specifically, the relative membrane-association of the native b_5 for POPC vesicles is 4 times that of the 108,112 at 6°C, and is approximately 30 times at 31°C. Since Trp 108 and 112 are only separated by three residues it is possible that Trp stacking within the α-helical membrane-binding domain increases protein stability.

W-Pos267

INDUCTION OF NON-BILAYER STRUCTURES BY α-HELICAL PEPTIDES IN MODEL MEMBRANES OF DIACYLPHOSPHATIDYLCHOLINE AND DIACYL-PHOSPHATIDYLETHANOLAMINE. ((J.A. Killian[a], M. de Planque[a], P. van der Wel[a], R.E. Koeppe II[b] and D.V. Greathouse[b])) [a]Dept. of Biochemistry of Membranes, University of Utrecht, Padualaan 8, 5384 CH Utrecht, The Netherlands, and [b]Dept. of Chemistry and Biochemistry, University of Arkansas, Fayetteville, Arkansas 72701

The effect of transmembrane α-helical model peptides was investigated on the phase behavior of different types of lipids. The peptides are uncharged and consist of a sequence with variable length of alternating leucine and alanine, flanked on both sides by two tryptophans. ^{31}P NMR measurements showed that the peptides lower the bilayer to hexagonal phase transition temperature in phosphatidylethanolamines, similar as observed previously for gramicidin. Upon incorporation of the peptides in diacylphosphatidyl-cholines, the preferred lipid organization (bilayer, isotropic phase, or H_{II} phase) depends on the precise extent of mismatch between the hydrophobic thickness of the bilayer and the length of the peptides. Using tryptophan modified analogs it was demonstrated that these aromatic amino acid residues are crucial for the effects on lipid organization. Sucrose density gradient centrifugation experiments showed that the peptide-induced H_{II} phase in diacylphosphatidylcholines is highly enriched in peptide. A molecular model of the peptide-induced H_{II} phase will be presented that is consistent with the results obtained thus far and that explains the important role of interfacially localized tryptophan residues.

W-Pos268

INTERFACIAL ACTIVATION OF PHOSPHOLIPASE A_2 IS ACCOMPANIED BY STRUCTURAL CHANGES IN THE ENZYME. ((S. A. Tatulian*, A. Fridie#, R. L. Biltonen# and L. K. Tamm*)) Dept. of Molec. Physiol. and Biol. Physics* and Pharmacol.#, Univ. of Virginia Med. Sch., Charlottesville, VA 22908

The phospholipid hydrolyzing enzyme phospholipase A_2 (PLA_2) is activated upon binding to aggregated, but not monomeric substrate. The mechanism of this interfacial activation is not yet well understood. Here we report FTIR evidence for structural changes in the wild-type (WTE) and modified (ME) enzyme of the venom of *A. p. piscivorus* (APPD49) upon binding to membranes. ME was prepared by attachment of 4-bromophenacyl bromide to His-48. Transmission spectra in D_2O buffer (pH 8.2) revealed broader amide I bands for WTE than ME. The α-helical component of ME occurred at higher frequencies (~1653 cm^{-1}) than that of WTE (~1650 cm^{-1}) and had a shoulder at 1658 cm^{-1}, indicating a larger fraction of more stable (less H/D exchangable) α-helices in ME than in WTE. In the presence of POPC/POPG (4:1) vesicles the amide I band of WTE was narrowed and a shoulder at ~1658 cm^{-1} appeared and the helical component of ME was shifted to higher frequencies (~1657 cm^{-1}), implying that interaction with negatively charged membranes converts some flexible residues of WTE to a rigid structure and that helices of ME become more stable. Attenuated total reflection (ATR)-FTIR measurements showed that the amount of POPC and DPPC (ester lipids), but not of DHPC (a non-hydrolyzable ether lipid), decreased in supported bilayers as a function of WTE concentration, demonstrating that the activity of WTE can be measured in this system. The α-helical component of the amide I bands of WTE bound to supported membranes was split (~1658 and ~1650 cm^{-1}); that of ME had a peak at ~1658 and a shoulder at ~1650 cm^{-1}, confirming the transmission FTIR results. We conclude that the attachment of the substrate or other hydrophobic compounds to the active center and the binding of the enzyme to membranes synergistically induce new and/or more stable helices. These structural changes are likely involved in the interfacial activation of PLA_2.

W-Pos269

EFFECT OF THE N-TERMINAL GLYCINE ON THE SECONDARY STRUCTURE, ORIENTATION AND INTERACTION OF THE INFLUENZA HEMAGGLUTININ FUSION PEPTIDE WITH LIPID BILAYERS. ((C. Gray, S. A. Tatulian, *S. A. Wharton and L. K. Tamm)) Dept. of Mol. Physiol., U. of Virginia, Charlottesville, VA 22903, and *MRC, Mill Hill, London, UK.

The amino-terminal segment of the membrane-anchored subunit of influenza hemagglutinin (HA) plays a crucial role in membrane fusion, and hence, has been termed the fusion peptide. We have studied the secondary structure, orientation, and effects on the bilayer structure of synthetic peptides corresponding to the wild-type and several fusogenic and non-fusogenic mutants with altered N-termini of the influenza HA fusion peptide by fluorescence, circular dichroism and Fourier transform infrared spectroscopy. All peptides contained segments of α-helical and β-strand conformation. In the wild-type fusion peptide, ~43% of all residues were in α- and ~27% in β-secondary structures. By comparison, the non-fusogenic peptides exhibited larger β/α secondary structure ratios. The order parameters of the helices and amide carbonyl groups of the β-strands of the wild-type fusion peptide were measured separately from the dichroism of the respective infrared absorption bands. Perhaps by coincidence, the same order parameter, 0.49, was found for the helical and β-strand segments of the wild-type peptide, which indicates that both segments are most likely aligned at oblique angles from the membrane normal. The non-fusogenic, but not the fusogenic, peptides induced a splitting of the infrared absorption band at ~1735 cm^{-1} which is assigned to stretching vibrations of the lipid ester carbonyl bond. This splitting, which reports on an alteration of the hydrogen-bonds formed between the lipid ester carbonyls and water and/or hydrogen-donating groups of the fusion peptides, correlated with the β/α ratio of the peptides, suggesting that unpaired β-strands may replace water molecules and hydrogen-bond to the lipid ester carbonyl groups.

W-Pos270

EFFECT OF ACYL CHAIN MISMATCH ON COEXISTING PHASES THAT ACTIVATE PROTEIN KINASE C ((A.K. Hinderliter, A.R.G. Dibble, M. Resnick, B. Vinton, R.L. Biltonen and J.J. Sando)) Dept. of Pharmacology, University of Virginia, Charlottesville, VA 22908.

The thermotropic phase behavior of the ternary mixtures dimyristoylphosphatidylcholine (DMPC) /dimyristoylphosphatidylserine (DMPS) /dioleoylglycerol (DO) and DMPC/DMPS/dimyristoylglycerol (DM) was analyzed and correlated with the ability of the mixtures to support protein kinase C (PKC) α activity. Differential scanning calorimetry was used to moniter the gel-to-liquid crystalline phase transition as a function of mole fraction DO (χ_{DO}) or DM (χ_{DM}) in DMPC:DMPS (1:1) multilamellar vesicles. Addition of either DM or DO to DMPC/DMPS broadened the transition in the range of $0 < \chi_{DO} < \sim 0.3$ for DMPC/DMPS/DO and in the range of $0 < \chi_{DM} < \sim 0.6$ for DMPC/DMPS/DM due to the appearance of overlapping transitions. The overlapping transitions were comprised of a broad and sharper component. The transitions became highly cooperative at $\chi_{DO} > \sim 0.3$ and $\chi_{DM} > \sim 0.6$. Activity in both lipid systems in the gel phase was biphasic and restricted to lipid compositions in which coexisting phases were observed in the region of $0 < \chi_{DO} < \sim 0.3$ for DMPC/DMPS/DO and $0 < \chi_{DM} < \sim 0.6$ for DMPC/DMPS/DM. Activation of PKC-α by the ternary mixture of DMPC/DMPS/DM was significantly reduced in comparison with activation by the ternary mixture of DMPC/DMPS/DO. We attribute the enzymatic behavior of PKC-α observed in the gel phase to the need for interface between the coexisting phases for activation.

(Supported by NIH grants DK07642, DK07320, and GM31184.)

W-Pos271

A SIMPLIFIED MODEL OF THE HYDROLYSIS OF LIPID VESICLES BY PHOSPHOLIPASE A2. ((P.F.F. Almeida and R.L. Biltonen)) Univ. Virginia, Dept. Pharmacology, Charlottesville, VA 22908.

We have developed a simple model for the hydrolytic activity of phospholipase A2 (PLA2) toward lipid vesicles. The key assumptions are: (1) PLA2 exists either bound to a vesicle or in solution; (2) PLA2 hydrolizes one reactant lipid to one product lipid; (3) PLA2 binds to reactant-rich and product-rich regions of a vesicle with low and high affinities, respectively; (4) for both protein and lipid (reactant or product), the lateral diffusivity is small in gel-phase regions, and is large in fluid-phase regions; (5) product-rich regions are fluid and reactant-rich regions are either gel or fluid depending on temperature. This model was simulated using Monte Carlo dynamics methods on a square lattice. The model qualitatively reproduces some key experimental observations: (1) if the system is initially in the gel phase, at low enzyme/vesicle there is an initial period of activity, followed by a lag period that ends at a burst of activity, and (2) addition of extra enzyme during the lag period has essentially no effect; (3) if the system is in the fluid phase initially, there is a lag time if binding is weak but activity starts immediately if binding is good. Snap-shots of the simulation indicate that small product-rich domains are formed at the burst; PLA2 binds to these domains and hydrolysis takes place mostly at the interface with the bulk reactant lipid. A substantial amount of enzyme is bound prior to the burst, but a rapid increase in the average diffusivity occurs concomitant with the burst. (Supported by NIH and NSF.)

W-Pos272

ANESTHETIC EFFECTS ON PROTEIN KINASE C AND LIPID DOMAIN FORMATION. ((Y.-M.A. Shen, A.R.G. Dibble, J.J. Sando, and R.L. Biltonen)) Dept. of Pharmacology, Univ. of Virginia Schl. of Med., Charlottesville, VA 22908

Protein kinase C (PKC) phosphorylates and regulates many of the membrane proteins that have been implicated in pathways affected by anesthetics. The purpose of this study is to understand the mechanism of anesthesia via anesthetic effects on PKC activity. Since PKC activity is dependent on physical properties of the membrane and various anesthetics can alter membrane properties, we tested the hypothesis that PKC activation is related to the dynamic structural state of the lipid bilayer and that anesthetic-induced alteration in PKC activity is the result of perturbation of that state.

We have investigated the effects of several anesthetics on the activity of PKC and on the phase behavior of lipid bilayers that support enzyme activity. In lipid system composed of phosphatidylcholine (PC)/phosphatidylserine (PS)/diacylglycerol (DAG), local anesthetics tetracaine and dibucaine and a general anesthetic chloroform had biphasic effects on PKC activity - activating the enzyme at low anesthetic concentrations and inhibiting at high concentrations. DAG was required for these effects. In contrast, octanol only activated PKC with increasing anesthetic concentration and could replace DAG in activating the enzyme. Differential scanning calorimetry (DSC) studies suggested that DAG-rich domains form in PC/PS/DAG ternary mixtures. Formation of DAG-rich domains was further enhanced as a function of increasing octanol and low local anesthetic concentration, consistent with the octanol and local anesthetic activation of PKC activity. These observations suggest that anesthetics are affecting PKC activity via their effects on formation of lipid domains that are required for PKC activation.

[supported by NIH grants GM-31184 and GM-37658]

W-Pos273

STUDY OF MEMBRANE TARGETING WITH MELITTIN. ((T. Benachir, M. Monette, J. Grenier and M. Lafleur)) Département de chimie, Université de Montréal, Montréal, Québec, H3C 3J7.

Melittin, an amphipathic helical peptide, is known to change the permeability of biological and model membranes. In this work we introduce the possibility of achieving specific membrane targeting with melittin. First, melittin-induced permeability is strongly dependant on lipid composition of the vesicles. The presence of cholesterol inhibits melittin-induced leakage of calcein, a fluorescence marker, from large unilamellar lipid vesicles. We propose that this inhibition is associated with the ordering effect of the sterol on fluid lipid membranes. This leads to a strong reduction in the affinity of melittin for bilayers containing cholesterol as shown by intrinsic fluorescence of the single tryptophan of melittin and by ^{2}H-NMR. Second, our results show that melittin discriminates cholesterol-free vesicles from those containing cholesterol when both populations are simultaneously present. We demonstrate that melittin first empties the cholesterol-free vesicles before causing leakage from the cholesterol-containing vesicles. Therefore, our work reveals a new feature of melittin namely the ability to target specifically cholesterol-free membranes.

W-Pos274

SOLUBLE PHOSPHATIDYLSERINE UPREGULATES FACTOR X_a AND DIRECTS THE ENZYME TO APPROPRIATE SUBSTRATE PEPTIDE BONDS DURING PROTHROMBIN ACTIVATION IN SOLUTION. ((M. Banerjee, J.-F. Wang, & B.R. Lentz)) Dept. of Biochemistry & Biophysics; Univ. of North Carolina; Chapel Hill, NC 27599-7260.

Platelet membrane phosphatidylserine (PS) plays an important but incompletely understood role in human prothrombin activation by factor X_a. Two peptide bonds in prothrombin must be cut during activation, resulting in the production and subsequent proteolysis of two intermediates, meizothrombin ($MzII_a$) or prethrombin 2 & fragment 1.2 (Pre2 & F1.2), for a total of four proteolytic reactions. We report here the effects of dicaproyl-p h osphatidylserine (C_6PS) on both the rate and pathway of prothrombin activation by X_a in solution. Activation was monitored in two ways: first, using dansylarginine-N-(3-ethyl-1,5-pentanediyl) amide (DAPA), whose fluorescence changes when bound to the activation products; second, using a chromogenic substrate (S-2238) to detect both thrombin and $MzII_a$ active site formation. All three data sets were well modelled by a steady-state kinetic model that assumed parallel sequential Michaelis-Menten reaction steps. Two kinetic constants ($MzII_a$ and Pre2&F1.2 consumption) were measured independently, and two were adjusted ($MzII_a$ and Pre2 formation). The results demonstrated that addition of C_6PS increased in a biphasic manner the rate of prothrombin activation. Low concentrations of C_6PS (0-0.3mM) increased the rate of Arg^{322}-Ile cleavage (leading to $MzII_a$ formation) 75-190 fold, while the rate of Arg^{273}-Thr cleavage increased or even *decreased* by only 6-12 fold. A second increase in the rate of thrombin formation occurred from 0.8 to 1.2mM C_6PS. Dynamic light scattering experiments detected formation of C_6PS aggregates at these concentrations. Over this range, the rates of meizothrombin formation and consumption increased by 4 and 20 fold, respectively, while the rate of Pre2 formation *decreased* by 2 fold. The data demonstrate that PS alters prothrombin activation in at least two ways: first, by upregulating X_a, especially in its ability to cleave the Arg^{322}-Ile bond leading to MzIIa formation; second, by altering the interaction between factor X_a and its substrates on a surface so as to favor the $MzII_a$ pathway. *Supported by USPHS grant HL54916.*

W-Pos275

STRUCTURE-FUNCTION STUDIES OF ANTIMICROBIAL PEPTIDE ACTIVITY IN LIPID MEMBRANES

((Lori Silvestro, Mario J. Citra, and Paul H. Axelsen))
Department of Pharmacology, University of Pennsylvania, Philadelphia PA

Cecropin A is a 37-residue antimicrobial peptide and a component of the host-defense mechanism in *Cecropia* spp. Its mechanism of action is unknown, but appears to require a membrane potential difference, and is inhibited by cholesterol. The interaction between these peptides and membranes surfaces is being studied in calcein-loaded liposomes, and in supported lipid membranes using internal reflectance infrared spectroscopy. Preliminary results indicate that cecropin-induced release of calcein from liposomes is markedly enhanced in the presence of a membrane potential generated by valinomycin/K^+, and that 38 mole% cholesterol inhibits most of this release. The activity of cecropin differs according to the sign of the membrane potential. Cecropin does not induce liposome aggregation or size changes. IR spectroscopy detects the presence of mixed α/β structure for cecropin bound to lipid monolayers at the lipid-water interface. The orientation of the helical structure is predominantly in the plane of the membrane. Studies of the form which facilitates calcien release, however, will requires a bilayer membrane, and possibly, a transmembrane potential difference.

Sponsored by J. Lear, and supported by the L. P. Markey Charitable Trust

VIDEO, FLUORESCENCE, CONFOCAL

W-Pos276

LOCALIZATION OF Ca2+ EXTRUSION SITES IN SINGLE POLARIZED EXOCRINE CELLS. ((P.V. Belan*, O.V. Gerasimenko, A.V. Tepikin and O.H. Petersen)) MRC Research Group, University of Liverpool, Liverpool, L69 3BX, U.K; *Bogomoletz Institute of Physiology, Kiev, Ukraine.

Hormone or neurotransmitter-evoked intracellular Ca2+ release is rapidly followed by activation of plasma membrane (PM) Ca2+ pumps extruding a considerable fraction of the Ca2+ liberated from the stores. Pancreatic acinar cells are highly polarized with an apical secretory pole that is particularly sensitive to Ca2+ mobilizing messengers. Recent indirect evidence suggests that continuous maximal agonist stimulation evoking a sustained global rise in the cytosolic Ca2+ concentration results in activation of PM Ca2+ pumps in all regions of these cells We have now devised a new method for direct visualization of the regional Ca2+ extrusion sites from single cells. To detect Ca2+ extruded from the stimulated cells as well as to slow down diffusion of Ca2+ in the external milieu, we use confocal microscopy and a Ca2+ sensitive fluorescent probe linked to heavy dextran in the extracellular solution. We now show directly that the secretory pole is the major Ca2+ extrusion site in pancreatic acinar cells following agonist stimulation. Ca2+ extrusion across the luminal membrane would help to confine physiological Ca2+ signals to the apical part of the cell. Furthermore, endocytosis which must follow Ca2+ -activated exocytosis requires extracellular Ca2+ and the Ca2+ pumping into the acinar lumen would secure this.

W-Pos277

CONFOCAL MICROSCOPY STUDIES OF SECRETION USING INSULIN-GREEN FLUORESCENT PROTEIN ((G. H. Patterson, M. A. Magnuson, and D. W. Piston)) Dept. of Molecular Physiology and Biophysics, Vanderbilt University, Nashville, TN 37232

Studies of pancreatic β cells have shown glucose-response differences between dispersed cells and those in the intact islet. Since isolation of β cells reduces their total insulin secretion, we expect to find functional differences as well. Existing methods to assay insulin secretion on single cells are difficult to temporally correlate with other cellular events and the non-invasive methods used to study secretion in whole islets inherently average over the entire population of β cells, impeding assignment of insulin release to individual cells. We are developing a method to study insulin secretion in single living β cells by expression of an insulin-green fluorescent protein (I-GFP) fusion. Such fusions have been utilized in many other systems to localize proteins of interest to various tissues or regions of cells. We have transfected a plasmid containing the I-GFP driven by the cytomegalovirus (CMV) promoter into cells and produced fluorescent insulin which can be monitored quantitatively using laser scanning confocal microscopy. Putatively, a decrease in fluorescent intensity within β cells during secretion will correlate with the exocytosis of insulin. This method is being used and compared with established techniques for studying insulin secretion in tissue culture and primary culture β cells. The green insulin technique should allow measurements of secretion in intact islets by introducing insulin-GFP through an adenovirus-mediated gene transfer or by development of a transgenic animal.

W-Pos278

NON-RANDOM MOTION IN A LIPID MEMBRANE OBSERVED ON A SINGLE MOLECULE LEVEL.
((Th. Schmidt, G.J. Schütz, H.J. Gruber and H. Schindler)) Institute for Biophysics, University of Linz, Altenberger Str. 69, 4040 Linz, Austria.

The recently developed fluorescence microscopy which allows for observations on the level of individual fluorophores in physiological environments is used to directly visualize non-random motion in a fluid phospholipid membrane. Submicron inhomogeneities of the membrane are observed by deviations from the expected Brownian trajectories of single fluorescence-labelled lipids. The data are interpreted in terms of the 'coralled' diffusion model. Deviations from the random motion of single antibodies on a hapten-containing membrane are interpreted in the framework of individual binding/unbinding events of the antibody to the membrane-bound hapten. The direct visualization allows to discern the lifetime of the antibody/hapten complex from the timescale of the antibody/hapten encounter.

(Supported by the Austrian Research Funds, project S06607-MED)

W-Pos279

FLUORESCENT ANTIGEN PROCESSING BY MACROPHAGES

((Todd French†, Peter T. C. So†, Enrico Gratton†, Jenny Carrero‡, and Edward W. Voss, Jr.‡))
†*Laboratory for Fluorescence Dynamics, Department of Physics, and* ‡*Department of Microbiology, University of Illinois at Urbana-Champaign, Urbana, IL 61801.*

We present a study of macrophage mediated antigen processing using laser scanning two-photon fluorescence lifetime microscopy. With this method, antigen processing can be continuously monitored non-destructively via the measured fluorescence intensity and lifetime. The primary antigen used was $FITC_nBSA$ (FITC, fluorescein-5-isothiocyanate; BSA, bovine serum albumin). Fluorescein moieties were covalently attached to BSA at sufficient concentration for efficient self quenching (typically 22 FITC per BSA molecule). Proteolysis of the antigen is indicated by an increase in the fluorescence intensity and lifetime. Absolute fluorescence intensity measurements *in vivo* are problematic because the local probe concentration also affects the observed intensity. When ratiometric measurement is not possible (as in this case), fluorescence lifetime is the only reliable way to measure the probe's state. Images of macrophages observed after incubation times of up to 36 hours indicate that the FITC-BSA is indeed proteolyzed. The average intervacuolar lifetime did increase with time. However after 24 hours the lifetime did not increase but was still significantly shorter than that of free fluorescein. To investigate other factors that may influence the observed lifetime, various FITC-BSA analogs were used. Questions as to the biological specificity of the antigen were investigated with two homopolymers of lysine (FITC-poly-L-lysine and FITC-poly-D-lysine). The low pH (as low as 4.0) reported in the lysosomes could also affect the lifetime. This work was supported by National Institutes of Health grant RR03155.

W-Pos280

PUMP-PROBE FLUORESCENCE MICROSCOPY: A NEW METHOD FOR TIME-RESOLVED IMAGING WITH HIGH SPATIAL RESOLUTION

((C. Y. Dong, P. T. C. So, and E. Gratton)) Laboratory for Fluorescence Dynamics, Department of Physics, University of Illinois at Urbana-Champaign, 1110 West Green Street, Urbana, IL 61801

We present a unique time-resolved, fluorescence microscope using the pump-probe technique. In this microscope, two laser sources with different repetition frequencies are focused onto the fluorescent sample. The wavelengths of the lasers are chosen such that one laser excites the sample, and another laser induces stimulated emission from the molecules in the excited states. Due to the difference in the lasers' repetition frequencies, the fluorescence generated contains a signal at the cross-correlation frequency, and its harmonics. The spatial distribution of the signal depends on the intensities of both lasers, and is the strongest at the focal point where both light sources have high photon flux. As a result, microscopic imaging with this technique results in strong axial depth discrimination and comparable spatial resolution as confocal microscopy. We will present data characterizing the point-spread functions of pump-probe fluorescence microscopy by imaging fluorescent latex spheres. We will also present similar data showing the additional improvement in spatial resolution achieved by combining pump-probe excitation with confocal detection. Unique features of the time-resolved images obtained with both methods will be shown. Finally, we will discuss the applications of this technique in spectroscopic studies inside cells, and further implementation using diode laser systems. This work is supported by the National Institute of Health RR03155.

W-Pos281

A NEW POTENTIOMETRIC DYE FOR MEASURING POTENTIAL CHANGES ACROSS ENDOPLASMIC RETICULUM. (C.C. Fink, B.P. Bouverat, and L.M. Loew) Dept. of Physiology, U. Conn. Health Center, Farmington, CT 06030.

The endoplasmic reticulum (er) plays a central role in intracellular calcium signalling. However, despite the importance of its role, the electrophysiology of the er has proven difficult to study in the intact cell because of its inaccessibility to both electrical and optical recording techniques. To address this issue, a ratiometric potential indicator dye that could specifically label the er was developed: Di-18:2-ANEPPS. In calibrations on plasma membrane-labelled N1E-115 neuroblastoma cells, Di-18:2-ANEPPS shows on average a 7%/100mv dual excitation wavelength ratio change. CV-1 kidney epithelial cells were the cell line of choice because of its highly detailed er structure apparent even using non-confocal imaging techniques. Experiments were done testing varying agents for their ability to stimulate calcium release from the er stores of these cells. Cells injected with indo-1 (conjugated to 10-kD dextran) showed significant and immediate intracellular calcium increases following addition of 50 mM caffeine, which specifically stimulates calcium release from ryanodine-receptor associated stores. CV-1 cells labelled with Di-18:2-ANEPPS were also treated with caffeine, with dual excitation ratio images of the masked er-network collected along a similar timecourse as the calcium experiments. In 15/16 cells, addition of 50 mM caffeine evoked a 10% decrease in ratio within seconds, followed by a steady-state at this lower ratio for several minutes, after which the ratio gradually relaxed back to its initial value. The cell appears to recover when the caffeine is replaced by normal buffer, and can be stimulated multiple times with further caffeine additions. Lower concentrations of caffeine (5 mM) trigger smaller er ratio decreases (3-6%) which recover in much shorter times (as quickly as 10 seconds). Experiments to establish the relationship between these ratio changes are changes in er membrane potential are underway. (supported by USPHS Grant GM35063)

W-Pos282

DNA SYNTHESIS IN HELA CELLS AFTER TWO-PHOTON EXCITATION ((Jennifer A. Nichols[1] and Watt W. Webb[2])) Departments of [1]Chemistry and [2]Applied Physics, Cornell University, Ithaca, NY 14853.

Minimal cellular phototoxicity is anticipated during two photon excitation (TPE) in fluorescence microscopy since the molecular excitation is confined to the imaged focal plane; in all other methods excitation occurs throughout the specimen. Although this advantage is being realized in practice, especially for UV absorbing fluorophores under the relatively benign conditions empirically selected for imaging, little is known about the limitations and possible damage mechanisms of this process. Parameters include excitation wavelength, excitation intensity, fluorophore selection, spatial and temporal exposures and total dose. We are measuring the inhibition of DNA synthesis by TPE in cultured HeLa cells. After exposures of controlled doses of 700nm pulsed illumination from a mode-locked Ti:sapphire laser in an imaging raster pattern, cell proliferation is assayed by monitoring the incorporation of bromodeoxyuridine into cellular DNA via immunofluorescence labeling. Doses (W^2s) are defined as the square of peak pulse power multiplied by the total illumination time in an average cell. The typical dose to form a ratio image of cellular calcium using Indo-1 fluorescence is ~0.05 W^2s at an average power of 5mW. The corresponding doses for the onset of DNA synthesis inhibition exceeds ~1 W^2s at average powers ~5 to 25mW with 150 to 200fs pulses. Intensity and dose dependence as well as action spectra will be presented.

Supported at Developmental Resource for Biophysical Imaging and Opto-electronics by the NIH (RR04224 and RRO7719) and NSF (BIR 9419978).

W-Pos283

CHARACTERIZATION OF SPONTANEOUS CALCIUM WAVES AND SPARKS IN PRIMARY CULTURES OF FETAL RAT MYOTUBES USING TWO PHOTON EXCITATION POINT AND LINE SCANNING MICROSCOPY. (Warren R Zipfel[1], James P. O'Malley[2], Dirk Van Helden[3], Rebecca M. Williams[1], Jeffrey B. Guild[1], Miriam M. Salpeter[2] and Watt W. Webb[1].) [1]Developmental Resource for Biophysical Imaging and Opto-Electronics (DRBIO), Applied and Engineering Physics, [2]Section of Neurobiology and Behavior. Cornell University, Ithaca, NY 14853. [3]Dept. of Physiology, University of Newcastle, NSW 2308, Australia.

Cultured skeletal muscle cells from fetal rats exhibit spontaneous rhythmic fluctuations in intracellular calcium activity after approximately 5-6 days in culture. We have observed two types of spontaneous calcium activities: (1) waves of calcium which appear to originate from a single point source and (2) calcium sparks that originate in a repetitive stochastic manner from multiple sites; the majority of which are localized to one region of the cell. Calcium waves propagate throughout the myotube, even in the absence of the characteristic "twitching " normally exhibited by these cultured cells, although waves are always found in actively twitching cells. The sparks remain localized to the region of origin and occasionally can be seen as rings of calcium, a few microns in diameter, presumably released from internal structures. Using two photon excitation point scanning (6 frames/sec) and line scanning (30 frames/sec) microscopy we have measured the rate of propagation and the frequency of both the waves and sparks in Fluo-3 and Indo-1 loaded cells and suggest possible sources of these two phenomenon.

Supported by NSF (DIR8800278), NIH (RR04224) and NIH (R07719) at DRBIO.

W-Pos284

PULSE DISPERSION BY HIGH NUMERICAL APERTURE OBJECTIVES FOR NONLINEAR MICROSCOPY USING TWO-PHOTON FLUORESCENCE EXCITATION. ((Jeffrey B. Guild, Chris Xu, and Watt W. Webb)) Applied Physics, Cornell University, Ithaca, NY 14853

Two-photon excitation (TPE) inherently achieves three-dimensional imaging resolution and background elimination by limiting fluorophore excitation to the focal point. The high peak powers required to simultaneously excite a blue absorbing chromophore with two red photons are typically achieved by focusing mode-locked ultra-short laser pulses (≈ 100 fs) through the same well corrected high numerical aperture (NA) microscope objectives used with confocal and conventional microscopy. However, the optical dispersion of the microscope system ultimately limits the minimum pulse-width that can be used in TPE. The temporal broadening of a Gaussian laser pulse-shape of width, t_i, by group delay dispersion (GDD) can be calculated exactly and the resulting pulse-width at the sample, t_s, would be $t_s = t_i\sqrt{1 + (4\ln 2\ \phi'')^2/t_i^2}$ where ϕ'' is a measure of the GDD of the system. Using second order interferometric autocorrelation with fluorescein TPE as the power square sensor we have directly measured the pulse-widths at the focal point of several commonly used microscope objectives. The pulse-widths at the sample could be compressed to their original value (≈ 55 fs) using conventional pre-chirp schemes although the measured quantity of GDD was quite large (-6000 – -1000 fs^2.) This suggests that higher order dispersions are minimal for these objectives at these pulse-widths. Without compensation of this GDD the resulting reduction of TPE as a result of pulse-width broadening can be significant (up to 90%), however, compensation can be easily optimized by maximizing fluorescence emission. We present the measurements of GDD for several objectives over a range of excitation wavelengths (700 – 780 nm) and discuss the effects of GDD on TPE photophysics.

Funded by NSF(BIR9419978), NIH(RR04224), and NIH(RRO7719) at the Developmental Resource for Biophysical Imaging and Opto-Electronics.

W-Pos285

HOMOGENEITY OF GLUCOSE METABOLISM WITHIN INTACT PANCREATIC ISLETS. ((B.D. Bennett and D.W. Piston)) Molecular Physiology and Biophysics, Vanderbilt University, Nashville, TN 37323.

Studies of dispersed β cells have been used to infer their behavior in the intact pancreatic islet. When dispersed, β cells exhibit multiple metabolic glucose-response populations with different insulin secretion properties. However, uncertainty remains whether β cell metabolic heterogeneity is functionally important in intact islets. We have used two-photon excitation microscopy to compare glucose-induced NAD(P)H autofluorescence responses in dispersed β cells and within intact islets. In intact islets, glucose induced elevation of NAD(P)H in > 90% of β cells and the magnitude of this response was nearly homogeneous. In contrast, less than 70% of dispersed β cells responded and the response was very heterogeneous. Also, all responding β cells within intact islets exhibited sigmoidal dose response behavior. Inflection occurred at ~8 mM glucose indicating control by glucokinase (GK, the putative rate-limiting enzyme in β cell glucose metabolism). If GK activity controls steady-state NADH levels, then glucokinase activity should be uniform to generate intra-islet NADH homogeneity. As a first step, we assayed glucokinase immunoreactivity in whole islets and dispersed β cells. We found that GK was indeed distributed homogeneously in islets, but not in isolated cells. These results suggest that β cell heterogeneity may be functionally less important in the intact islet than has been predicted from studies of dispersed β cells, and support the role of glucokinase as the rate-limiting enzyme in the β cell glucose response. Supported by the Beckman Foundation and Vanderbilt Diabetes Center.

W-Pos286

MEMBRANE-PROXIMAL CALCIUM TRANSIENTS IN STIMULATED NEUTROPHILS SEEN BY TOTAL INTERNAL REFLECTION FLUORESCENCE
((Geneva M. Omann[1] and Daniel Axelrod[2])) VA Medical Center[1] and Depts. of Biological Chemistry[1], Surgery[1], Physics[2] and Biophysics Research Division[2], Univ. of Michigan, Ann Arbor, MI 48109.

Numerous signal transduction mechanisms involve the alteration of intracellular calcium levels, either by releasing calcium from internal stores or by opening calcium channels in the plasma membrane. Many of the events triggered in cells occur at the plasma membrane. A long-standing question in the signal transduction field is whether calcium levels at the plasma membrane are the same as that in the bulk cytoplasm. To address this question, we have developed a novel fluorescence microscope/laser optical system to measure membrane-proximal vs. bulk cytoplasmic intracellular calcium levels in single human neutrophils labeled with fluo-3. A set of acousto-optical modulators rapidly chops the excitation illumination between epi-illumination ("EPI", which excites the bulk intracellular region) and total internal reflection ("TIR", which excites only the region near membrane at the cell-substrate contact). This allows simultaneous observation of the activation kinetics in both region while neutrophils are activated by the chemoattractant N-formylpeptide FMLP. We find that: (a) the cells show a transient increase in both EPI and TIR lasting several seconds; (b) the great majority of these show a larger fractional change in TIR than in EPI illumination. The ratio of TIR:EPI fluorescence generally increases in the range of 20% to 60% after FMLP stimulation, and the ratio increase is somewhat longer-lived, on the order of tens of seconds. This shows that the free calcium concentration near the membrane increases more than the free calcium concentration deeper in the cell, and the relative elevation of membrane-proximal calcium persists well after the main transient is over. (Supported by the National Science Foundation).

W-Pos287

IN VIVO VISUALIZATION OF DOXORUBICIN-INDUCED OXIDATIVE STRESS IN ISOLATED CARDIAC MYOCYTES.
((*N.A.Sarvazyan*)) Department of Physiology, Texas Tech University Health Sciences Center, Lubbock, 79430 TX

Spatial and temporal features of intracellular oxidation were studied in isolated cardiac myocytes from adult rats using laser scanning confocal microscopy. Cells were exposed to doxorubicin, an important anticancer drug with well-known cardiotoxicity. To determine the changes in the intracellular production of oxygen free radicals, cells were preloaded with an oxidant-sensitive fluorescent probe 2'7'-dichlorofluorescein diacetate. High resolution fluorescent images were obtained from living cells using low intensity (0.25mW) laser excitation at 488nm. Images were collected using two channels simultaneously, which allowed to visualize both, the intracellular distribution of doxorubicin (channel I, emission >610nm), and the change in oxidation (channel II, emission 520-550). The images revealed extensive accumulation of doxorubicin in different subcellular compartments, with highest accumulation in the nucleus. The uptake of doxorubicin was associated with a rapid increase in intracellular oxidation. The phenomenon was quantified for different doxorubicin concentration (10-200μM). These data indicate that oxygen free radicals are involved in the mechanism of doxorubicin cardiotoxicity. They also show the advantages of the new techniques to monitor intracellular oxidation *in vivo*.

W-Pos288

CYTOPLASMIC VISCOSITY NEAR THE CELL PLASMA MEMBRANE: TRANSLATIONAL DIFFUSION OF BCECF MEASURED BY TIR-FRAP
((A.S. Verkman, R. Swaminathan, H. Pin Kao, S. Bicknese and N. Periasamy)) U.C.S.F. San Francisco, CA 94143-0521.

Total internal reflection-fluorescence recovery after photobleaching (TIR-FRAP) was applied to measure solute translational diffusion in the aqueous phase of membrane-adjacent cytoplasm. TIR excitation in aqueous solutions and cells was produced by laser illumination at a sub-critical angle through a quartz prism; μs-resolution FRAP was accomplished by acousto-optic modulators and fast PMT gating. A mathematical model was developed to determine solute diffusion coefficient from the photobleaching recovery, bleach time, bleach intensity, and evanescent field penetration depth; the model included irreversible and reversible photobleaching processes, with triplet state diffusion. Model predictions were tested in aqueous fluorophore solutions. Diffusion coefficients for FITC-dextrans (10-2000 kDa) determined by TIR-FRAP (recovery times 0.1-4 ms) agreed with values from conventional spot photobleaching. Model predictions for the dependence of recovery curve shape on solution viscosity, bleach time and bleach depth were validated using aqueous fluorescein solutions. Swiss 3T3 fibroblasts and MDCK epithelial cells were fluorescently labeled with the small solute BCECF. Recovery half-times for TIR-FRAP were in the range 3-8 ms; analysis of recovery curves obtained with different bleach times indicated that BCECF diffusion in membrane-adjacent cytosol was 4-8-fold less than in water. These results establish the theory and first experimental application of TIR-FRAP for measurement of aqueous-phase solute diffusion, and indicate similar solute diffusion in membrane-adjacent and bulk cytosol.

W-Pos289

HIGH ORDER FLUORESCENCE FLUCTUATION AUTOCORRELATION WITH IMAGING FLUORESCENCE CORRELATION SPECTROSCOPY
((Willem Vanden Broek, Zhengping Huang, and Nancy L. Thompson)) Department of Chemistry, University of North Carolina, Chapel Hill, NC, 27599-3290

Fluorescence correlation spectroscopy is useful for detecting and characterizing molecular clusters that are smaller than or approximately equal to optical resolution in size. Here, we report the development of an approach in which the pixel-to-pixel fluorescence fluctuations from a single fluorescence image are spatially autocorrelated. Calculation of a series of high order autocorrelation functions from a single image generates several independent parameters which may be used to characterize the distribution of clusters of differing intensities. The method is demonstrated on fluorescent beads and applied to tetramethylrhodamine-labelled, anti-trinitrophenyl IgE specifically bound to substrate-supported planar membranes composed of trinitrophenylaminocaproylphosphatidylethanolamine and dipalmitoylphosphatidylcholine. Supported by NIH GM-37145 and by NSF GER-9024028.

W-Pos290

MODELLING FLUORESCENCE INTENSITY DISTRIBUTIONS IN CONFOCAL MICROSCOPE IMAGES. APPLICATION TO MITOCHONDRIAL MEMBRANE POTENTIAL..
((L. M. Loew, S. M. Krueger and M.-d. Wei)) Center for Biomedical Imaging Technology and Department of Physiology, U. Conn. Health Center, Farmington, CT 06030.

Fluorescence intensity measured from a homogeneous solution in a fluorometer is proportional to the concentration of the fluorophore. It would be of great value to be able to extend this simple measurement to determine the relative concentrations of a fluorescent marker or indicator in different regions or compartments within a cell. Digital imaging microscopy does provide a means for measuring intensities, but these intensities are a function of the thickness of the sampled region as well as the concentration of fluorophore. Confocal microscopy improves this situation by confining the thickness of the sampled region to a subcellular volume, but even this can be larger than that of many intracellular compartments. We have been able to devise a correction scheme by using an experimental point spread function, derived from sub-resolution fluorescent beads and acquired directly from the confocal microscope, as the kernel in a convolution of a model of the subcellular region. This has been applied to the measurement of mitochondrial membrane potential with the Nernstian dye TMRE in which the relative concentrations of dye in the mitochondria and cytosol must be determined. Mitochondrial models were constructed for both N1E-115 neuroblastoma cells and NIH-3T3 fibroblasts based on the typical mitochondrial dimensions determined from electron micrographs. Data from both pinhole and slit aperture confocal microscopes are compared. For the latter, the correction depends on the orientation of the mitochondrion with respect to the slit. (supported by USPHS grant GM35063)

W-Pos291

SINGLE MOLECULE PROTEIN:DNA BINDING STUDIES USING KINETIC BEAD-TRACKING MICROINTERFEROMETRY
((J.D.B. Sutin, and J.M. Beechem)) Vanderbilt Univ., Dept. of Molecular Physiology and Biophysics, Nashville, TN 37232

We have constructed a microinterferometer to study single molecule protein/DNA interactions using tethered particle motion analysis (See Sutin & Beechem, *Biophys. J. 68*: A290). In this method, a microsphere is tethered by a DNA fragment to a coverslip. Changes in conformation of the DNA during binding are reported by changes in Brownian motion of the bead which are observed by microinterferometry. Since microinterferometry has never been used for tethered particle motion analysis of protein:DNA interactions, we have performed simulations to demonstrate that microinterferometry is sensitive to structural transitions caused by protein binding. For these simulations, we have modeled DNA as a worm-like chain using software provided to us by D. Crothers and J. Kahn (See Crothers, et al., 1992; *Methods in Enzymol. 212*: 3). We modified the software for our boundary conditions and incorporated the structure of TBP bound DNA using the coordinates from the X-ray structure of the co-crystal (See Kim, et al., 1993, *Nature 365* : 520). These simulations indicate microinterferometry has the potential to monitor TBP induced DNA bending. Experiments are now on going to measure single molecule TBP binding to DNA.

W-Pos292

Imaging a Single Fluorophore using Two-Photon Excitation
((Tim Ragan, Keith Berland, Peter T.C. So, Weiming Yu and Enrico Gratton)) Laboratory For Fluorescence Dynamics, Department of Physics, University of Illinois at Urbana-Champaign, Urbana, IL 61801

We have developed a detection system for recording the time arrival of single photons with high throughput. We have incorporated this detection system into the two-photon excitation microscope. We have obtained single fluorophore detection sensitivity. The low background inherent in two-photon excitation and single-photon counting enable us to achieve very high sensitivity and large (15 bit) dynamic range.

The sensitivity and dynamic range of this system has been characterized in model systems. The linearity of the instrument is investigated in terms of fluorescence signal intensity and pixel residence time. High sensitivity imaging of cells and macromolecular assemblies will be presented. Finally, the statistics of single chromophore photobleaching in a biological system has been studied. [Supported by NIH grant RR03155.]

W-Pos293

EXPERIMENTAL VERIFICATION OF A QUANTITATIVE MODEL TO DESCRIBE FLUORESCENCE IN HOMOGENEOUS TISSUES

((J. S. Maier, A. Cerussi, S. Fantini, M. A. Franceschini, S. A. Walker, E. Gratton)) Laboratory for Fluorescence Dynamics, Department of Physics, Univ. of Illinois at U-C, 1110 West Green Street, Urbana, IL 61801.

Fluorescence spectroscopy is a potentially valuable tool for the investigation of tissues because of its high specificity. *In vivo* fluorescence spectroscopy has several potential advantages over standard near-infrared tissue spectroscopy in non-invasive medical applications. The multiple scattering of light in tissues (with effective photon mean free paths less than 1 mm) complicates quantitative analysis of tissue fluorescence. Our work unites fluorescence spectroscopy with the diffusive theory for light transport in highly scattering media such as tissues. We developed a model which uses the photon density of the excitation light to derive the spatially extended source at the emission wavelengths. This model relates the measured emission photon density to the optical coefficients of the tissue, and the undistorted fluorescence spectrum, probe concentration, quantum yield, and lifetime of the probe. We demonstrate the effectiveness of this model in describing frequency-domain data collected on a tissue-like sample of Rhodamine B and ink dissolved in water suspending Titanium Oxide particles. Several conclusions based on this model will be presented. This work is supported by the National Institutes of Health grants RR03155 and CA57032.

W-Pos294

Study of Protein Aggregation In Solution Using Scanning Two Photon Fluorescence High Order Correlation Spectroscopy ((Yan Chen, Keith Berland, Peter T. C. So, W. W. Mantulin and Enrico Gratton)) Laboratory for Fluorescence Dynamics, University of Illinois at Urbana-Champaign, Urbana, IL 61801

Two photon scanning fluctuation correlation spectroscopy is a powerful technique for measuring diffusion coefficients and particle number concentrations in dilute solutions of biomolecules (K. Berland, P. T. C. So and E. Gratton, 1995, Biophysical Journal, 68, 694-701). By comparing measured number concentrations with nominal concentrations (known weight concentrations), one can detect the presence of molecular aggregates. We have applied this technique to study protein association /dissociation equilibrium at dilute concentrations (sub micromolar). We demonstrate accurate detection of changes in oligomeric state as protein concentration, pH, or other relevant experimental parameters are varied. These measurements are shown for the proteins Malate Dehydrogenase (MDH), and rabbit muscle Phosphofructokinase (PFK). Also presented are kinetic measurements of dissociation following dilution using PFK. PFK has a complicated distribution of aggregate sizes. We have examined the oligomerization process by calculating high order correlation function. The intensity fluctuation is Poisson distributed up to 1 μM in less than 0.1 fL^3 defined by the excitation geometry. The statistics allows extraction of the moments of oligomerization distribution by high order correlation. [This work is supported by NIH grant R30155.]

W-Pos295

Two-Photon Excitation for Low Background Fluorescence Microscopy: Detection of Single Molecules and Single Chromophores in Solution. ((Keith Berland, Peter T. C. So, Tim Ragan, Weiming Yu and Enrico Gratton)) Laboratory for Fluorescence Dynamics, Dept. of Physics. University of Illinois at Urbana-Champaign, Urbana, IL 61801.

The capability to observe single fluorescent molecule in solution opens up many exciting experimental possibilities, including the development of ultra-sensitive bioassays, and studies of single molecular chemical reactions or ligand binding. A major experimental difficulty in observing single molecule (single chromophore) fluorescence is a low signal to background ratio. In one-photon excitation, scattered fluorescence excitation (Raman and Rayleigh) overlaps with the fluorescence emission spectrum. Time gating techniques are often needed to reduce scattered light. Two-photon excitation is particularly suitable for single molecular detection. First, the excitation and emission wavelengths are widely separated, and filters can be chosen to greatly attenuate the detection of scattered light while maintaining high fluorescence emission collection efficiency. Second, the two-photon excitation volume can be as low as 0.1 femtoliters, which corresponds to an average of 0.06 molecules in a 1 nM sample. Single chromophore detection can be performed at nanomolar range and which maintains high sample to contaminant ratio. We show results for the detection of single dye molecules, fluorescein and Cascade Blue, as well as single chromophore labeled proteins in solution. Essentially all scattered photons can be rejected and photomultiplier dark current contributes only 5 counts sec-1 at the room temperature in our apparatus. Monte Carlo simulations of particle diffusion (including photobleaching effects and triple-state transitions) are presented to compare the expected fluorescence count distribution (calculated using the known chromophore properties and instrument optical characteristics) with the measured photon detection rates. This work is supported by NIH RR03155.

W-Pos296

FIBER OPTIC METAL ION BIOSENSORS BASED ON FLUORESCENCE ENERGY TRANSFER
((Richard B. Thompson, Zhengfang Ge, Marcia W. Patchan, and Carol A. Fierke)) Dept. of Biological Chemistry, Univ. of Maryland School of Medicine, 108 N. Greene St., Baltimore, MD 21201; and Dept. Of Biochemistry, Box 2711, Duke University Medical Center, Durham, NC 27710

We have been developing fluorescence-based fiber optic sensors for continuous monitoring of several analytes in complex matrices such as sea water or serum. As a transducer we have employed variants of a metalloenzyme, human carbonic anhydrase II (CA), which binds certain metal ions with higher selectivity than typical metallofluorescent indicators. Zn(II) present in the active site permits binding of a colored inhibitor to the CA; if the CA has been previously labeled with a suitable fluorescent dye, the fluorophore becomes partially quenched and exhibits a reduction in intensity and lifetime. Lifetime changes are readily quantifiable through a length of optical fiber by means of phase fluorometry. If Zn(II) is absent, the inhibitor binds weakly or not at all to apo-CA, no energy transfer occurs, and the fluorophore is not quenched. Thus the fraction of CA with bound metal is readily determined and simply related to the metal ion concentration. This approach has been extended to other metal ions which exhibit weak d-d absorbance bands such as Cu(II), Co(II), and Ni(II); the weak absorbance serves as an energy transfer acceptor for a correctly placed fluorescent donor. Finally, some anions serve as weak inhibitors, and upon binding perturb the absorbance of Co- or Ni-CA, which thereby alters the efficiency of energy transfer from suitable fluorophores. Recent results will be shown. Sponsored by the Office of Naval Research.

W-Pos297

THREE-PHOTON EXCITED FLUORESCENCE AND APPLICATIONS IN NONLINEAR LASER SCANNING MICROSCOPY. **((Chris Xu, Warren Zipfel and Watt W Webb)) Applied and Engineering Physics, Cornell University, Ithaca, NY 14853**

Molecular fluorescence excited by absorption of three photons can be used in three-dimensional biological imaging by nonlinear microscopy as a direct extension of two-photon excitation. Three-photon microscopy provides an alternative wavelength window for conveniently available laser sources to probe biological specimens and potentially to minimize photodamage. Three-photon excited fluorescence of several common biological fluorophores (indo-1, DAPI, fura-2, dansyl etc.) are measured. Their three-photon fluorescence excitation cross-sections are measured in the wavelength range from 960 nm to 1050 nm. Three-photon induced fluorescence of intrinsic biological chromophores, including tryptophan and serotonin, were also observed in the wavelength range of 700 nm to 900 nm. Three-photon fluorescence images are obtained using existing two-photon laser scanning microscopes. Principles of nonlinear microscopy for qualitative comparisons between two- and three-photon excitation and cross-section measurements will be presented.

Funded by NSF(DIR8800278), NIH(RR04224) and NIH(RR07719) at the Developmental Resource for Biophysical Imaging and Opto-electronics.

W-Pos298

SINGLE MYOFIBRIL IMAGED IN PHYSIOLOGICAL BUFFER BY LATERAL SHEAR-FORCE MICROSCOPY. ((E.J. Seibel and G.H. Pollack)) Center for Bioengineering Box 357962, University of Washington, Seattle, WA 98195.

We have recently added shear-force microscopy to a near-field scanning optical microscope and obtained unexpected results. The near-field probe is a single-mode optical fiber pulled to 50-200 nm tip diameter, and coated with ~50 nm aluminum except at the tip aperture. To determine probe-to-sample separation, the probe tip is laterally vibrated, parallel to the sample surface, at ~20 kHz. When the vibrating probe tip approaches the surface, the amplitude of vibration decreases due to increasing lateral shear force. At constant probe height, a plot of vibration amplitude versus scan position along the sample generates a shear-force topographic image. Image resolution is approximately the probe tip diameter. Our sample, the single myofibril in physiological buffer, is expected to have a smooth surface based upon electron microscopic data. However, when sample-to-probe separation is ≤ 500 nm, our shear-force images show high-relief topography consisting of three prominent peaks per sarcomere. We are investigating whether these shear-force images provide more information than just a very sensitive measure of surface topography. Possibly, the lateral shearing of liquid above the sample exerts a normal component of force which deforms the surface of the soft sample. The image of the myofibril may then derive from a combination of genuine topography and sample compliance. Or possibly, the shear-force microscope is able to detect spatial differences in viscous properties of the solution surrounding the myofibril. Nevertheless, these results imply that there are three regions along the myofibrillar sarcomere of different topography, sample compliance, and/or solution viscosity.

W-Pos299

ENHANCED MULTIWAVELENGTH FLUORESCENCE IMAGING OF LIVE SPECIMENS ((D. L. Farkas, W. Niu, Y. Garini, D. Fishman, and E. Wachman)) Center for Light Microscope Imaging and Biotechnology, Carnegie Mellon University, Pittsburgh, PA 15213.

The non-destructiveness, spatial resolution and speed of optical imaging provide high versatility for investigating biological structure and function. We have previously developed new approaches[1] to meeting the challenges posed by the fluorescence-based imaging of living cells[2] and tissues[3], and we report here on imaging with increased spectral content and resolution. We applied two techniques of spectral selection: (a) microinterferometry, yielding a spectral imaging microscope with high wavelength-discrimination intra-image classification, and (b) acousto-optic tunable filtering, allowing for no-moving-parts multiwavelength fluorescence microscopy with a spatial imaging resolution of 0.35 microns and sub-millisecond temporal resolution. Improved implementations of existing optical technologies, coupled with Fourier analysis and image processing, enabled these enhancements. We summarize our results in applying these advances to imaging a variety of live biological specimens, and the extension of these approaches to the mesoscopic domain, suitable for *in vivo* imaging.

[1]Farkas *et al.* (1993) Ann. Rev. Physiol., 55: 785-817; [2]Farkas *et al.* (1994) Proc. SPIE, 2137: 2-16; [3]Farkas *et al.* (1995) Proc. SPIE,2386: 138-149.

W-Pos300

IMAGING OF SINGLE PROTEIN MOLECULES BY SURFACE PLASMON RESONANCE. ((K. Saito, H. Yokota & T. Yanagida)) Yanagida Biomotron Project, ERATO, JRDC, Mino, Osaka, Japan & Department of Biophysical Engineering, Osaka University, Toyonaka, Osaka, Japan (Spon. by K. Namba)

We have recently demonstrated that single fluorescent dye molecules can be seen at a full video rate in aqueous solution by total internal fluorescence microscopy (*Nature*. **374**, 555(1995)). We refined surface plasmon resonance microscopy to visualize single molecules more clearly. The penetration depth of the surface plasmon is smaller than that of the evanescent field, so the background noise would be further reduced.
The surface plasmon was generated on a metal(Ag)-solution interface with the evanescent field of the totally reflected light (Nd:YAG 532 nm).
Single actin filaments labeled with rhodamine phalloidin were imaged by the surface plasmon. The images were ~10 times brighter than that imaged with the evanescent field at the same power of the incident laser. Single Cy3 fluorescent dyes attached to single myosin subfragments were clearly visualized in aqueous solution.

W-Pos301

SUPER-RESOLUTION DISTANCE MEASUREMENTS BY NON-RESONANT DUAL-COLOR IMAGING OF SINGLE MOLECULES ((S. Weiss[1], T. Ha[1,2], Th. Enderle[1], D.S. Chemla[1,2], P.R. Selvin[3,4])) [1]Molecular Design Institute, Material Sciences and [3]Structural Biology Divisions, Lawrence Berkeley National Laboratory, and [2]Physics and [4]Chemistry Depts., University of California, Berkeley.

Spatial resolution much better than the classical diffraction limit can be achieved with fluorescence if the two points of interest are labeled with fluorophores whose emission can be optically distinguished (E.Betzig, Optics Letters, **20**, 237, 1995). The center of the point-spread function (PSF) can be located approximately 100x more accurately than the of width of the PSF (diffraction limit for far-field, aperture size for near-field microscopies). We used simultaneous dual-color excitation and dual-color detection with the near-field scanning optical microscope (NSOM) to simultaneously acquire two separate images of two different single fluorophores. Due to the identical excitation volume and imaging by scanning, both images were optically in perfect registry. The distance between the fluorophores could be determined by locating the center of the PSFs of the two fluorophores with an accuracy much better than the NSOM aperture size (we typically used apertures of 100 nm). FITC and Texas Red fluorophores were randomly dispersed on a cover-slip. 488nm and 568nm excitation lines were simultaneously coupled to the NSOM fiber probe and dual-color emission images were taken by separating the collected photons with a dichroic mirror and acquiring the data on two detectors. To minimize crosstalk between the channels, the two excitation colors were crossed-polarized. Non-resonant dual-color imaging (NRDCI) can potentially be applied in NSOM, confocal and wide-field microscopies.

W-Pos302

FLUORESCENCE RESONANCE ENERGY TRANSFER BETWEEN A SINGLE DONOR AND A SINGLE ACCEPTOR MOLECULE ((P.R. Selvin[1], T. Ha[2,3], Th. Enderle[3], D.F. Ogletree[3], D.S. Chemla[2,3], S. Weiss[3])) [1]Chemistry and [2]Physics Depts., University of California, Berkeley, and [1]Structural Biology and [3]Material Science Divisions, Lawrence Berkeley National Laboratory.

We report the detection of fluorescence resonance energy transfer (FRET) between a single donor fluorophore (tetramethylrhodamine) and a single acceptor fluorophore (Texas Red) linked by a 10 or 20 base pair double-stranded DNA molecule. We use the near-field scanning optical microscope (NSOM) to excite the donor molecule in the near-field and use high-numerical optics to efficiently collect the fluorescence. The DNA is placed on amino-silanized glass coverslips. 2-color imaging and emission spectra from the donor-only, acceptor-only and donor-acceptor pair are demonstrated. Integration times range from 10 msec to a few seconds. Photodestruction dynamics of the donor or acceptor are used to confirm that we are looking at single fluorophores and to determine the presence and efficiency of energy transfer. Photodestruction of the acceptor leads to an increase in donor emission if energy transfer is occuring. Photodestruction of the donor leaves only the direct-fluorescence of the acceptor, and the extent of energy transfer is measured by comparing the relative net areas of donor and acceptor emission. The classical equations used to measure energy transfer on ensembles of fluorophores are modified for single-molecule measurements. The detection of FRET between a single donor and single acceptor opens up the possibility of monitoring conformational changes - rotations and distance changes on a nanometer scale - within single biological macromolecules.

W-Pos303

POLARIZED AND DEPOLARIZED DYNAMIC LIGHT SCATTERING STUDY OF MUCIN. ((X. Cao, R. Bansil, K.R. Bhaskar* , J.T. LaMont*, N. Afdhal† and Niu Niu†)) Boston University, *BUSM, †BCH, Boston, MA 02215. (Spon. by B. Chasan)

Dynamic light scattering was applied to study the effects of pH and concentration on pig gastric mucin (GM) and bovine gallbladder mucin (GBM). At low concentration of GM (C=2.0mg/ml), the distribution of diffusion constants is independent of pH. Depolarized DLS could be observed at pH2 even at low concentration (C=5.0mg/ml). The rotational and translational diffusion constants were analyzed using the Kirkwood-Riseman model for rods and showed that at pH2 gastric mucin is a rod-like molecule of length 390 nm, diameter 55 nm, with an axial ratio of 7. However, at pH7, no significant depolarized signals could be detected at any of the concentrations examined in the study. Similar studies on GBM showed that while the gallbladder mucin formed aggregates as concentration increased, no depolarized DLS could be observed at the various concentrations and pHs studied. These results suggest that the gastric mucin monomer undergoes a conformational change from a flexible to a rod-like conformation upon lowering pH from 7 (neutral) to 2 (acidid), whereas the gallbladder mucin does not. Such conformational change and aggregation of the gastric mucin molecule at acidic pH may provide a mechanism by which the gastric mucin layer prevents the stomach from digesting itself, since the back diffusion of acid from the lumen to the gastric epithelium is retarded by the gel layer.

W-Pos304

DESIGN OF A SMALL ANGLE SPECTROMETER: APPLICATION TO MILK CASEIN. ((M. Alexander and F.R. Hallett)) University of Guelph, Guelph, Ontario, CANADA, N1G 2W1. (Spon. by F.R. Hallett)

A Small Angle Integrated Light Scattering (SAILS) Spectrometer was designed with the innovative use of a CCD camera. As opposed to previous spectrometers, SAILS has minimum number of optical surfaces that interfere with the main beam and allows the recovery of low angle scattering data.

The scattered light falls on a diffusive plate which is photographed by the CCD camera. The image on this plate produces a digitized two dimensional array, covering the scattering angles from 9 to 20 degrees. This data is then stored as an ASCII file.

Due to this non-invasive technique and the speed of data collection (in the order of 40 s) we are able to study dynamic phenomena such as casein micelle aggregation. By the addition of rennet, caseins are forced to aggregate . As this process takes place, the intensity of the scattered light is recorded as a function of time. The size distribution of the scatterers is obtained from the experimental data by a discrete inversion of the angle dependent scattering. By fitting this information to different aggregation theories, we can get an insight into the possible structure of these elusive proteins.

W-Pos305

Determining the Optical Properties of Inhomogeneous Turbid Media Using Known Structural Information

M. A. O'Leary, D. A. Boas, X. D. Li, B. Chance and A. G. Yodh
University of Pennsylvania, Philadelphia, PA, 19104

There has recently been much interest in obtaining spectroscopic information from highly scattering media. Previously, researchers have concentrated on determining the reduced scattering and absorption coefficients of homogeneous media [2]. Many systems of interest however, are heterogeneous. An important example of such a system is tumor bearing breast or brain tissue.

We have previously presented experimental images of heterogeneous turbid media derived from measurements of diffuse photon density waves traveling through highly scattering tissue phantoms, and showed that this method is sensitive to the optical properties of the heterogeneity[2]. However, these images require many measurements, and are highly sensitive to noise and resolution problems. In this work, we propose an algorithm which combines optical tomography with other imaging modalities to accurately determine the optical properties of heterogeneous media. (Xray tomography and magnetic resonance imaging are viable imaging options.) This simple algorithm reduces the number of unknowns in the problem from the number of voxels in the image, to the number of tissue types. This reduces both the complexity of the inverse problem and the number of measurements neccesary for an accurate reconstruction.

[1] M. S. Patterson, D. J. Moulton, B. C. Wilson, K. W. Berndt, J. R. Lakowicz, Applied Optics, 30(31), (1991).
[2] M. A. O'Leary, D. A. Boas, B. Chance, and A. G. Yodh, Optics Letters, 20(5), p 426 (1995).

W-Pos306

DIFFUSION OF TEMPORAL FIELD CORRELATION WITH SELECTED APPLICATIONS. ((D.A. Boas, I.V. Meglinsky, L. Zemany, L.E. Campbell, B. Chance, A.G. Yodh)) Dept. of Physics, Dept. of Biophysics, University of Pennsylvania, Philadelphia, PA 19104.

We demonstrate that the dynamical properties of turbid media can be probed and imaged using diffusing light. Information is derived from temporal autocorrelation measurements of emerging speckle fields produced by the diffusing light. Experimental results for strongly scattering media with spatially separated static and dynamic components are presented and show the sensitivity of these measurements to the spatially varying dynamical properties of turbid media. Low resolution "dynamical" images of such media are obtained using autocorrelation measurements taken along the surface of the sample. Our analysis is based on a diffusion approximation to the field correlation transport equation [1]. Systems where the dynamics are governed by Brownian motion, shear flow, and random flow will be considered. The application of this technique to diagnosing tissue burn depth and measuring blood flow will be discussed.

[1] D.A. Boas, L.E. Campbell, A.G. Yodh, Phys. Rev. Lett, Vol. 75, pp.1855-1858, 1995.

W-Pos307

3-D SCANNING PROBE MICROSCOPE BASED ON OPTICAL TWEEZERS AND 2-PHOTON EXCITATION BY A cw-Nd:YAG LASER

((Ernst-Ludwig Florin, J.K. Heinrich Hörber and Ernst H.K. Stelzer)) Cell Biophysics Programme, European Molecular Biology Laboratory (EMBL), Meyerhofstrasse 1, Postfach 10.2209, D-69012 Heidelberg, Germany

Understanding biological structures and related functions is a 3-dimensional rather than a 2-dimensional task. New microscopic techniques for 3-D *in situ* investigations are required to overcome the restrictions of conventional scanning nearfield techniques to probe and manipulate surfaces.

The 3-D scanning probe microscope demonstrated uses the 2-photon absorption process with fluorophores bound to a probe (e.g. a latex bead). The probe is trapped by optical tweezers (Fig.) in cw-mode, which is sufficient for fluorescence excitation by 2-photon absorption.

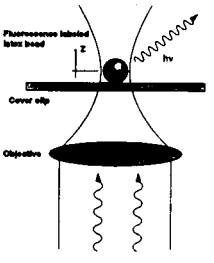

Figure: Schematics of the 2-photon absorption experiment.

Initially, the position sensitivity of the fluorescence emission was investigated. As a result, a lateral resolution and a resolution along the z- axis better than 10 nm can be reported and will be discussed theoretically. First images will be presented.

W-Pos308

NANOANTENNAE EQUIPPED MOLECULAR PROBES: A NEW APPROACH TO NONLINEAR OPTICAL MICROPROBING OF BIOSYSTEMS. ((O. Bouevitch, A. Lewis, and L. Loew)) The Hebrew University of Jerusalem, Israel. (Spon. by A. Lewis)

The application of nonlinear optics to investigate biological problems is a field of considerable and growing interest. It was shown previously that the nonlinear optical phenomenon of second harmonic generation by a submonolayer of potential sensitive dyes can be used to monitor the potential of a lipid bilayer membrane.[1] However, nonlinear optics is often restricted by a relatively low efficiency of nonlinear optical interactions that underlie these processes. We report on experiments that permit the use of the well-known phenomenon of surface enhancement, similar to that which is observed for Raman scattering, to increase the efficiency of non-linear optical molecular probes. To prepare the probes, a dye was adsorbed to a silver colloid forming what we call a dye colloid aggregate (DCA). The DCA particles are in essence nanoantennae equipped with molecular probes. We can freely and selectively place these enhanced probes in a biological system, such as a cell, to amplify at a specific location optical non-linearities to probe biological structure and function. Specifically, we have used an electrochromic potential sensitive dye having significant nonlinear optical coefficients that are dependent on membrane potential.[1] We show by direct microscopic experiments with a living cell culture that the probes can emit second harmonic scattering, two-photon and multiphoton luminescence with enormously high efficiency. A 0.5 μ DCA particle emits about 720 second harmonic photons/s at only 3 W/cm^2 average intensity of infrared illumination at 1.06 μ. Connecting DCA particles to membrane channels in a neural network using presently available immunolabelling techniques should open an unprecedented opportunity of studying the electrical activity of neural networks in parallel and with high spatial/temporal resolution.

1. Bouevitch et al. *Biophys. J.* **65**, 672-679 (1993).

W-Pos309

THEORY OF TRANSPARENCY OF THE EYE USING PHOTONIC BAND STRUCTURE. ((David B. Ameen, Marilyn F. Bishop, and Tom McMullen)) Department of Physics, Virginia Commonwealth University, Richmond, VA 23284-2000.

The propagation of visible light through the corneal stroma of the eye is studied using photonic band structure theory. The stroma consists of long, parallel, cylindrical collagen fibers embedded in a clear ground substance. These fibers are uniform with constant diameter and are oriented so that the wave vector of plane polarized light characteristically incident on the cornea is perpendicular to the long axes of the fibers. Such an arrangement suggests that a regular lattice model could be used to study light propagation in the cornea. The collagen fibers are assumed to be cylindrical rods that intersect the plane formed by parallel rays of incident light. Each lattice point then is the circle formed by this intersection such that a triangular lattice is produced, enabling the application of the theory of photonic band structure. The theory begins with Maxwell's equations, from which the wave equation, a differential equation for either the magnetic or electric field vector, is derived as a function of position in the lattice plane and propagating frequency. The periodicity of the lattice enables the use of Bloch's theorem, which states that the solution to this wave equation is the product of a plane wave with wave vector $\boldsymbol{k}$ and a function that has the periodicity of the lattice. To solve the problem, we expand the periodic function in plane waves, which converts the differential equation to a matrix eigenvalue equation. The eigenvalues for each wave vector $\boldsymbol{k}$ are then the frequencies that are allowed to propagate in the medium, or the photonic band structure. We solve the eigenvalue equation numerically and find that good convergence is achieved with a 343×343 matrix. We find that no band gaps appear, and thus the corneal stroma is transparent for all frequencies.

W-Pos310

HEPARIN INHIBITS ACTIVATION OF MAP KINASE IN CULTURED TRACHEAL MYOCYTES. ((M.C. Stephens, A.J. Halayko, E. Rector* and N.L. Stephens)) Dept Physiology and the Flow Cytometry Lab*, U Manitoba, Winnipeg, MB, R3E 0W3.

Stimulation of quiescent cells with a mitogen, such as Fetal Bovine Serum (10% FBS), leads to activation of mitogen activated protein kinases (MAP kinases). MAP kinase activation is coincidental with G_0 to G_1 cell cycle transition and has been shown to occur in bovine tracheal myocytes (Kelleher et al, AJP 268:L894, 1995) in which proliferation correlates with the timing of activation of the kinases. Heparin, a highly charged anionic glycosaminoglycan, is known to inhibit smooth muscle proliferation but its mode of action remains unresolved. We assessed the responsiveness of cultured canine tracheal smooth muscle cells to FBS stimulation in the presence and absence of heparin using two methods: 1) measurement of MAP kinase activity using an in gel assay, and 2) measurement of cell cycle progression using flow cytometry and propidium iodide staining to determine cellular DNA content. Cells were arrested for 96 hrs in serum free media prior to being stimulated with media containing 10% FBS for up to 1 hour. Parallel experiments in which heparin was included in the FBS medium were also run. Kinase assays showed that enzyme activity peaked 10 min after FBS addition for both groups, however, there was a 50% decrease in peak activity in heparin treated cells compared to controls (n=6). Additionally, ANOVA of all time points showed that heparin decreased the activity by 20% overall (p=.002). Similarly, cell cycle analysis revealed that the fraction of cells entering the cell cycle was decreased by about 40% when heparin was included (n=6, p=.006). However, the time for G_0 to G_1 transition was the same for all cells recruited to the cell cycle by FBS stimulation in the presence or absence of heparin. These data suggest that reduced recruitment of FBS-stimulated tracheal myocytes into the cell cycle in the presence of heparin may be related to inhibition of MAP kinases activation in a particular sub-population of cells. (Supported by the Medical Research Council of Canada).

W-Pos311

PHOSPHORYLATION OF THE SODIUM CHANNEL INACTIVATION GATE BY MYOTONIC DYSTROPHY PROTEIN KINASE. ((Mical J. Kupke, Glenn E. Meixell, J. Paul Mounsey, Christina M. Nall, Erik W. Bush, M. Benjamin Perryman, J. Randall Moorman)) University of Colorado, Denver, CO; University of Virginia, Charlottesville, VA.

Coexpression of human myotonic dystrophy protein kinase (DMK; the product of the gene which is abnormal in myotonic muscular dystrophy) reduces amplitude and speeds decay of currents through skeletal muscle Na channels expressed in *Xenopus* oocytes. The effect requires the presence of the phosphorylation site (*S*1321) in the III-IV linker, the Na channel inactivation gate. DMK, which has sequence homology to protein kinase C and to cAMP-dependent protein kinase (PKA), is composed of two immunoreactive polypeptides of 72 (DMK-1) and 84 (DMK-2) kD which we hypothesize are regulatory and catalytic in function, respectively. To test the hypothesis that the Na channel is directly phosphorylated at S1321 by DMK, we measured the specific activity of DMK-2 (in pmol phosphate/min/mg protein) on synthetic Na channel peptides mimicking the III-IV linker phosphorylation site. DMK-2 was purified from transiently transfected BC3H1 cells by immunoaffinity, anion exchange, and size-exclusion column chromatography. We conclude (1) the Na channel inactivation gate is phosphorylated by DMK-2, (2) the upstream lysines inhibit phosphorylation (unlike PKA) while the downstream lysines are required for substrate recognition by the kinase.

peptide	*DMK-2*
AMKKLGSKKPQK (wild type)	13
AMKKLGAKKPQK (no serine; phos(-))	0
AMNNLGSKKPQK (no upstream Ks)	85
AMKKLGSNNPQN (no downstream Ks)	0

W-Pos312

MODULATION OF OOCYTE-EXPRESSED SKELETAL MUSCLE SODIUM CHANNELS BY NIMA KINASE ((J. Paul Mounsey, James E. John, Anthony R. Means, J. Randall Moorman)) University of Birmingham, UK; Duke University, Durham, NC; University of Virginia, Charlottesville, VA.

Phosphorylation of Na channels by protein kinases modulates Na current amplitude and kinetics. This effect may be mediated by phosphorylation of a site (S1321) in the conserved cytoplasmic linker between domains III and IV. NIMA is a newly-described Ser/Thr protein kinase isolated from *A. nidulans*. To test the idea that Na channels are a substrate for phosphorylation by NIMA kinase, we measured I_{Na} through *Xenopus* oocyte-expressed skeletal muscle Na channel α-subunits alone, and in the presence of mRNA encoding NIMA kinase. Coexpression of NIMA reduced I_{Na} by an average of 56% (1st and 2nd boxes; p<0.001; 82-86 oocytes; 7 frogs). This reduction in I_{Na} was not observed when Na channels were coexpressed with NIMA inactivated by the mutation K39N (3rd box; p=NS; 25; 3). To test the idea that this reduction of I_{Na} is mediated by phosphorylation at S1321, we measured I_{Na} through channels where this site had been disabled by the mutation S1321A ((phos(-)). We find no reduction of S1321A I_{Na} upon coexpression of NIMA (4th and 5th boxes; p=NS; 36-49; 3). We conclude that skeletal muscle Na channels can be modulated directly or indirectly by NIMA kinase. This effect requires phosphorylation at S1321.

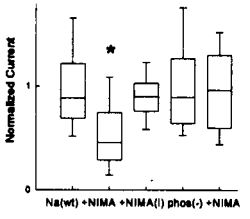

W-Pos313

THE SOLUTION STRUCTURE OF cGMP-DEPENDENT PROTEIN KINASE (PKG) AND ITS ALTERATION UPON ACTIVATION BY cGMP. ((R. D. Mitchell, G. A. Olah, Gu, W., J. Corbin, S. H. Francis, D. A. Walsh, and J. Trewhella)) Dept. of Biol Chem, Univ of California, Davis, CA 95616; Los Alamos National Laboratory, NM 87545; and Dept. of Mol. Physiol and Biophys, Vanderbilt Univ, Nashville, TN 37232-0615

The solution structure of PKG in the presence and absence of cGMP has been determined by small-angle x-ray scattering (SAXS) and Fourier-transform infrared spectroscopy (FTIR). Guinier and P(r) analysis of the SAXS data revealed that PKG in solution is an asymmetric molecule characterized by a R_g of 41.8 ± 0.8 Å and a d_{max} of 135 Å. Upon activation by cGMP, PKG undergoes a large conformational change that results in further asymmetry as evidenced by a d_{max} of 169 Å and an R_g of 54.1 Å. The P(r) function indicates that the extensive conformational change induced by cGMP is the result of a shift of the molecular mass away from the center of the molecule. The overall secondary structure composition of PKG, as determined by FTIR, is unaltered by cGMP indicating that the conformational change is more a consequence of domain movement than of changes within the individual domains. Monte Carlo modelling of the SAXS data has been used to obtain low resolution models of PKG with and without cGMP. Optimum adherence of the modelling constraints is best met by a model for PKG in which a central amino-terminal coiled coil leucine zipper dimerization domain is flanked asymmetrically by the pair of combined contiguous autoinhibitory-regulatory-catalytic domains that each are patterned as asymmetric ellipsoids. PKG activation is envisioned as the partial disassembly of this latter structure leading to overall elongation and movement of the mass away from the central coiled coil.

W-Pos314

PROTEIN KINASE Cα CONTAINS TWO ACTIVATOR BINDING SITES THAT BIND PHORBOL ESTERS AND DIACYLGLYCEROLS WITH OPPOSITE AFFINITIES. ((Simon J. Slater, Cojen Ho, Mary Beth Kelly, Jonathan D. Larkin, Frank. J. Taddeo and Christopher D. Stubbs)) Dept. of Pathology and Cell Biology, Thomas Jefferson University, Philadelphia, PA 19107.

Recently, based on marked differences in the enzymatic properties of diacylglycerol (DAG) compared to phorbol ester activated protein kinase C (PKC), we proposed that these activators may each bind to separate sites on the enzyme (Slater et al., (1994) *J. Biol. Chem.* 269, 17160-17165). In the present study, using a novel binding assay based on the fluorescent phorbol ester, sapintoxin-D (SAPD), direct evidence is provided showing that phorbol esters and DAG may bind simultaneously to two distinct high and low affinity sites on PKCα. Thus, both SAPD binding and activation dose-response curves contained two distinct transitions indicating two sites of high and low affinity for the phorbol ester, respectively. Low affinity SAPD binding was inhibited by *sn-1,2*-dioleoylglycerol (DAG), while binding to the high affinity site was enhanced. Based on this, it is proposed that binding of DAG to the low affinity site allosterically promotes binding of phorbol ester to the high affinity site. Consistent with this, the level of activation in the presence of SAPD *and* DAG *together* was greater than that achievable with either activator individually. By contrast, bryostatin-I (B-I), inhibited SAPD binding to its high affinity site, while low affinity binding was unaffected. Overall, the results provide direct evidence that PKCα contains two distinct binding sites with affinities in the order DAG > SAPD > B-I and B-I > SAPD > DAG, respectively. Further, it was found that, similar to DAG, n-alkanols (long chain) and anesthetics inhibited low affinity SAPD binding and enhanced high affinity binding. Thus, it is proposed that PKCα contains a hydrophobic binding site for these agents corresponding to the low affinity phorbol ester binding site.

W-Pos315

CATALYTIC DOMAIN OF MYOSIN I HEAVY CHAIN KINASE (MIHC KINASE) CLONING EXPRESSION AND CHARACTERIZATION ((H. Brzeska, J. Szczepanowska, J. Hoey, B. Martin* and E.D. Korn)) LCB:NHLBI, *CNB:NIMH Bethesda, MD 20892 (Spon. by X. Wu).

Acanthamoeba MIHC kinase is a 97-kDa monomeric serine/threonine kinase, whose activity is highly (~50-fold) enhanced by autophosphorylation occurring at multiple (up to 11) sites. The exact positions of these sites are not known nor which of them are essential for activation. MIHC kinase is also activated by acidic phospholipids and inhibited by calcium/calmodulin. Recently we have mapped the catalytic domain of MIHC kinase to the 35-kDa COOH terminal segment of the molecule and have shown that phosphorylation causes a conformational change in the region located 11-kDa from the COOH-terminus. The catalytic domain obtained from native fully phosphorylated protein contained at least 1 phosphorylation site located in the COOH-terminal 11-kDa segment. Now, utilizing sequences obtained from the native protein, we cloned the cDNA corresponding to the MIHC kinase catalytic domain and expressed it in SF9 insect cells. The deduced amino acid sequence shows all the characteristics common to kinase catalytic domains. The expressed protein has the same activity as fully activated MIHC kinase and the 35-kDa catalytic domain obtained by proteolytic cleavage of native protein (44 μmol/min•mg) and undergoes rapid autophosphorylation. We are in the process of mapping the position of the phosphorylation site(s) and studying the effect of phosphorylation on activity and conformation of the expressed catalytic domain.

W-Pos316

REGULATORY DOMAINS OF Ca^{2+}/CALMODULIN-DEPENDENT PROTEIN KINASES. ((GANG ZHI AND JAMES T. STULL)) DEPT. PHYSIOL., UT SOUTHWESTERN MEDICAL CENTER, DALLAS, TX 75235

Smooth and skeletal muscle light chain kinases (SmMLCK and SkMLCK) and Ca^{2+}/calmodulin-dependent protein kinase II (CaMKII) catalytic cores are regulated intrasterically by respective autoinhibitory and calmodulin CaM-binding domains. We have investigated the functional properties of these regulatory domains by expressing catalytic cores containing chimeric regulatory domains (denoted in [ ]). SkMLCK and SkMLCK[SmMLCK] had similar activities (V_{max}/K_m values) towards regulatory light chain from smooth (SmRLC) and skeletal (SkRLC) muscles, and similar CaM activation properties (K_{CaM} = 1 nM). SkMLCK[CaMKII] also had a similar K_{CaM} value but had a 7-fold decrease and undeterminable V_{max}/K_m values for SmRLC and SkRLC, respectively. In comparison to CaMKII, CaMKII[SkMLCK] and CaMKII[SmMLCK] had similar high K_{CaM} values (26-50 nM), but V_{max}/K_m values for SmRLC were 10-20 fold lower. All kinase activities were Ca^{2+}/CaM dependent. Thus, heterologous regulatory domains affect substrate recognition. Furthermore, the sensitivity to CaM activation is determined primarily by the respective catalytic cores, not the CaM binding domains.

W-Pos317

FUNCTIONAL EXPRESSION OF THE NINA-C KINASE DOMAIN.
((K.P. Ng*, M. Matsuura†, M. Ikebe‡ and M. Burke*)) Departments of * Biology, and ‡ Physiology and Biophysics, Case Western Reserve University, Cleveland, Ohio 44106, USA. † Nutrition Science Institute, Meiji Milk Products Co. Ltd., 1-32-3 Sakae-Cho, Higashimurayama-Shi, Tokyo 189, Japan

ninaC is one of eight neither inactivation nor afterpotential (*nina*) genes identified from mutations that reduce the amount of rhodopsin in *Drosophila melanogaster* photoreceptor cells. The *ninaC* gene encodes for two photoreceptor specific proteins (NINAC proteins, p132 and p174). NINAC proteins are thought to be involved in *Drosophila* phototransduction and play a structural role in the rhabdomeres. Both the NINAC proteins contain an amino terminus region homologous to a protein kinase joined to a domain homologous to myosin heavy chain motor domain. NINAC has been classified as a class III myosin in the myosin superfamily that currently consist of nine distinct classes. To examine the possibility that the amino terminus domain has kinase activity, a mutant ninaC cDNA for the putative kinase domain (amino acid residue 1-327) was constructed. The construct, encoding a 38 kDa protein (MYOIIIPK), was expressed using the baculovirus expression system and purified to homogeneity. The kinase activity of the purified MYOIIIPK was determined by incubating MYOIIIPK with a number of common protein kinase substrates and radioactive ATP. MYOIIIPK was found to phosphorylate two of the protein substrates examined - NINAC (p132) and smooth muscle regulatory light chain (LC_{20}). To our knowledge, this is the first demonstration of kinase activity for NINAC.

HEAT SHOCK PROTEINS

W-Pos318

LOCAL ANESTHETICS STIMULATE THE HEAT SHOCK RESPONSE BY INCREASING THE EXPOSURE OF HYDROPHOBIC DOMAINS OF DENATURED PROTEINS. ((Senisterra, G. A., Benwell, B., Frey, H. and Lepock, J.R.)). Department of Physics , University of Waterloo, Waterloo, Ontario, N2L 3G1. Canada.

Some agents which stimulate the heat shock response (i.e. sensitize cells to heat shock response and induce the synthesis of heat shock proteins (HSP's)) function by either decreasing the conformational stability of the same set of proteins denatured by heat shock (e.g. ethanol) or denature or destabilize a different set of sensitive proteins (e.g. diamide and menadione). These agents also cause protein aggregation and reduce the stability of nuclear proteins, detectable as an increase in the protein/DNA ratio of isolated nuclei or as an increase in the protein mass of the nuclear matrix. Local anesthetics (LA) stimulate the induction of HSP's, sensitize cells to heat shock, and reduce the extractability of nuclear proteins. The stability of proteins is slightly reduce by LA, however, the reduction in the conformational stability of proteins in hole cells, isolated nuclei or nuclear matrices, or the soluble protein citrate synthase (CS) is not sufficient to account for sensitization to heat shock. These LA do increase the apparent surface hydrophobicity of the thermally denatured state of the nuclear matrix and CS as determined by ANS fluorescence, and they increase the rate and extent of aggregation of CS as determined by light scattering.
Thus, we propose that LA sensitize cells to heat shock and stimulate the heat shock response by increasing the surface hydrophobicity of cellular proteins denatured during heat shock either by increasing the exposure of normally buried hydrophobic residues or by direct binding to the denatured state.

W-Pos319

DYNAMIC LIGHT SCATTERING STUDIES SUGGEST THAT THE BINDING OF HSP70 INDUCES A CONFORMATIONAL CHANGE IN CLATHRIN. ((Albert J. Jin[1], Ralph Nossal[1], Rodolfo Ghirlando[2], Lois Greene[3], and Evan Eisenberg[3])), [1]Phys. Sci. Laboratory, DCRT; [2]Laboratory Mol. Biology, NIDDK; [3]Laboratory of Cell Biology., NHLBI, National Institutes of Health, Bethesda, MD 20892.

The heat shock protein, hsp70, is able to dissociate clathrin from clathrin-coated vesicles in an ATP dependent reaction. This uncoating process leads to the formation of a clathrin-enzyme complex which can also be formed by the direct binding of hsp70 to clathrin. In these complexes three hsp70 molecules appear to bind to the vertex of each clathrin molecule[1]. We have now carried out dynamic light scattering studies on both free clathrin and clathrin saturated with hsp70. Since hsp70 binds extremely slowly to clathrin in pure ADP, these studies were carried out in 90% ADP and 10% ATP which maximizes the binding strength of hsp70 to clathrin but still allows the binding to occur at a reasonable rate[1]. Preliminary scattering intensity and particle sizing analyses suggest that, with hsp70 bound, the clathrin has a mean diameter of 29 nm, compared to the mean diameter of free clathrin of 35 nm. This effect of hsp70 was clearly related to its binding to clathrin since it could be reversed by adding high concentrations of cytochrome C peptide which dissociates the hsp70 from the clathrin by binding competitively with the clathrin. Therefore the binding of hsp70 to clathrin induces a marked decrease in the size of clathrin possibly because it changes the conformation and/or flexibility of the clathrin arms. Such a change in clathrin conformation could be related to the ability of hsp70 to dissociate clathrin from clathrin-coated vesicles.

[1] Prasad, K., Heuser, J., Eisenberg, E., and Greene, L. (1994). *J. Biol. Chem.*, 269(9): 6931-6939.

W-Pos320

FLUORESCENCE STUDIES OF THE LIGAND INDUCED CONFORMATIONAL CHANGES IN THE *E. coli* HSP70, DNAK ((Diana Montgomery & Richard Morimoto)), BMBCB, Northwestern University, Evanston, IL 60208

Fluorescence energy transfer (FET) has been used to measure the distance, and the ligand dependency of the distance between unique functional sites in DnaK. The three sites include: W102, C15 (both in the N-terminal domain), and the peptide binding site (C-terminal domain). DnaK labeled at C15 with AEDANS can serve as an acceptor for FET with W102. In the crystal structure of bovine hsc70[1], the sequentially conserved C15 is located near the nucleotide binding site. DnaK-C15-AEDANS retains nucleotide binding activity and displays the same W102 emission maximum as unlabeled DnaK, suggesting that the label does not dramatically perturb the structure of the protein. FET experiments indicate a molecular distance of 25 Å. In the presence of 0.5 mM ADP or ATP the distance increases by 3 and 4 Å respectively. At saturating concentrations of peptide, the distance is not significantly changed. In order to measure distances between the nucleotide binding domain and the peptide binding domain, a fluorescently labeled peptide has been used to localize the peptide binding site. A 22 residue peptide has been labeled at a N-terminal cysteine with fluorescein. Peptide binding affinity has been determined by fluorescence anisotropy, Kd=76 nM. In 0.5 mM ADP the affinity is lower, Kd=0.28 uM. The fluorescein labeled peptide will be used as an acceptor in FET experiments with DnaK-AEDANS to measure the distance between the nucleotide binding site and the peptide binding site and how the distance changes in the presence of nucleotides. 1. Flaherty, K.M., DeLuca-Flaherty, C., & McKay, D. B. (1990), *Nature* 346,623-628.

W-Pos321

INVESTIGATING NUCLEOTIDE BINDING TO THE HEAT SHOCK PROTEIN DNAK USING ESR-SPECTROSCOPY ((‡Pia D. Vogel, ‡Sonja Neuhofen, #Holger Theyssen, #Jochen Reinstein and ‡Wolfgang E. Trommer)) ‡ Fachbereich Chemie, University of Kaiserslautern, 67663 Kaiserslautern, Germany and # Abteilung Physikalische Biochemie, Max Planck Institut, 44139 Dortmund, Germany.

We employed ESR spectroscopy using spin-labeled adenine nucleotides to investigate nucleotide binding to the HSP 70 analog DnaK from *Escherichia coli*. Of the spin-labeled adenine nucleotides available in our laboratory, only the derivatives with the spin label attached to the C-8-position of the adenine moiety (C8-SL-ATP and C8-SL-ADP, 8-(2,2,6,6-tetramethyl-piperidin-4-yl-1-oxyl-)amino-adenosine-5'-tri- or di-phosphate) were bound sufficiently tightly by the heat-shock protein. The resulting ESR spectra (2Azz-value = 54 G) were typical for protein-bound radicals with considerable intrinsic mobility. Maximum binding of both nucleotide analogs was reached at about one mol of nucleotide analog per mol DnaK monomer in the presence of magnesium ions. In the absence of Mg^{2+}-ions, only approximately 0.5 mol were bound. Subsequent addition of Mg^{2+} led to the previously observed maximum binding of one mol per mol. Both C8-SL-ATP and C8-SL-ADP were fully exchangeable upon addition of excess ATP or ADP. C8-SL-ADP-release was also observed in the presence of the co-chaperone GrpE, indicating that the spin-labeled analogs of adenine nucleotides function like the natural nucleotide-substrates of the heat-shock protein. Maximal GrpE-induced nucleotide release was observed at a GrpE to DnaK ratio of 2 : 1. A significant conformational difference of the protein having bound either SL-ADP or SL-ATP was not observed. Independent experiments, however, showed that the ATP-derivative was hydrolyzed by DnaK. It is therefore possible, that in the time needed for the ESR experiment SL-ATP had already been hydrolyzed to the corresponding ADP-form. We will be able to circumvent this problem in the future by using the non-hydrolizable ATP analog, SL-AMPPNP, which is presently being synthesized in our laboratory.

W-Pos322

INCREASED EXPRESSION OF HEAT SHOCK GENES IN CELLS EXPOSED TO WEAK 60Hz ELECTROMAGNETIC FIELDS. ((M. Blank[1] and R. Goodman[2])) Columbia University Health Sciences, Departments of Physiology and Cellular Biophysics[1], and of Pathology[2] New York, NY 10032.

In dipteran salivary gland cells, yeast and human HL-60 cells, exposure to weak (0.8μT-80μT) electromagnetic (EM) fields increases transcript levels for the stress gene, HSP70. Protein synthetic patterns show similar elevated levels of several heat shock proteins (particularly in the 27kD and 70kD regions) in samples exposed to either EM fields (at constant growth temperature) or sudden elevated temperature (**Bioelectrochem Bioenerg** 31:27-38, 1993; 33:109-114,1994; 33:115-120, 1994; **Advances in Chemistry 250,** 1995). In light of these results, we propose that EM fields stimulate the general pathway used by cells in response to thermal and other physical stresses. The response to EM fields occurs at a very much lower energy density, 10^{-7} joules/m^3 for 0.8μT magnetic field compared to 10^{+7} joules/m^3 for 5.5°C rise in temperature. Thus, EM fields are the preferred stimulus for studying the stress response with minimal perturbations (i.e., compared to accelerated reactions at heat shock temperatures). In recent studies, we have shown that EM activation of the HSP70 gene occurs between -155 and -230 (the c-*myc* binding sites) on the HSP70 promoter. We have also found evidence for negative feedback control in EM-stimulated transcription by showing that a short exposure to EM fields induces a longer sustained response compared with continuous exposure.

(We thank EPRI and the Heineman Foundation for their support.)

W-Pos323

PHOSPHORYLATION OF THE 27 kDa HEAT SHOCK PROTEIN (HSP27) IN SMOOTH MUSCLE ((J. Larsen, I. Yamboliev, and W.T. Gerthoffer)) Dept. Pharmacology, Univ. Nevada School of Medicine, Reno, Nevada, 89557-0046.

HSP27 is expressed in a variety of tissues in the absence of stress and even though overexpression of the protein confers thermotolerance, its function remains unclear. We showed previously the canine HSP27 protein sequence has three serine residues which correspond to the known sites of phosphorylation by MAPKAP kinase-2 in human HSP27. MAPKAP kinase-2 is activated by MAP kinase in signal transduction cascades initiated by mitogenic stimuli as well as being activated by cytokines in non-proliferating cells. Here we show the expression of HSP27 in canine tracheal smooth muscle and its ability to be phosphorylated in intact muscle. Results suggest that HSP27 phosphorylation is rapid (within one minute) after carbachol stimulation of muscle tissue. In addition, we expressed a recombinant canine HSP27 in E. Coli and conducted an *in vitro* assay of its phosphorylation by MAPKAP kinase-2. MAPKAP kinase-2 phosphorylated HSP27 *in vitro*. These findings suggest that HSP27, in addition to being a stress response protein, may be phosphorylated in receptor-initiated signalling cascades. These sequence of events may include MAPKAP kinase-2 phosphorylation of HSP27. (Supported by HL48183.)

HEME PROTEINS AND PORPHYRINS II

W-Pos324

A MOLECULAR DESCRIPTION OF POLYMER FORMATION IN A RECEPTOR SITE MUTANT OF SICKLE HEMOGLOBIN ((Dan Liao*, Zhiqi Cao*, Rossen Mirchev*, Jose Javier Martin de Llano §, Juha-Pekka Himanen§, James M. Manning § and Frank A. Ferrone*)) *Department of Physics and Atmospheric Science, *Drexel University*, Philadelphia, PA 19104 and §*The Rockefeller University*, New York, New York 10021

Sickle hemoglobin forms polymers composed of 7 pairs of double strands. The mutation site β6V contacts another monomer at β88L, among other sites. By site directed mutagenesis at β88 the Leu has been replaced by an Ala. We have determined the solubility of this mutant in 0.15 M phosphate buffer from 15 to 45 °C and find it has risen to 29.6 g/dl at 25°C versus 17.4 g/dl for HbS. Homogeneous nucleation occurs with a rate significantly slowed, so that at 40.8 g/dl it is only 1.3×10^{-7} mM/s rather than 3.3×10^{-4} mM/s for HbS. Heterogeneous nucleation is also slowed, and the exponential growth of the polymer mass has an exponent of 1.4 /s vs 400 /s for HbS. When the measured solubility is used with the double nucleation model, the prediction of the homogeneous nucleation rate is exact with no adjustment of parameters, while the heterogeneous rate shows significant discrepancy. This argues that the double nucleation model needs adjustment.

W-Pos325

AN IMPROVED DESCRIPTION OF HETEROGENEOUS NUCLEATION IN SICKLE HEMOGLOBIN POLYMERIZATION ((Frank A. Ferrone, Dan Liao and Zhonglin Hu)) Department of Physics and Atmospheric Science, *Drexel University*, Philadelphia, PA 19104

The polymerization of sickle hemoglobin occurs by homogeneous nucleation (from monomers alone), and heterogeneous nucleation (onto pre-existing polymers). These nuclei have no special structure, and are concentration dependent thermodynamically determined species. A critical aspect of the description is the inclusion of large solution nonideality to account for the crowded solutions in which polymers form *in vivo*. New precision techniques and site directed mutants (cf. related posters) now allow the contributions of the various effects to be assessed with much greater discrimination. While the homogeneous nucleation process appears to be well described, weaknesses appear in the treatment of the heterogeneous process, and affect the ability of the model to describe mutants as well as hemoglobin mixtures. Directions for addressing this discrepancy will be discussed.

W-Pos326

HOMOGENEOUS NUCLEATION OF SICKLE HEMOGLOBIN POLYMERS: TESTING THE THEORY ((Zhiqi Cao and Frank A. Ferrone)), Department of Physics and Atmospheric Science, *Drexel University*, Philadelphia, PA 19104

Sickle hemoglobin polymerizes by homogeneous and heterogeneous nucleation. As a molecular process, homogeneous nucleation is fundamentally stochastic, and we have used the fluctuations in time of nucleation to determine the rate of nucleation. The nucleation rates so obtained can be compared with previous theories based on light scattering measurements.[1] When directly measured polymer elongation rates[2] are incorporated, the magnitude and high (50th order) concentration dependence of the nucleation process are reproduced accurately by the theory with no parameter adjustment. Nucleation involves the interplay between the entropy of motional freedom, lost upon assembly, and the entropy of polymer vibrations and energy of polymer bonding which are both gained upon assembly. From the temperature dependence of the nucleation rate we can deduce the temperature dependence of polymer vibrational entropy, and find it similar to an Einstein lattice, also in agreement with previous assumptions.

1 F. A. Ferrone, J. Hofrichter & W. A. Eaton (1985), J. Mol. Biol. 183 611-631
2 Samuel, Solomon, & Briehl (1990) Nature 345 833-835

W-Pos327

RELIGATION KINETICS OF SICKLE CELL HEMOGLOBIN POLYMER ((Daniel B. Shapiro[1], Raymond M. Esquerra[1], Robert A. Goldbeck[1], Samir K. Ballas[2], Narla Mohandas[3], and David S. Kliger[1]))[1]Dept. of Chemistry & Biochemistry, Univ. of California, Santa Cruz, CA 95064, [2]The Caldeza Foundation, Dept. of Medicine, Jefferson Medical College, Philadelphia, PA 19107, [3]Life Sciences Division, Lawrence Berkeley Laboratory, Berkeley, CA. 94720.

We present kinetic measurements of the religation of sickle cell hemoglobin (HbS) polymers following laser photolysis of the carbonyl adduct. These measurements are accomplished through the application of an ultrasensitive, ellipsometric time-resolved linear dichroism technique developed for this purpose. Linear dichroism measurements can discriminate between religation of the polymer phase and ligand rebinding to the monomer (free tetramers) phase. We find that the return of the polymer phase to its equilibrium ligation state is about 1000 times slower than that of the solution phase hemoglobin tetramers. Several models describing the mechanism of this slow religation to the polymer are presented: 1) religation occurs through a bimolecular process involving all polymer hemes characterized by slow diffusion of carbon monoxide (CO) through the polymer phase, perhaps due to dampened internal motions within the hemoglobin molecule 2) religation occurs through a bimolecular process in which only hemoglobin molecules at the polymer ends can participate 3) religation occurs through the exchange of ligated molecules in the monomer phase with unligated ones in the polymer phase. Results of experiments to distinguish between these models are presented. *This work is supported by NIH grants HL08969 (D.B.S.), HL31579 (N.M.), GM35158 (D.S.K.) and the NIH Comprehensive Sickle Cell Center Grant no. HL38632 (S.K.B.).*

W-Pos328

POLYMERIZATION OF DEOXY-SICKLE HEMOGLOBIN IN HIGH PHOSPHATE BUFFER. ((Z. P. Wang, Y. M. Chen and R. Josephs)) Dept. of Molecular Genetics and Cell Biology, Univ. of Chicago, Chicago, Illinois 60637

The intracellular polymerization of deoxy-sickle hemoglobin (HbS) to form fibers is the primary cause of sickle cell anemia. We have previously determined the three dimensional structure of HbS fiber electron micrographs and synthesized a model depicting the contacts stabilizing the fiber. In order to test the contacts predicated by the model we are preparing site directed mutants. However high concentrations of hemoglobin (ca. 150mg/ml) are required for polymers to form. Quantities of the order of 10-20mg are available from most site directed mutant preparations. Increasing the phosphate buffer concentration to 1.5M can reduce the concentration of HbS required for polymerization. However the work of high concentrations of phosphate buffer to induce polymerization had been criticized because there is no data relating the structure of fibers formed in high phosphate to the structure of fibers formed under physiological conditions. We have characterized the structures formed in high phosphate to determine if they are similar to those formed under physiological conditions. HbS polymerizes in 1.5M phosphate at a concentration of 25mg/ml. Fibers form first and after about 10 hours fibers begin to form other types of structures such as bundles, macrofibers and crystals which have the same appearances as the corresponding particles formed in low phosphate buffer. The pathway of polymerization in high and low phosphate is similar. In addition optical diffraction of the micrographs reveals the spacings are $1/32Å^{-1}$ and $1/64Å^{-1}$ respectively which are the same as those in low phosphate. On the basis of these preliminary studies, these HbS fibers formed in high phosphate appear to have the same structure as those formed in low phosphate.

W-Pos329

LYSINE 313 OF ERYTHROID 5'-AMINOLEVULINATE SYNTHASE IS REQUIRED TO FORM THE QUINONOID INTERMEDIATE

Gregory A. Hunter and Gloria C. Ferreira

Department of Biochem. and Mol. Biol., USF College of Medicine

5'-Aminolevulinate synthase is a pyridoxal phosphate enzyme that catalyzes the condensation of glycine and succinyl coenzyme A to yield aminolevulinate, coenzyme A, and carbon dioxide. At the active site of the enzyme lysine 313 covalently binds pyridoxal phosphate to form the holoenzyme. Site directed mutagenesis of lysine 313 to glycine or alanine does not eliminate the ability of the enzyme to bind pyridoxal phosphate, but does result in a complete loss of measurable enzymatic activity, indicating lysine 313 also has some catalytic function. The mutants do bind and form stable external aldimines with glycine and, in the reverse direction, aminolevulinate, but show no evidence of forming the quinonoid intermediate which arises from the loss of the pro-R C-α proton of glycine, or the pro-R C-5 proton of aminolevulinate. These results suggest that the role of lysine 313 in catalysis by the wild type enzyme is in the removal of these protons, perhaps through a general base mechanism.

W-Pos330

INTERACTION OF TWO WATER SOLUBLE PORPHYRINS WITH BOVINE SERUM ALBUMIN: STEP-BY-STEP AGGREGATION MODEL ((Iouri E.Borissevitch, Tania T.Tominaga, Hidetake Imasato and Marcel Tabak)), Instituto de Química de São Carlos-USP, S.P.780, 13560-970, São Carlos, S.P., Brasil.

The importance of porphyrins (PPh) as therapeutic drugs has increased significantly over the last decade due to the application of natural and synthetic porphyrins in medicine, for instance, as active compounds in fluorescence, radiological and Magnetic Resonance Imaging cancer detection and as photosensitizers in photodynamic therapy of cancer. The aggregation phenomenon plays an important role in physico-chemical properties and photophysical behavior of porphyrins. In particular, the formation of aggregates changes their absorption spectra, quantum yields and lifetimes of triplet states, affinities to biological structures, water solubilities and other characteristics. On the other hand, many biological structures are self-assembling or are able to form aggregates and superaggregates. In the present work we report studies of interaction of *meso*-tetrakis(*p*-sulfonatophenyl)porphyrin and *meso*-tetrakis(4-*N*-methyl-pyridiniumyl)porphyrin with bovine serum albumin (BSA) using optical absorption and fluorescence and calculation of aggregation numbers according to our step-by-step model. Two types of aggregation are considered: the aggregation of PPh on the surface of BSA and the aggregation of BSA around PPh. The aggregation number in the first process can reach 60 and in the second one 10, depending on the nature of PPh, pH and [BSA]/[PPh] ratio. Consideration of the aggregation is very important for correct evaluation of association constants.

Support: CNPq, FAPESP and FINEP.

W-Pos331

INTERACTION OF CATIONIC PORPHYRINS WITH DNA

((Shirley C. Monte, Janice R. Perussi, Hidetake Imasato, Marcel Tabak, Iori Borissevitch)). Departamento de Química e Física Molecular, IQSC/USP, CP 780, 13560-970, São Carlos, SP, Brazil

The great interest on porphyrins is due to its useful biochemical and medical applications. The interactions of porphyrins with nucleic acids are of primary importance in photodynamic therapy since DNA is one of the major targets in cancer cells. Several cationic porphyrins are known to bind to DNA in different ways depending on the structure of the porphyrin and the sequence and structure of the DNA. In this work we have used the cationic tetra(N-methyl-4-pyridyl)porphyrin (TMPyP) in the forms of free base, Fe(III) and Mn(III) derivatives in order to assess its interaction with DNA from calf thymus (CT-DNA) using VIS-UV optical absorption spectroscopy. The Convex Constraint Analysis (CCA) method of Fasman et al was used to decompose the optical spectra. In the case of free base and manganese porphyrins a simple two-component equilibrium of free and bound species is observed. The association constant is around 2-5 x 10^4 M^{-1}. In iron porphyrin a complex equilibrium is observed involving aggregation of porphyrin which is dependent on DNA concentration. In this case free porphyrin, aggregated bound porphyrin and monomeric bound porphyrin coexist in equilibrium.

CNPq, FAPESP, FINEP

W-Pos332

KINETICS OF THE OXIDATIVE REACTIONS IN A HEMOGLOBIN - LIPID VESICLE MIXTURE ((Sharron Jenkins and L. W.-M. Fung)) Department of Chemistry, Loyola University of Chicago, Chicago, IL, 60626.

It has been hypothesized that abnormal oxidation of sickle hemoglobin (HbS) might promote the deposit of denatured hemoglobin (metHb, hemichrome, choleglobin) on erythrocyte membranes, decreasing the life time of erythrocytes. We have compared the heme oxidation kinetics of normal adult hemoglobin (HbA) and HbS in the presence of lipid vesicles of phosphatidyleserine. The oxidation studies were carried out at various ionic strengths (from 0 to 110 mM NaCl) and pH values (6.4 & 7.4). Optical measurements of the disappearance of oxyHbA and oxyHbS in the hemoglobin-vesicle reaction mixtures were carried out. Rate constants for the initial disappearance of oxyHemoglobin were obtained. The oxidation rate constants of HbA and HbS under physiological conditions (110 mM NaCl and pH 7.4) were similar. However, the rate constants of HbA and HbS under low ionic strength at pH 7.4 were quite different, with rate constants for HbS being 1.4 times higher than those for HbA. The rate constants of HbA and HbS at low pH (6.4) and low ionic strength were also different, with the rate constants for HbS being 4 times higher than that of HbA. These studies provide insight of the oxidative processes in sickle cells. (Supported by Loyola University of Chicago.)

W-Pos333

CRYSTALLOGRAPHIC STUDIES OF *LUMBRICUS* ERYTHROCRUORIN ((Kristen Strand and William E. Royer, Jr.)) Program in Molecular Medicine and Dept.of Biochemistry and Molecular Biology, University of Massachusetts Medical Center, Worcester, MA 01605 (spon. by T.T. Tibbitts)

Lumbricus erythrocruorin is an extracellular respiratory protein complex located in the hemolymph of the common earthworm, where it functions to transport O_2 and CO_2. It is composed of four unique heme binding chains (**abcd**) which bind O_2, and three linker chains which are required for assembly of the entire molecule. We are investigating the crystal structure of the entire molecule and isolated subunits in order to learn the mechanism for the self-limited assembly of a cooperative complex from more than 200 polypeptide chains. We have recently crystallized the **abcd** assemblage in 2.2 M phosphate buffer, pH 6.7. These crystals show symmetry of the space group $C222_1$ with cell constants of **a**=138.2 **b**=171.1 and **c**=201.2 Å and show diffraction corresponding to at least 2.8 Å resolution . We have also grown crystals in which the Ca^{2+} has been replaced with Gd^{3+} and Ho^{3+}. The modulation of diffraction intensities at different wavelength due to anomalous scattering of these lanthanides will be used to solve the phase problem. The structure of the **abcd** complex will then be fitted into cryo-electron microscopy images of *Lumbricus* erythrocruorin in order to provide initial phases for the whole molecule crystal diffraction data. (Supported by NIH and AHA)

W-Pos334

HIGH RESOLUTION CRYSTAL STRUCTURE OF DEOXY SICKLE CELL HEMOGLOBIN ((D. J. Harrington, K. Adachi, W. E. Royer, Jr.)), University of Massachusetts Medical Center, Worcester, MA 01605 and the University of Pennsylvania School of Medicine, Philadelphia, PA 19104 (spon. by A. Ross)

We have refined the crystal structure of deoxy sickle cell hemoglobin (β6 glu → val) at 2.0 Å resolution to an R-factor of 18 % (free R = 24%) using crystals isomorphous to those originally grown by Wishner and Love. A predominant feature of this crystal form is a double strand of hemoglobin tetramers that has been shown by a variety of techniques to be the fundamental building block of the intracellular sickle cell fiber. The double strand is stabilized by lateral contacts involving the mutant valine interacting with a pocket between the E and F helices on another tetramer. The new structure reveals some marked differences from the previously refined 3.0 Å resolution structure, including several residues in the lateral contact which have shifted by as much as 3.5 Å. The lateral contact includes, in addition to the hydrophobic interactions involving the mutant valine, hydrophilic interactions and bridging water molecules at the periphery of the contact. This structure provides insight into hemoglobin polymerization and may be useful for the structure-based design of therapeutic agents to treat sickle cell disease.

W-Pos335

Resonance Raman Investigations of P450$_{CAM}$ / Putidaredoxin Electron Transfer Complex

((M. Unno,[1] J. F. Christian,[1] D. Benson,[2] N. Gerber,[2] S. G. Sligar,[2] and P. M. Champion[1])) [1] Department of Physics, Northeastern University, Boston, MA 02115; [2] Departments of Biochemistry and Chemistry, University of Illinois, Urbana, IL 61801

Cytochrome P450$_{CAM}$ (P450) accepts two electrons in discrete steps from putidaredoxin (Pdx) in its reaction cycle. In this report we characterize the effects of Pdx binding on P450 using resonance Raman and optical spectroscopies. The complex formation of ferric substrate-bound P450 with oxidized Pdx leads to optical changes, which are characteristic of high-spin to low-spin change. In accordance with this observation, resonance Raman spectrum of the complex shows that Raman intensity for the high-spin marker bands decreases in the presence of Pdx. The effect of Pdx on heme iron–axial ligand (Fe–S) stretching mode was also examined. The Pdx upshifted the mode by ~3 cm^{-1}, as can be seen from the figure. This indicates that the formation of the complex strengthens the Fe–S bond, possibly due to a Pdx-induced conformational change and/or an electrostatic effect of Pdx.

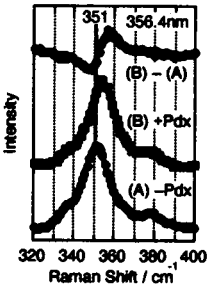

W-Pos336

CHROMOPHORE DESIGN AND PEPTIDE ENGINEERING REQUIREMENTS FOR SYNTHETIC TETRA-α-HELICAL ELECTRON TRANSFER ASSEMBLIES. ((J. A. Baker, V. S.-Y. Lin, F. Rabanal, D. Pilloud, C. Moser, P. L. Dutton, and M. J. Therien)). University of Pennsylvania Department of Chemistry and the Department of Biochemistry and Biophysics, Philadelphia, PA 19104.

Incorporation of synthetic porphyrins and covalently-linked multiporphyrin systems into tetra-α-helical peptide assemblies provide simple experimental constructions in which to study energy and electron transfer in a predesigned anisotropic environment. Work to date has shown that the structure of the tetra-α-helical peptide exerts considerable influence on the types of synthetic systems that can successfully utilize the peptide's available (porphinato)metal axial ligation sites. Equally important for the binding of artificial chromophores to the peptide assembly is the nature of the porphyrin's peripheral substituents. These results are discussed in the context of elucidating the minimal design criteria required for the engineering of new biomimetic analogues for the electron and energy transfer proteins.

W-Pos337

A STUDY OF HEME-HEME AND HEME-PROTEIN INTERACTIONS IN SYNTHETIC PEPTIDES.((J.M. Shifman, F. Rabanal, P.L. Dutton)). The Johnson Research Foundation, Department of Biochemistry and Biophysics, University of Pennsylvania, Philadelphia, PA 19104

The present work is aimed at designing and synthesizing a 4-helix protein bundles capable of binding hemes.The goal is to examine for packing constraints, electrochemical interactions and interheme electron transfer.

A 62 residue helix-loop-helix segment was synthesized and proved to assemble into 4-helix bundles in aqueous environment. The 4-helix bundle was intended to bind four hemes through bis-hystidyl ligations with histidines two turns apart from each other on the alpha helix, at positions 10 and 17, which brings bound heme edges to close proximity.

Steric and electrostatic interactions permit only two hemes to bind in the oxidized state, showing negative binding cooperativity. In the reduced state, when there is no charge repulsion between heme groups , a third, but not a fourth heme binds. These results suggest that the first two hemes bind diagonally to each other at positions 10'an 17 with similar intrinsic Kd values. Spectroscopic characterization of this protein helps to undestand binding affinities and redox properties of each heme site and to improve the present design towards a functional electron transfer center.

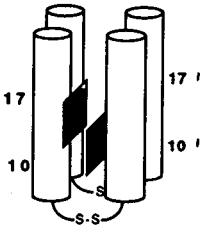

W-Pos338

FAR & NEAR UV TIME-RESOLVED CIRCULAR DICHROISM STUDIES of PROTEIN FOLDING in CARBON MONOXIDE BOUND CYTOCHROME c. ((Eefei Chen, Matthew J. Wood, Sangita Seshadri, Anthony Fink & David S. Kliger)) University of California, Department of Chemistry & Biochemistry, Santa Cruz, California 95064.

Carbon monoxide (CO) bound cytochrome c is an interesting biochemical system where protein unfolding or refolding can be triggered by a photoevent. Time-resolved absorption (TROD) methods have been used to study CO rebinding at the heme group on this system (Jones et. al., (1993) *Proc. Natl. Acad. Sci. USA 90,* 11860), and have demonstrated the potential that this system has for studying protein folding dynamics. We used time-resolved circular dichroism (TRCD) spectroscopy in the near UV to the examine the kinetics of aromatic residue interaction with the heme group after photolysis of the CO, and in the far UV to monitor the resulting changes in secondary structure. Currently, our TRCD results indicate that while the photoevent triggers significant protein refolding it is localized to the region of the heme group. Significant changes in the secondary structure have not been observed. The behaviour of the ground state fluorescence intensity of the tryptophan (Trp, W59) residue, which is located in close proximity to the heme plane, in the CO unbound vs bound form of the reduced cytochrome c supports these TRCD results. Additionally, the results of near UV TROD studies are similar to that for heme-CO. *This work is supported in part by NIH GM-35158 (DSK) and a University of California President's Postdoctoral Fellowship (EC).*

W-Pos339

SPECTROSCOPIC INVESTIGATIONS OF THE HEME COFACTORS AND THEIR ENVIRONMENT IN A CYTOCHROME *b* MODEL ((W. A. Kalsbeck[1], D. E. Robertson[2], F. Rabanal[2], P. L. Dutton[2], R. K. Pandey[3], K. M. Smith[3], and D. F. Bocian[1]))
[1]Department of Chemistry, University of California, Riverside, CA 92521, [2]Johnson Research Foundation, Department of Biochemistry and Biophysics, University of Pennsylvania, Philadelphia, Pennsylvania 19104, [3]Department of Chemistry, University of California, Davis, CA 95616 (Spon. by R. Cardullo)

The structure and protein environment of the heme cofactors in a synthetic cytochrome has been investigated using electronic and resonance Raman spectroscopies. The protein, described by Robertson *et al* (*Nature*, **368**, 425-432 (1994)), binds one heme via bis histidine ligation of the iron atom, the protein dimerizes in solution to form a four helix bundle. Previous work has shown that the two hemes are electrochemically inequivalent, with their redox couples separated by 115 mV. In order to gain a better understanding of the structural and electronic properties of the heme cofactors in the synthetic protein and the nature of the protein environment surrounding these groups, spectroscopic studies were conducted on protein reconstituted with a number of different hemes, including 2- and 4-monovinyl-hemes, symmetric and asymmetric divinyl-hemes, and 2-oxoheme.

W-Pos340

CHARACTERIZATION OF THE IRON-BINDING SITE IN MAMMALIAN FERROCHELATASE BY KINETIC AND MÖSSBAUER METHODS

Ricardo Franco[1], José J.G. Moura[1], Isabel Moura[1], Steven G. Lloyd[2], William Forbes[3], Boi Hanh Huynh[2], and Glória C. Ferreira[3]

[1]Universidade Nova de Lisboa, Portugal

[2]Department of Physics, Emory University, Atlanta, GA

[3]Department of Biochem. and Mol. Biol., USF College of Medicine

All organisms utilize ferrochelatase (protoheme ferrolyase, EC 4.99.1.1) to catalyze the terminal step of the heme biosynthetic pathway, which involves the insertion of ferrous ion into protoporphyrin IX. Kinetic methods and Mössbauer spectroscopy have been used in an effort to characterize the ferrous ion-binding active site of recombinant murine ferrochelatase. The kinetic studies indicate that dithiothreitol, a reducing agent commonly used in ferrochelatase activity assays, interferes with the enzymatic production of heme. Ferrochelatase specific activity values determined under strictly anaerobic conditions are much greater than those obtained for the same enzyme under aerobic conditions and in the presence of dithiothreitol. Mössbauer spectroscopy conclusively demonstrates that, under the commonly used assay conditions, dithiothreitol chelates ferrous ion and hence competes with the enzyme for binding the ferrous substrate. Mössbauer spectroscopy of ferrous ion incubated with ferrochelatase in the absence of dithiothreitol shows a somewhat broad quadrupole doublet. Spectral analysis indicates that when 0.1 mM Fe(II) is added to 1.75 mM ferrochelatase, the overwhelming majority of the added ferrous ion is bound to the protein. The spectroscopic parameters for this bound species are $\delta = 1.36 \pm 0.03$ mm/s and $\Delta E_Q = 3.04 \pm 0.06$ mm/s, distinct from the larger ΔE_Q of a control sample of Fe(II) in buffer only. The parameters for the bound species are consistent with an active site composed of nitrogenous/oxygenous ligands and inconsistent with the presence of sulfur ligands. This finding is in accord with the absence of conserved cysteines among the known ferrochelatase sequences. The implications these results have with regard to the mechanism of ferrochelatase activity are discussed.

W-Pos341

STRUCTURE-FUNCTION OF COBALAMIN DEPENDENT ENZYMES: X-RAY ABSORPTION STUDIES ON METHIONINE SYNTHASE FROM *E. COLI*.

((E. Scheuring[1], S. Huang[2], R. G. Matthews[2], and M. R. Chance[1]))
[1]Department of Physiology and Biophysics, A. Einstein College of Medicine, Bronx, N.Y., 10461, and Biophysics Research Division and Department of Biological Chemistry, University of Michigan, Ann Arbor, MI, 48109.

The first crystallographic data on an enzyme bound cobalamin cofactor, methylcobalamin bound to the 27 kDa fragment of methionine synthase from *E. coli* (Drennan, C. L. et al. *Science*, **1994**, *266*, 1669) revealed dramatic changes in the structure of the cofactor upon enzyme binding. The most striking change is that the 5,6-dimethylbenzimidazole (DMB) group of the cofactor is displaced and replaced by a His group of the enzyme. The DMB base with the sugar phosphate linkage penetrates into a deep pocket of the enzyme to stabilize enzyme binding. His^{759} of the enzyme, bound to the Co atom, is part of a hydrogen bonding network involving Asp^{757} and Ser^{810} residues. Examination of different mutants, affecting the three catalytically important residues, His^{759}, Asp^{757}, Ser^{810}, provides insights into how the enzyme controls the Co-C bond cleavage. X-ray edge results on the Co(II) form of mutant H759G shows that replacing His^{759} with a Gly residue causes the formation of a four-coordinate species with no Gly ligation to the Co. The Co(II) form of mutant D757E, in which Asp^{757} is replaced by Glu, indicates similar geometry to that of the wild-type Co(II). Both mutants have edge positions at significantly lower energies indicating higher electron density on the Co with respect to the wild-type Co(II) form. This work is supported by NIH grants, RR-01633 (M.R.C.) and GM-24908 (R.G.M.).

W-Pos342

Conversion of α-Hydroxyhemin to Verdoheme in Heme Oxygenase. ((K. Mansfield Matera†, S. Takahashi¶, H. Fujii§, H. Zhou‡, K. Ishikawa‡, T. Yoshimura§, D. L. Rousseau¶, T. Yoshida‡ and Masao Ikeda-Saito†)) †Dept. of Physiol. and Biophys. Case Western Reserve Univ., Cleveland, OH 44106, ¶AT&T Bell Labs., Murray Hill, N. J. 07974, §Division of Bioinorg. Chem., Yamagata High-Tech. and Res. Dev. Center, Yamagata 990, Japan, and ‡Dept. of Biochem., Yamagata Univ., Yamagata 990-23, Japan

The α-hydroxyheme-heme oxygenase (HO) complex has been prepared and its active site structure and reactivity were studied. Resonance Raman studies have revealed that the α-hydroxyheme group in the complex exists as a keto-enol tautomer. In the ferric form, the prosthetic group is an oxophlorin where the α–meso hydroxy group is deprotonated, and in the ferrous form, it is a porphyrin with the hydroxy group protonated. Verdoheme is formed either by the reaction of oxygen with the ferrous hydroxyheme complex or by the addition of a reducing equivalent to the ferric complex in the presence of oxygen. It is found that molecular oxygen and one reducing equivalent are required for the conversion of the ferric α-hydroxyheme to verdoheme in the heme oxygenase catalysis.

Supported by NIH GM-51588 & GM-48714.

W-Pos343

THE EFFECT OF WATER IN THE QUANTITATION OF HEMOGLOBIN CONCENTRATION IN A TISSUE-LIKE PHANTOM BY NEAR-INFRARED SPECTROSCOPY.

((S. Fantini, M. A. Franceschini, A. Cerussi, J. S. Maier, S. A. Walker, B. Barbieri*, B. Chance**, and E. Gratton)) Laboratory for Fluorescence Dynamics, Department of Physics, University of Illinois at Urbana-Champaign, Urbana, IL 61801. *ISS Inc., Champaign, IL 61821. **Univ. of Pennsylvania, Dept. Biophys/Biochem., Philadelphia, PA 19104.

The quantitative measurement of tissue oxygenation is of paramount importance to prevent dangerous hypoxic or hyperoxic conditions in ill patients. A non-invasive, accurate, real-time, *in situ* monitor of tissue oxygenation is one of the goals of near-infrared tissue spectroscopy. The quantitative optical oximeter developed so far in our laboratory which operates at 715 and 825 nm assume that the absorption of near-infrared light in tissue is solely due to oxy- and deoxy-hemoglobin. We have investigated the effect of a third chromophore (water) in the quantitative determination of hemoglobin concentration and saturation. Our study consists of *in vitro* measurements on an aqueous solution containing Liposyn, bovine blood, and yeast, pH buffered at 7.2. The optical coefficients of the solution match those of biological tissue in the near-infrared (μ_a~0.03-0.08 cm^{-1}, μ_s'~6 cm^{-1}) and the hemoglobin concentration (23 μM) is also of the same order of magnitude than that in tissue. We were able to reversibly saturate and desaturate hemoglobin in the full range 0-100% by flowing either oxygen or nitrogen through the medium. At these wavelengths we found that the additional absorption of water must be taken into account to obtain accurate results of hemoglobin concentration and saturation. However, the water correction has a small effect on deoxy-hemoglobin concentration, and on hemoglobin saturation in the high saturation limit. Instead oxy-hemoglobin concentration and hemoglobin saturation in the low saturation limit are the parameters most sensitive to water correction. [Supported by NIH grants RR03155 and CA57032.]

W-Pos344

A Technique for Nanosecond Time-Resolved Magnetic Optical Rotatory Dispersion: Application to the Photolysis Intermediates of Myoglobin

((Raymond M. Esquerra, Daniel B. Shapiro, Robert A. Goldbeck, Diping Che and David S. Kliger)) Department of Chemistry and Biochemistry, University of California at Santa Cruz, Santa Cruz, CA 95064.

We present a simple and sensitive technique for nanosecond time-resolved magnetic optical rotatory dispersion (MORD) spectral measurements. This is a pseudo-null technique based on the fact that magnetic rotatory dispersion rotates the plane of linearly polarized light. The theoretical basis of the technique is presented using Mueller calculus and a signal analysis describes the effects of some optical imperfections as well as complications due to the Faraday effect. The accuracy of the technique is demonstrated by comparison of static MORD data collected using this method with the Kramers-Kronig transform of static magnetic circular dichroism (MCD) data. The technique is applied to the rebinding of the carbonyl adduct to horse skeletal myoglobin from nanoseconds to milliseconds following ligand photolysis in both the visible and Soret bands. This work is supported by NIH GM38549.

W-Pos345

INVOLVEMENT OF SUBCELLULAR ORGANELLES IN PHOTOINDUCED CELL DEATH BY HEMATOPORPHYRIN DERIVATIVE.

Rajesh Sreenivasan, Preeti G. Joshi and Nanda B. Joshi, Department of Biophysics, National Institute of Mental Health and Neuro Sciences, Bangalore-29 (India).

Subcellular organelle membranes were isolated from U-87MG cells after treating them with HpD for 1 or 24h. Photoinduced structural changes in the membranes were studied using lipid specific fluorescent probes DPH and TMA-DPH whereas, the functional alterations were assessed by measuring the activities of organelle marker enzymes Na(+)-K(+)-ATPase, succinic dehydrogenage (SDH) and NADPH cytochrome c. The limiting anisotropy of lipid probes showed an increase on light irradiation both in plasma membrane and endoplasmic reticulum(ER) but the increase was more in case of ER after treating the cells with HpD for 24h. The photoinduced inhibition in the Na(+)-K(+)-ATPase was almost same after treating the cells with HpD for 1 or 24 h whereas, NADPH cytochrome c was inhibited completly after 24h of HpD treatment. These results have been correlated with HpD binding and photosenitivity of cells.

W-Pos346

PHOTODYNAMIC ACTION OF MC540 CAUSES STRUCTURAL ALTERATIONS IN PLASMA MEMBRANE OF U-87MG CELLS. Mrinalini Sharma, Preeti G. Joshi and Nanda B.Joshi, Department of Biophysics, National Institute of Mental Health and Neuro Sciences, Bangalore-29 (India).

Photodynamic action of Merocyanine 540 (MC540) on the plasma membrane of U-87MG cells was investigated using lipid and protein specific fluorescent probes TMA-DPH and PM respectively. Steady state anisotropy, decay time and time dependent anisotropy of these probes in cells have been measured. Light irradiation caused a decrease in the steady state anisotropy and decay time of TMA-DPH in cells. The time dependent anisotropy measurements of TMA-DPH in cells were performed and the data were analyzed using wobbling in cone model. Photosensitization of cells caused an increase in the rotational relaxation time, cone angle and a decrease in the order parameter of TMA-DPH. An increase in lipid peroxidation, inhibition of protein SH groups, increase in relaxation time of PM and cross linking of proteins as evidenced by a decrease in excimer to monomer fluorescence intensity ratio of PM was also found. These results can be explained in terms of lipid-protein interactions.

FOLDING AND SELF-ASSEMBLY III

W-Pos347

METAL ION INTERACTIONS WITH ALZHEIMER MODEL PEPTIDES: INDUCED β -SHEET STRUCTURE AND SELECTIVE REVERSIBILITY WITH SILICATES AND CITRATES. ((Su-Hwi Hung and Gerald D. Fasman)) Department of Biochemistry, Brandeis University, Waltham, Massachusetts 02254-9110 (Spon. by Gerald D. Fasman)

Exposure to trace metal ions such as, Al^{3+}, Fe^{3+}, and Zn^{2+} has been proposed as risk factors in Alzheimer's disease (AD). Previous studies demonstrated that sodium orthosilicate reversed the Al^{3+} ion effect of the induction of the β-sheet back to random coil conformation. However, citrate, an Al^{3+} ion chelator, failed to reverse the Al^{3+} effect but did reverse the Ca^{2+} ion effect on the conformational change of the unphosphorylated and phosphorylated NF-M 13 and NF-17 peptides. In order to characterize the reversibility by sodium orthosilicate and citrate on the metal ion effects on the model Alzheimer peptides (phosphorylated and unphosphorylated NF-M13), circular dichroism (CD) studies were carried out to examine the effect of sodium orthosilicate and citrate on the conformational state induced by various metal ions: Al^{3+}, Fe^{3+}, Mg^{2+}, Ca^{2+}, Mn^{2+}, Fe^{2+}, Cu^{2+} Zn^{2+}, Pb^{2+} on the phosphorylated and unphosphorylated peptides. Our results showed that silicates selectively reversed the effect of Al^{3+}, Fe^{3+}, and Ca^{2+} on the induction of the β-sheet structure of model Alzheimer peptides (NF-M13), and their phosphorylated species. Silicates did not reverse the effect Mg^{2+}, Mn^{2+}, Fe^{2+}, Cu^{2+}, Zn^{2+}, and Pb^{2+} on the induction of partial β-sheet of the phosphorylated NF-M13 peptides. It is suggested that silicates should be investigated for their therapeutic use in treating Alzheimer patients. (Research supported by a NIH grant).

W-Pos348

COMPARISON OF NMR AND MOLECULAR MODELING RESUTLS FOR A RIGID AND A FLEXIBLE OLIGOSACCHARIDE ((Qiuwei Xu, Rossitza Gitti and C. Allen Bush)) Department of Chemistry & Biochemistry, University of Maryland Baltimore County, Baltimore, MD 21228.

We show that antiphase methods for measuring $^3J_{CH}$ in oligosaccharides have limited reliability but that the coupling constants can be reliably measured in natural abundance by quantitative J-correlation methods. Interpretation of $^3J_{CH}$ data for a pentasaccharide (lacto-N-fucopentaose 2) from human milk are consistent with a rigid model for the Lewis^a trisaccharide epitope but for an antigenic tetrasaccharide fragment from the cell wall polysaccharide of viridans streptococci, $^3J_{CH}$ data imply a considerably more flexible model. Nuclear Overhauser effect (NOE) data are reported for a heptasaccharide repeating unit isolated from the cell wall polysaccharide of *Streptococcus gordonii* 38. The results for a tetrasaccharide fragment are similar to data reported for the same fragment in the cell wall polysaccharide from *S. mitis* J22. This result implies a similar conformation for the tetrasaccharide fragment in the polysaccharide and in the heptasaccharide and also implies that anisotropy of motion is not significant in the interpretation of the nuclear Overhauser effects in the polysaccharide. Interpretation of the NOE results for the tetrasaccharide fragment, like the $^3J_{CH}$ data, implies a flexible model with three conformations in fast exchange. The results of the two experimental techniques are combined with molecular modeling results including molecular dynamics simulation to provide a clear delineation between flexible and rigid oligosaccharide epitopes. The blood group Lewis^a trisaccharide antigenic determinant is highly restricted in its motions by steric interactions while the antigenic tetrasaccharide fragment of the *S. gordonii* 38 heptasaccharide is considerably more mobile. We propose that some branched oligosaccharides are relatively rigid and some are flexible depending on subtle details of the linkages.

W-Pos349

MIMICRY OF THE CALCIUM-INDUCED CONFORMATIONAL STATE OF TROPONIN C BY HIGH PRESSURE AND LOW TEMPERATURE. ((D.Foguel, M.D.Suarez, C. Barbosa, M. Sorenson, L. B. Smillie* and J. L. Silva)) Depart.of Biochem, Federal University of Rio de Janeiro 21941-590, RJ, Brasil and * Depart. of Biochem., University of Alberta, Edmonton, Alberta, Canada T6G 2H7. (Spon. by CNPq, FAPERJ, EEC, CAPES, FINEP, PADCT).

Calcium binding to the N-domain of troponin C (TnC) initiates a series of conformational changes that lead to muscle contraction. In one hypothesis, Ca^{2+} binding provides the free energy for a hydrophobic region in the core of N-domain to assume a more open configuration. Steady-state fluorescence measurements on a tryptophan mutant (F29W) of the N-domain of chicken skeletal muscle TnC show that a similar conformational change occurs in the absence of Ca^{2+} when the temperature is lowered to -11 ^oC at 2.2 kbar pressure. The conformation induced by low temperature binds the hydrophobic probe bis-ANS, and the tryptophan has the same fluorescence lifetime (7 nanoseconds) as the Ca^{2+} bound form. The decrease in volume (-25.4 ml/mol) correspond to an increase in surface area, as predicted by the model. The thermodynamic parameters obtained from measurements at different teperatures and pressure suggest an enthalpy-driven conformational change that leads to an intermediate with an exposed N-domain core. This form is stabilized by the free energy from Ca^{2+} binding.

W-Pos350

Trifluoroethanol-induced β-sheet→α-helix→intermolecular β-sheet structural transition in β-proteins [(J.F. Carpenter and A. Dong)] Dept. of Pharmaceutical Sciences, University of Colorado Health Sciences Centers, Denver, CO 80262 and Dept. of Chemistry, University of Northern Colorado, Greeley, CO 80639.

Trifluoroethanol (TFE) is known to induced α-helical structure in non-helical peptides and proteins and has been used widely to probe α-helical propensity for potential transmembrane segment of proteins. However, the relative stability of the TFE-induced α-helical structure in non-helical proteins has not been studied. In the present study, we have monitored the stability of TFE-induced α-helix in β-lactoglobulin, trypsin, and α-chymotrypsin as a function of time using Fourier transform infrared (FT-IR) spectroscopy. Immediately after dissolving the lyophilized protein powder in 50% TFE/10 mM KPO_4, pH 7.3, at concentration of 10, 20, and 30 mg/ml, a strong band component at 1655 cm^{-1} assignable to α-helix in the conformationally-sensitive amide I region was observed. The intensity of the 1655 cm^{-1} band decreased as a function of time, concomitant with appearance and intensification of two new bands at 1617 and 1695 cm^{-1}, a typical band pattern associated with intermolecular β-sheet aggregates. A clear gel was formed in all three proteins under this condition. Similar spectral changes at much slower rate were also observed for deuterated protein samples at lower concentration (2 mg/ml protein in 50% TFE-d_3). These results suggest that the TFE-induced α-helix in non-helical proteins in extremely unstable and readily converts to an intermolecular β-sheet structure.

W-Pos351

CORRELATION OF INFLUENZA VIRUS FUSION AND INACTIVATION WITH CONFORMATIONAL CHANGES IN HEMAGGLUTININ. ((T. Shangguan[1], D. P. Siegel,[2], J. D. Lear[3], P. Axelsen[4], D. Alford[5] & J. Bentz[6])) [1]The Liposome Co., Inc., Princeton, NJ 08540,[2]Procter & Gamble Co., Cin. OH 45253, [3]Dept. Biochem. & Biophys.& [4]Dept. Pharmacol., U. of Pennsylvania, Phil. PA 19104, [5]Center for Blood Res., Boston MA 02115, [6]Dept. Biosci. Biotech, Drexel Univ., Phil. PA 19104,

We studied the fusion of A/PR/8/34 influenza virus with ganglioside (GD1a)-bearing liposomes at pH 4.9 and 30°C, using the CPT/DABS lipid mixing assay. A pre-binding step was introduced to achieve lipid mixing rate-limited kinetics. The rate of viral inactivation at pH 4.9 was indicated by differences in the initial lipid mixing rate and in the final extent of lipid mixing for virus that was preincubated at pH 4.9 for different intervals, reneutralized, bound to target liposomes, and re-acidified. We made cryoelectron microscopy (Cryo-TEM) specimens of virions exposed to pH 4.9 for the same intervals at 30°. Virus preincubated for 2 or 10 minutes at pH 4.9 retained extensive lipid mixing activity, with only ca. 30-40% inactivation after 10 min. By 30 min lipid mixing activity was drastically reduced, and was absent by 60 min. Cryo-TEM showed that, relative to virus at pH 7, no major conformational changes occurred in the HA spikes of the virus until after 10 min at pH 4.9. Spike layers were mostly disordered after 30 min, and completely disordered after 60 min. Molecular models show that formation of the hypothetical coiled-coil structure by native HA would break the HA1-HA1 contacts in the trimer and introduce motional freedom in that part of the spike, drastically changing spike appearance in cryo-TEM. No such change was observed in virus preincubated at pH 4.9 on the time scale of lipid mixing in virus/liposome mixtures at pH 4.9. This suggests that neither formation of coiled-coil HA, nor perhaps any drastic conformational change in HA, is a precursor to HA-induced lipid mixing.

W-Pos352

CONTRACTION OF FILAMENTOUS PHAGE BY CHLOROFORM: IMPLICATIONS FOR MOLTEN GLOBULAR INTERMEDIATES IN VIRAL UNCOATING ((A. K. Dunker, J. L. Uehara, and J. Oh)) Dept. of Biochemistry & Biophysics, Washington State University, Pullman, WA 99164

Interaction of the fd filamentous phage with a chloroform/water interface induces an approximately 3-fold reduction in length, leading to rod-shaped, I-form particles. Further contraction to spheroidal-shaped, S-form particles is associated with DNA release. A deeper understanding of the chloroform-induced contraction should provide insight into the phenomenon of virus uncoating. Previous studies from our laboratory suggest that the I-form and S-form particles have properties in common with protein folding intermediates known as molten-globules; the cardinal feature of molten globules - their nonrigid side chain packing, which leads to flexible tertiary structure - would be an ideal characteristic for the process of viral uncoating (Dunker et al., FEBS Lett 292: 275, 1991; Roberts and Dunker, Biochemistry 32, 10479, 1993). To further probe chloroform-induced contraction, we are isolating and characterizing chloroform-resistant mutants. Three different mutants have been isolated so far - H5D, L31V, and T37I. The same mutations were formed by site-directed mutagenesis in the absence of chloroform selection and all exhibited chloroform resistance, suggesting that these amino acid changes alone are responsible for chloroform resistance. Charge imbalance plays a key role in the formation of molten globules when these folding intermediates are induced at low or high pH; pH profiles of chloroform resistance for each of the mutants indicate charge imbalance of the phage coat protein also plays a key role in the contraction mechanism. Indeed, if chloroform induces fd phage to form molten globular intermediates, then low and high pH treatment of wild type fd phage in the absence of chloroform should also yield I-forms and S-forms at appropriate temperatures and ionic strength. This prediction appears to hold except that intermediates between filaments and I-forms also appear at high pH.

W-Pos353

THE VOLUME CHANGES OF THE MOLTEN GLOBULE TRANSITIONS OF HORSE HEART FERRICYTOCHROME C: A THERMODYNAMIC CYCLE. ((Kira Foygel, Shari Spector, Sukalyan Chatterjee, and Peter C. Kahn)) Rutgers University, New Brunswick, NJ 08903.

The volume changes among the unfolded (U), native (N), and molten globule (MG) conformations of horse heart ferricytochrome c have been measured. U to N (pH 2 to pH 7) was determined in the absence of added salt to be -136 ± 5 mL/mole protein. U to MG (pH 2, no added salt to pH 2, 0.5 M KCl) yielded +100 ± 6 mL/mole. MG to N was broken into two steps, N to NCl_x at pH 7 by addition of buffered KCl to buffered protein lacking added salt (NCl_x = N interacting with an unknown number, X, of chloride ions), and MG to NCl_x by jumping MG at pH 2 in 0.5 M KCl to pH 7 at the same salt concentration. The ΔV of N to NCl_x was -30.9 ± 1.4 mL/mole protein, while MG to NCl_x entailed a ΔV of -235 ± 6 mL/mole. Within experimental error the results add up to zero for a complete thermodynamic cycle. We believe this to be the first volumetric cycle to have been measured for the conformational transitions of a protein. The results are discussed in terms of hydration contributions from deprotonation of the protein, other hydration effects, and the formation and/or enlargement of packing defects in the protein's tertiary structure during the steps of folding. In addition, the ΔVs of the pH jump legs depend sensitively upon the initial pH, and the cycle is also sensitive to the protein concentration. These unexpected results are also presented and discussed.

W-Pos354

EFFECT OF CYCLODEXTRINS ON AGGREGATION AND REFOLDING OF PROTEINS IN MOLTEN GLOBULE STATE. ((J. Horsky and J. Pitha)) NIA, NIH, Baltimore, MD 21224 (Spon. by J. Horsky)

Cyclodextrins (CDs), cyclic oligosaccharides, were recently suggested for reducing protein aggregation because unlike other agents usually used for this purpose CDs bind exclusively to aromatic amino acid residues. Protein aggregation may lead ultimately to precipitation, however, the decrease in protein activity is often more important. Here, we report the results indicating the difference between the effect of CDs on the protein solubility and on renaturation/refolding. We investigated the effect of hydroxypropyl β-cyclodextrin (HPBCD) on three proteins (containing aromatic amino acid residues) in the molten globule state at low pH. (i)The solubilities of α-Lactalbumin (aL) and Ribonuclease A (RNA) increased almost linearly with HPBCD concentration. Application of the denaturant binding model to solubility analysis provided estimates of HPBCD binding constants per site of 2.3 M^{-1} and 1.4 M^{-1} for aL and RNA, respectively. These constants are lower then values for binding between HPBCD and aromatic amino acids. (ii) The extent of the renaturation of ß-Lactamase (bL) decreased with the time bL spent in the molten globule state. In spite of the fact that this decrease is caused by aggregation the extent of bL renaturation decreased identically in the presence and in the absence of HPBCD. (iii) Theoretical analysis shows that although no protective effect of HPBCD was observed in the renaturation experiment the effect of HPBCD on bL aggregation might be comparable to that found in solubility experiments. The increase in protein solubility is given by the increased concentration of all types of aggregates in solution; only reversible aggregates and/or non-aggregated molecules are relevant for renaturation.

W-Pos355

OSMOLYTE INDUCED A-STATE FORMATION

((Aleister J. Saunders[1], Jennifer L. Marmorino[2], and Gary J. Pielak[2])) Departments of Biochemistry & Biophysics[1] and Chemistry[2], University of North Carolina at Chapel Hill, Chapel Hill, NC, 27599.

Acid-denatured cytochrome *c* substantially refolds in the presence of nonionic osmolytes (glucose, sucrose, trehalose, and glycerol) alone. Like the salt-induced state, this osmolyte-induced state has spectroscopic properties indicative of an A-state or "molten globule" conformation. Comparisons of far-UV circular dichroism (CD) spectra, for both the salt- and osmolyte-induced A-states, indicate native-like amounts of secondary structure. Tertiary structure in both A-states is disrupted as judged by near-UV and visible CD spectra. These results suggest that salt-induced charge screening is not the only mechanism for A-state formation. Removal of osmotically labile solvent may be sufficient to drive A-state formation.

W-Pos356

A THEORETICAL INVESTIGATION ON BINDING OF IONIC SURFACTANTS TO PROTEINS. ((A.K. Bordbar, A.A. Saboury and A.A. Moosavi-Movahedi)) Institute of Biochemistry & Biophysics, University of Tehran, Tehran, Iran. & Dept. of Chemistry, Tarbiat-Modarres University, Tehran, Iran.

Macromolecular binding of ionic surfactants can lead to some conformational changes in tertiary structure of proteins. So study the process of binding can help us to obtain a better underestanding of surfactant denaturation and conformational stability of proteins. In this article the theoretical approaches of Wyman-Jones and Hill-Tanford on binding of ionic surfactants to water soluble proteins have been investigated and modified. This modification caused that the estimation of intrinsic and statistical Gibbs free energy of electrostatic and hydrophobic binding become possible. The trend of variation of these thermodynamical binding parameters with respect to Hill coefficient discussed and the differences between these two approaches have been investigated. These modified theories have been applied for analysis of the binding data for interaction of sodium n-dodecyl sulphate to lysozyme and ribonuclease A.

W-Pos357

MONOCLONAL EPITOPE LOCALIZATION: IMPLICATIONS FOR SODIUM CHANNEL STRUCTURE ((Sylvia Kolibal, Sabu George, Candace Brady, Weijing Sun, and Sidney A. Cohen)) University of Pennsylvania School of Medicine, Philadelphia, PA 19104.

We localized the epitopes for 28 monoclonal antibodies (mAbs) generated against purified rSkM1 sodium channel protein using immunoblotting of fusion proteins containing various channel segments. Five major immunogenic regions were identified: the origin of the N-terminus, the ID 1-2 region, the mid-ID 2-3 region, the far-ID 2-3 region, and the C-terminus. No antibodies had epitopes in the ID 3-4 region. A map of antibody binding sites obtained from competition studies using metabolically labeled monoclonal antibodies (J Neurochem **48**:773-778, 1987) was reexamined with knowledge of the antibody epitopes. The antibody topology map confirms several aspects of our recent model of sodium channel cytoplasmic domain structure (JBC **270:** 22271-22276). These data also suggest that the early N-terminus is closer (<3.5 nm distance) to the distal-ID 2-3 region than to the mid-ID 2-3 region and that segments of the relatively long ID 1-2 region extend >3.5 nm away from each of the other channel cytoplasmic segments. Therefore: 1) immunogenic regions of the sodium channel are all cytoplasmic, located on four of the five sodium channel cytoplasmic segments; 2) the topology of monoclonal epitopes provides independent support for our model of the structure of sodium channel cytoplasmic domains; and 3) the ID 3-4 segment, modeled to be involved in channel inactivation, has a low surface probability and/or antigenicity, consistent with its short length and proposed interaction with the channel's cytoplasmic surface.

W-Pos358

REGULAR DISTRIBUTIONS OF ACYL CHAINS IN BINARY LIPID SYSTEMS

((Daxin Tang, S.-Y. Simon Chen and B. Wieb Van Der Meer)) Department of Physics and Astronomy, Western Kentucky University, Bowling Green, KY 42101.

The lateral distribution of acyl chains in two binary lipid systems was studied by steady-state fluorescence intensity and anisotropy. These two binary lipid systems were constituted from DMPC/DPPC, and DPH-propionic acid/DMPC. The former system is a mixture of a two-chain lipid with a two-chain lipid, the latter is a mixture of a two-chain lipid with a one-chain lipid. Some strong fluorescence quenching was found at critical concentrations that can be predicted from mathematical equations. The observation implies that a stable hexagonal super-lattice distribution in the matrix of the acyl chains of host molecules is formed at critical concentrations. This regular acyl chain distribution in the mixture of DMPC and DPPC appeared not only in the liquid-crystalline phase but also in the gel phase. A similar phenomenon was also observed in mixtures of DPH-propionic acid/DMPC above the phase transition temperature of DMPC. This work is supported by NASA (NCCW-60).

W-Pos359

FREE ENERGY DETERMINANTS OF α-HELIX INSERTION INTO LIPID BILAYERS AND HELIX-HELIX INTERACTIONS IN THE BILAYER. ((N. Ben-Tal, A. Ben-Shaul, and B. Honig)) Columbia University. (Spon. by A. Palmer)

The insertion of a helix into a lipid bilayer is driven by nonpolar (hydrophobic) interactions. Electrostatic desolvation effects, interactions of the helix with the lipid tails in the bilayer (lipid perturbation), and the confinement of the helix motion in the membrane (immobilization effect) oppose insertion. We calculated the nonpolar and electrostatic contributions to the free energy of insertion of helices into lipid bilayers, using continuum models, and estimated the effects of lipid perturbation and immobilization based on microscopic model for lipid organization. Two configurations of a membrane-bound 25-polyalanine helix were found to be lower in free energy than the isolated helix in the aqueous phase. The first corresponds to the case of complete vertical insertion where the helix termini protrude from either side of the bilayer. The free energy calculated for this configuration is in good agreement with the measured one. The second minimum is for the case of horizontal insertion where the helix is adsorbed on the surface of the bilayer. Our results suggest that helices are inserted by first adsorbing in a horizontal configuration, and then having one terminus "swing around" so as to penetrate the bilayer. Concerning helix-helix interactions, an anti-parallel orientation is much more stable than a parallel orientation when the helix termini are inside the membrane. However, it is sufficient for them to protrude a few Å from the two ends of the bilayer for their dipole-dipole interaction to diminish almost completely.

W-Pos360

(Moved to Su-AM-H10)

W-Pos361

SEDIMENTATION EQUILIBRIUM ANALYSIS OF TRANSMEMBRANE HELIX-HELIX INTERACTIONS. ((K.G. Fleming and D.M. Engelman)) Yale University, Department of Molecular Biophysics and Biochemistry, New Haven, CT 06520-8114.

Our goal is to advance the molecular understanding of the specific packing interactions important for the determination of membrane protein tertiary and quaternary structure. A major focus has been the development of techniques using the transmembrane domain of erythrocyte glycophorin A as a model system for membrane protein helix-helix interactions. We have begun a program to evaluate transmembrane helix-helix interactions in detergent solutions using the analytical ultracentrifuge. Sedimentation equilibrium experiments have been done in both denaturing and non-denaturing detergent solutions. We have used the calculated buoyant density factor as well as density matching techniques to analyze our concentration *versus* radius equilibrium distributions in order to obtain the protein molecular weight and association state. We anticipate that these techniques will be widely applicable to other transmembrane protein systems.

W-Pos362

MEMBRANE INSERTION AND GLYCOSYLATION OF TRUNCATION MUTANTS OF BOVINE OPSIN. ((J.A.W. Heymann and S. Subramaniam)) Johns Hopkins University School of Medicine, Baltimore, MD 21205.

We have investigated the structural requirements for membrane insertion, glycosylation and transport to the cell surface of a multispanning transmembrane protein using bovine opsin as a model system. Mutants of bovine opsin were constructed by progressive truncation of the protein from the C-terminus resulting in opsins containing the first 5, 3, 2, 1.5 or 1 transmembrane (TM) segment(s) of the 7 helices of wild-type opsin. All mutant and wild-type opsins were transiently expressed in COS-1 cells at comparable levels. Wild-type opsin was glycosylated at the N-terminus and transported to the cell surface whereas all mutants were localized in the endoplasmic reticulum. As expected from their localization, the mutants with 2, 3 or 5 TM segments displayed high-mannose type *N*-glycosylation, and could be extracted from membranes by the non-ionic detergent n-dodecyl maltoside. Despite its extractability, the extent of glycosylation in the mutant with 2 TM segments was typically lower and subject to variation. The mutants containing 1 or 1.5 TM segments were not glycosylated and could not be extracted from membranes except under denaturing conditions. None of the mutant opsins could be extracted by 4M urea or under alkaline conditions (pH ~ 11) demonstrating that all the mutants were integral membrane proteins. These results show that the first 5 TM segments are not sufficient for transport and that glycosylation requires at least the first two TM segments. The lack of glycosylation with 1 and 1.5 TM segments may be due to an inverted membrane topology. (This work was supported by the Deutsche Forschungsgemeinschaft (to J.H.) and the National Institute of Health (to S.S.))

W-Pos363

CALORIMETRIC DISCOVERY OF A SUB-MAIN TRANSITION IN LONG-CHAIN PHOSPHATIDYLCHOLINE LIPID BILAYERS

K. Jørgensen
[1]Department of Physical Chemistry, The Technical University of Denmark, DK-2800 Lyngby, Denmark

The existence of a sub-main transition in multilamellar bilayers composed of long-chain saturated diacyl phosphatidylcholine ($DC_{17}PC$, $DC_{18}PC$, $DC_{19}PC$, and $DC_{20}PC$) is reported for the first time using high-sensitivity differential scanning calorimetry. The highly cooperative sub-main transition which takes place over a narrow temperature range positioned between the well-known pre-transition and main-transition is characterized by a heat capacity curve with a half height width of $\Delta T_{1/2} \sim 0.15°C$ and an enthalpy change, ΔH, which is a few percent of the transition enthalpy for the main-transition of the lipid bilayer.

W-Pos364

THE VAPOR PRESSURE PARADOX -- POSTULATED, FORMULATED AND OBSERVED.

((Rudi Podgornik, Adrian Parsegian; Nola Fuller, Peter Rand)) Brock Univ., NIH, Bethesda, MD; St. Catharines, ON.

A perpetually troubling phenomenon in lipid physics is the repeated observation that multilamellar phases often imbibe more water in aqueous solutions than they do when bounded by an air/water interface or are attached to a solid substrate. One postulated explanation for this "vapor pressure paradox" is that the surface energy of high-energy surfaces suppresses the lamellar undulations that enhance the swelling pressure of hydration or electrostatic double layer forces. A recent formulation (J. de Phys. II 2:487 (1992), Biophys.J. 68(2):A341 (1995)) suggested that this suppression can reach into a multilayer to macroscopic distances, on the order of the longest wavelengths of undulations along the multilayer surface -- even developing to millimeters in carefully formed samples.

This is observed. By x-ray diffraction we watch spacings in hydrated lipid multilayers after creation of a vapor space within. Over a period of days, the initial uniform spacing of lipids disappears. Near the vapor, the bilayer separations decrease by several Angstroms compared to the original spacing. A gradient of spacings develops to a depth of several millimeters from the vapor interface, after and beyond which no significant change is seen. The long time of evolution is possibly due to the spreading of coherent domains to lower the energy of the air/multilayer surface. Generalizations to consideration and observation of linear molecules are under way.

W-Pos365

THE SOLVENT EFFECTS ON THE CONFORMATIONAL INTERCONVERSION OF A POLYPEPTIDE AND THEIR IMPLICATIONS FOR MEMBRANE PROTEINS IN A LIPID ENVIRONMENT

((Xu, F., Wang, A., Vaughn, J., Cross, T.)) Department of Chemistry, Florida State University, Tallahassee, FL 32306-3006

It's still largely unknown how the lipid environment modulates membrane protein function through lipid-protein interactions. In an attempt to understand the process, we have investigated the solvent-dependent conformational behavior of a polypeptide, Gramicidin A (GA), in a variety of solvent systems. While the non-specific bulk solvent effects generally dictates the overall conformational distribution at equilibrium, the specific solvent effects, which usually involves H-bonding, promote the conformational interconversion process, hence serving the role of a solvent catalyst. GA exists in several conformational forms in nonpolar solvents such as dioxane, which serves as a kinetic trap to maintain the conformations present. On the other hand, the addition of 1% alcohol by volume will enhance the rate of the conformational interconversion into a dominating anti-parallel double helix by several orders of magnitude. These observations suggest that in the lipid environment, small molecules such as water may play a pivotal role in inducing the functional conformation of membrane proteins.

W-Pos366

THE RELATIVE ORDER OF HELICAL PROPENSITY FOR AMINO ACIDS IN POLYPEPTIDES CHANGES WITH SOLVENT ENVIRONMENT.

((C. Krittanai and W.C. Johnson, Jr.)) Department of Biochemistry and Biophysics, Oregon State University, Corvallis, OR 97331

The 16 residue polypeptide sequences, Y-$(VAXAK)_3$ with 20 amino acid substitutions at the X position, were studied with circular dichroism in a water-methanol environment. All the sequences demonstrate a random coil conformation in sodium phosphate buffer, and adopt the alpha helical conformation in methanol. Titration of these polypeptides in buffer with methanol shows a two-state transition with an equilibrium at each point between random coil and helix. This gives us a free energy of helix stability (ΔG^0) as a function of methanol concentration, which is a measurement of helix propensity. We find that the relative order of helix propensity for the 20 amino acids are different in water and methanol, supporting the implication that helical propensity of amino acids changes according to the environment.

W-Pos367

Conformational Interconversion of a polypeptide Induced by "Catalytic' Solvent

Anping Wang, Feng Xu, Jeoseph Vaughn and T. A. Cross*
National High Magnet Field Laboratory and Florida State University

Polypeptide conformational interconversion is hindered in hydrophobic environment such as a lipid bilayer due primarily to the increased stability of electrostatic interactions. The addition of certain solvent, such as protic solvent can dramatically increase the conformational interconversion rate. These effects are illustrated with the polypeptide gramicidin A in an organic solvent, by monitoring conformational changes as a function of solvent. In organic solvent it is known that gramicidin can be found in a variety of specific conformational states. Numerous specific solvent peptide interactions have been observed with the ROESY experiment.

A new concept of catalytic solvent is presented here, which very much improve in the understanding of protein solvation in general and of conformational interconversion of gramicidin A in organic solvent. Catalytic effect in the conformational interconversion is probed by monitoring the conformational changes with and without the catalytic solvent. From the ROESY experiment, it is clear that solvent ethanol strongly interact with Val-6 NH which made the first bridging hydrogen bond with Leu-14 CO, provide evidence of initiation site of conformational interconversion. The catalytic activity is expected to occur via inducing hydrogen bond exchanges. Also, study of the specific solvent-peptide interaction on the peptide surface, instead only consider bulky solvent effect, improve the understanding of protein solvation and function in organic solvent.

W-Pos368

SOLVATION ENERGIES OF AMINO ACID RESIDUES AND SALT-BRIDGES IN PROTEINS.

((William C. Wimley[†], Trevor P. Creamer[§], Klaus Gawrish[‡] and Stephen H. White[†])) [†]Department of Physiology and Biophysics, University of California, Irvine, CA, 92717. [§]Department of Biophysics and Biophysical Chemistry, Johns Hopkins University School of Medicine, Baltimore, MD 21205. [‡]Membrane Biophysics and Biochemistry Lab, NIAAA,NIH, Bethesda, MD 20892

A proper solvation energy scale is important for understanding protein folding. At present, experimental solvation energy scales are invariably based on the partitioning of small model compounds that approximate fully exposed single residues. The amino acids of unfolded proteins, however, differ from the model compounds because they are flanked by neighboring sidechains and because they are linked to a polypeptide backbone. A new, experimental solvation energy scale is introduced that was determined in a peptide system which is a more appropriate model of unfolded proteins. The scale gives both sidechain and backbone solvation energies as well as the solvation energies of salt bridges. It is based on the water to octanol partitioning of two families of peptides: A complete set of host-guest pentapeptides of the form AcWL-X-LL and a set of peptides of the form $AcWL_n$ (n=1-6). The largest differences between the pentapeptides and the model compounds are seen in the polar residues, which are more hydrophobic in the pentapeptide system. However, the favorable solvation energy of the backbone makes the whole-residue solvation energy favorable for all but the large hydrophobic residues. We show that salt bridge formation cancels the solvation energy cost of the charged sidechains so that the solvation energy of a salt bridge is essentially zero. The total solvation free energy of folding for a set of proteins of known structure will be examined using this scale.

W-Pos369

PERTURBATION OF WATER STRUCTURE BY AMINO ACID SIDE CHAINS ((A. Pertsemlidis[a], A.M. Saxena[b], A.K. Soper[c], T. Head-Gordon[d], and R.M. Glaeser[a,d])) [a]University of California at Berkeley, [b]Brookhaven National Laboratory, [c]Rutherford Appleton Laboratory, United Kingdom, [d]Lawrence Berkeley National Laboratory. (Sponsored by R.M. Glaeser)

Neutron scattering techniques are used to determine the scattering profiles for aqueous solutions of hydrophobic and hydrophilic amino acid analogs. Solutions of hydrophobic solutes show unexpected differences from pure water in a range of scattering angles associated with the structure of water. Half-molar solutions of N-acetyl-leucine-amide and isobutanol cause the peak of the water ring to shift slightly to smaller angle, an effect that is clearly seen as a positive-negative ripple under the water ring when the scattering from pure water is subtracted from the scattering by the aqueous solution. Solutions of hydrophilic solutes, N-acetyl-lysine-amide and N-acetyl-glutamine-amide, do not show this shift in the water ring, however. This difference in behavior for solutions of hydrophobic and hydrophilic side chains is predicted by molecular dynamics simulations. The observed peak shift in the characteristic water ring provides new evidence for the widely held view that the water of hydration around hydrophobic solutes is organized in a different way than bulk water.

W-Pos370

COMPARISON OF VINCRISTINE-, VINBLASTINE- AND VINORELBINE-INDUCED PC-TUBULIN SELF-ASSOCIATION ((Sharon Lobert+, Bojana Vulevic++, and John J. Correia++)) +School of Nursing and ++Department of Biochemistry, University of Mississippi Medical Center, Jackson, MS, 39216

Vinca alkaloids are important chemotherapeutic agents currently used in cancer therapy. They are known to induce tubulin self-association and their effects have been described using a ligand-mediated isodesmic model and Wyman linkage. We have previously reported enhancement of vinblastine-induced tubulin self-association by GDP compared to GTP (Lobert et al., 1995, **Biochemistry** 34, 8050-8060). In these studies binding affinities were determined from sedimentation velocity data fit with ligand-mediated or combined ligand-mediated plus -facilitated models (Na & Timasheff, 1986, **Biochemistry** 25, 6214-6222). We have now carried out similar experiments with two other vinca alkaloids, vincristine and vinorelbine. We find the same extent of GDP enhancement with both these drugs (mean 0.85 kcal M^{-1}). Additionally we find that the overall affinity is highest for vincristine and lowest for vinorelbine, with vinblastine falling in between. This difference in vinca alkaloid interactions with tubulin correlates with the weekly clinical dosage of these drugs. Most interestingly, we find that the drug affinity for tubulin heterodimers, K_1, is, within error, identical for all 3 drugs (range 1.0×10^5- 1.9×10^5 M^{-1}). The main difference is in K_2, the affinity of liganded heterodimers for polymers. Supported by NR00056 (S.L.) and BIR9216150 (J.J.C.).

W-Pos371

THERMODYNAMICS OF MICROTUBULE ASSEMBLY: THE ROLE OF NUCLEOTIDE HYDROLYSIS ((B. Vulevic* and J.J.Correia*)) *Department of Biochemistry, University of Mississippi Medical Center, Jackson, MS 39216

Microtubule polymerization was studied as a function of nucleotide content. The thermodynamic parameters of tubulin assembly with GMPCPP(a weakly hydrolyzable analog), GMPCP- and GTP-2 M glycerol (glycerol decreases critical concentration) were obtained together with data for taxol-GTP/GDP assembly in Pipes (30-100 mM), 1 mM $MgCl_2$, 2 mM EGTA, pH 6.9. All the processes are characterized by positive enthalpy, entropy and negative heat capacity change. GMPCP induced assembly has the largest negative heat capacity, GMPCPP second largest, while GTP and taxol have more positive values respectively. This corresponds to a larger release of water in the case of polymerization with GMPCP and GMPCPP. Thermodynamic analysis suggests that in the absence of hydrolysis, assembly occurs via rigid body association and that taxol induced polymerization includes protein conformational changes. Nucleation is least favorable for GMPCP-tubulin assembly and most favorable for taxol- and GMPCPP- tubulin assembly. We propose that GTP hydrolysis and taxol promote changes in tubulin folding and surrounding water structure that promote microtubule closure.

W-Pos372

SEDIMENTATION VELOCITY AND LIGHT SCATTERING STUDIES OF VINCA ALKALOID-INDUCED TUBULIN SELF-ASSOCIATION ((Sharon Lobert*, Anthony Frankfurter+ and John J. Correia++)) *School of Nursing and ++Dept. of Biochemistry, Univ. of MS Medical Center, Jackson, MS 39216 and +Dept. of Biology, Univ. of Virginia, Charlottesville, VA 22901.

We have purified αβ-II and αβ-III tubulin using sequential immunoaffinity columns and compared vinca alkaloid (vincristine, vinblastine and vinorelbine) -induced isotype self-association by sedimentation velocity. Data were fit with an isodesmic ligand-mediated or ligand-mediated plus -facilitated model to obtain binding affinities. In the presence of vincristine, αβ-III tubulin self-associates less readily than PC-tubulin or αβ-II tubulin ($\Delta G = 0.35$ kcal-M^{-1}). This difference is not observed in the presence of vinblastine or vinorelbine. Drug-induced tubulin self-association was further investigated by stopped-flow light scattering experiments. PC-tubulin relaxation data in the presence of vinblastine or vinorelbine can be fit with single exponentials. These data suggest association of oligomers or annealing occurs as well as addition of heterodimers to growing spirals. Vincristine relaxation times were more than 20-fold longer and required two exponentials for adequate fits. The long relaxation time (513 ± 90 sec) may be due to denaturation or alignment of spirals. These interesting differences in isotype binding and kinetics in the presence of vincristine may be implicated in the dose-limiting clinically observed vincristine-induced neurotoxicity. Neurotoxicity is not dose-limiting for vinblastine or vinorelbine. Supported by NR00056 (S.L.), BIR9216150 (J.J.C.) and NS21142 (A.F.).

W-Pos373

SEQUENCE EFFECTS ON THE DUPLEX TO SINGLE STRAND TRANSITION IN B-Z JUNCTION FORMING DNA OLIGOMERS: MISMATCHES AND SLIPPAGE. ((E. Otokiti, E. Dilone & R. D. Sheardy)) Department of Chemistry, Seton Hall University, South Orange, NJ 07079.

An intensive investigation of sequence effects on the stability of DNA oligomers capable of forming B-Z conformational junctions is underway. Two families of sequence analogous oligomers are being considered: **I**: 5'-(5meC-G)$_4$-**LMN**GACTG (where **L** is either A or G and **MN** are permutations of T and C); and **II**: 5'-(TG)$_{3-6}$ACTGACTG-3'. The variations of **L**, **M** and **N** in family **I** oligomers influence the free energies of duplex formation in a predictable fashion for the perfect duplexes arising from these oligomers. By mixing various non self-complementary strands together, a series of duplexes with mismatched bases at or near the potential B-Z junction have been generated. These mismatches destabilize the duplex relative to the perfect duplex by 1 to 10 kcal/mol depending upon the position of the mismatch, the bases involved (i.e., G/T vs A/C) and the salt condition (i.e., 115 mM NaCl vs 4.5 M NaCl). The melting profiles for oligomers of family **II** were determined in 115 mM NaCl and 1.0 M NaCl. Examination of the derivative plots for the melting profiles for these oligomers indicates varying degrees of biphasic behavior. The degree of this biphasic behavior depends upon the length of the (TG) segment as well as the concentration of NaCl. The results for both families of DNA oligomers will be discussed in terms of base stacking and slippage. Supported by ACS PRF grant 27471-AC7.

W-Pos374

ALLOSTERIC LINKAGE IN DNA QUADRUPLEX ASSEMBLY: LINKAGE THERMODYNAMICS. ((Bernard A. Brown II, Matthew J. Corregan and Charles C. Hardin)) Department of Biochemistry, North Carolina State University, Raleigh, NC 27695.

Absorbance thermal denaturation data and circular dichroism (CD) equilibrium binding curves were measured in order to determine the nature of the cooperative transitions that occur during DNA quadruplex formation in the $[d(TG_4)_4{}^*(K^+)_n]$ system. Melt experiments done in 100 mM Tris-HCl (pH 7) containing 100 or 400 mM KCl yielded equilibrium association constants ranging from *ca.* 10^{11} to 10^{12} M^{-1} at the respective melting temperatures (70 - 80°C) to *ca.* 10^{21} M^{-1} at 23°C. Enthalpic and entropic contributions to the overall free energies of the reactions were found to be of almost equal magnitude and opposite sign at the T_ms, resulting in relatively modest association energies ($\Delta G^\circ_{70\text{-}80^\circ}$) of -2.2 to -2.3 kcal mol^{-1}). Enthalpic energies predominate over inhibitory entropic energies at 23°C, producing very strong association free energies in the range of -29.6 kcal mol^{-1}. The timecourse of quadruplex formation in the presence of 5 to 350 mM strands was followed by CD at 264 nm in 100 mM Tris-HCl (pH 7) containing 100 mM KCl to assure that sufficient time had elapsed to attain equilibrium. Complete complex formation required >10 h under these conditions. Scatchard and Hill binding isotherms were constructed from the binding data. Hill plots demonstrated that initial steps in the multistep pathway are positively cooperative, presumably due to strong strand-cation and strand-strand binding interactions. Intermediate steps, with strand-dependences up to order 3, are positively cooperative, apparently due to dominant charge-charge attraction energies. Subsequent transitions involving incorporation of four, five and six strands occur with strong negitive cooperativity, apparently associated with forcing the anionic strand onto the negitively charged triplex intermediate in an association pathway which requires assembly of a product-limiting 6-stranded entity. A model is presented which rationalizes these observations in terms of cooperative allosteric transitions from cation-deficient "relaxed" (R) structures to cation-containing "tense" (T) structures driven by the allosteric effector K^+.

W-Pos375

THERMODYNAMIC CHARACTERIZATION OF A DNA DUPLEX THAT CONTAINS A SINGLE *cis*-[Pt(NH_3)$_2${d(GpG)-N7(1), -N7(2)}] INTRASTRAND CROSS-LINK. ((Nataša Poklar[1], Daniel S. Pilch[1], Elizabeth A. Redding[2], Stephen J. Lippard[2], and Kenneth J. Breslauer[1])) [1]Department of Chemistry, Rutgers University. [2]Department of Chemistry, Massachusetts Institute of Technology.

cis-Diamminedichloroplatinum(II) (cisplatin) is an antitumor drug that is used in the treatment of numerous human cancers. Despite this important application, relatively little is known about the thermodynamic consequences of cisplatin adduct formation on duplex DNA, a deficiency that inhibits our understanding of the molecular forces that dictate the pharmacological activity of this drug. To alleviate this situation, we have used a combination of calorimetric and spectroscopic techniques to determine the thermodynamics for formation of a 20mer DNA duplex in the presence and absence of a single cisplatin 1,2-d(GpG) intrastrand cross-link. Our results reveal the following information: (i) Adduct formation does not induce significant alterations in the global conformation of the host duplex, as assessed by CD, despite well documented adduct-induced deformations (e.g. bending and unwinding); (ii) Formation of the cisplatin adduct reduces the thermal stability of the duplex (ΔT_m = -8.3 °C at 10 μM duplex); (iii) Adduct formation reduces the duplex-to-single strand transition enthalpy by 17 kcal/mole duplex, while not altering the two-state nature of the transition (i.e. $\Delta H_{cal} \approx \Delta H_{vH}$); (iv) The reduction in transition enthalpy is partially compensated by an enhancement in the transition entropy of 36 cal/K·mole duplex, thereby resulting in an adduct-induced destabilization free energy of 6.3 kcal/mole duplex at 25 °C. Taken together, our results reveal that a single cisplatin 1,2-d(GpG) intrastrand cross-link alters the energetics of duplex formation. We discuss potential molecular origins for these large adduct-induced energetic effects, as well as how energetic/structural perturbations may facilitate binding to adducted duplexes by HMG domains of both natural and recombinant proteins.

W-Pos376

OBSERVATION OF K^+-INDUCED SUPRAMOLECULAR CHIRAL SELF-ASSEMBLY IN $d(TGG)_4$ WITH A SINGLE T → C REPLACEMENT. ((Fu-Ming Chen)) Department of Chemistry, Tennessee State University, Nashville, TN 37209-1561.

We have recently uncovered a rather interesting phenomenon in which molar [K^+] induces chiral aggregate formation in $d(CGG)_4$. The kinetics of this transformation are greatly facilitated in acidic conditions and their profiles resemble those of autocatalytic reacting systems with characteristic induction periods. Time dependent CD spectral characteristics indicate the formation of parallel G-tetraplexes prior to the onset of aggregation. Both $d(TGG)_4$ and $d(CGG)_4T$ fail to exhibit the observed phenomenon, strongly implicating the crucial roles played by the terminal G and base protonation of cytosines. A plausible mechanism for the formation of a novel self-assembled structure was speculated: Aided by the C^+•C base pair formation, parallel quadruplexes are initially formed and subsequently converted to quadruplexes with contiguous G-tetrads and looped-out cytosines due to high [K^+]. These quadruplexes then vertically stack as well as horizontally expand via inter-quadruplex C^+•C base pairing to result in dendrimer-type of self-assembled super structures. (Chen, F.-M. (1995) *J. Biol. Chem. 270*, 23090-23096). In an effort to elucidate the roles played by the cytosines, studies are now made with $d(TGG)_4$ having one of its T replaced by C. It was found that a single T → C replacement is sufficient to observe the K^+-induced aggregation, with d(TGGTGGCGGTGG) the most effective and d(TGGCGGTGGTGG) the least.

W-Pos377

CONFORMATION OF THE DNA BACKBONE IN CRYSTAL AND SOLUTION STRUCTURES OF CYCLIC TRIDEOXYRIBOADENYLIC ACID [$c(dAp)_3$]: RAMAN MARKERS OF THE *GAUCHE*$^+$,*GAUCHE*$^+$ PHOSPHODIESTER GROUP. ((Y. Guan, J. M. Benevides, A. H.-J. Wang and G. J. Thomas, Jr.)) Division of Cell Biology and Biophysics, School of Biological Sciences, University of Missouri, Kansas City, MO 64110.

The cyclic adenine trinucleotide, $c(dAp)_3$, crystallizes in space group *R3* and its crystal structure reveals an unusual *gauche*$^+$, *gauche*$^+$ (g^+, g^+) conformation for each of the three phosphodiester moieties of the DNA backbone. We have obtained Raman spectra of the $c(dAp)_3$ single crystal and its H_2O and D_2O solutions in order to identify Raman markers diagnostic of the novel g^+, g^+ conformation. Comparison with canonical *B*-DNA and other models which exhibit the g^-, g^- phosphodiester conformation shows that Raman markers in the region 750-900 cm^{-1} are sensitive in frequency, intensity and apparent polarization to the $g^- \rightarrow g^+$ change in dihedral angles α (∠ O3′-P-O5′-C5′) and ζ (∠ O5′-P-O3′-C3′) of the DNA backbone. On the basis of the Raman correlations for the *R3* crystal, it is concluded that in a second crystal form of $c(dAp)_3$ (space group *P3*) two different phosphodiester conformers contribute to the Raman spectrum, whereas only one (g^+, g^+) is detected by X-ray diffraction. The experimental results are considered in the light of recent normal coordinate calculations on the conformational dependence of phosphodiester stretching vibrations of DNA (Guan & Thomas, *J. Mol. Struct.* in press).
[Supported by NIH Grant GM54378.]

W-Pos378

Single DNA Mesophases Observed by Electron and Polarization Microscopy. ((S.L. Keller, H.H. Strey, R. Podgornik, D.C.Rau and V.A. Parsegian)) UCSB, Santa Barbara, CA 93106, LSB/DCRT, OD/NIDDK, NIH, Bethesda, MD 20892.

The motivation of this work is to investigate the structure of single-phase samples of long (>10μm) DNA fragments prepared at known activities of salt and water.
Like short DNA fragments (Livolant, Biophys. J. 1994), long DNA fragments at physiologically relevant DNA concentrations (100-600 mg/ml) show a phase transition from a columnar hexagonal phase at high DNA densities to a cholesteric phase at lower densities.
Although packing of long DNA fragments is biologically more interesting, little is known about how exactly long molecules pack in high-density liquid-crystalline arrays. Especially in the cholesteric phase it is not clear how DNA, whose molecular length is on the order of the sample dimensions, arranges in a macroscopically twisted phase.
To visualize these arrangements we have combined freeze fracture electron microscopy, polarization microscopy and small angle x-ray scattering to determine the structures of the different phases under osmotic stress.
The method of preparation, setting all intensive parameters in the system, allows us to prepare single-phase samples rather than the mix of phases that often emerges from stoichiometric mixtures. It also makes it possible to measure the free energy to create each phase whose structure is observed from the nm to the μm scale.
In the cholesteric regime both electron microscopy and polarization showed the characteristic fingerprint pattern of the twisted cholesteric phase.

W-Pos379

DNA Mesophases: An Osmotic Stress Study ((H.H. Strey, R. Podgornik, J. Wang, E. Sirota, D.C. Rau, A. Rupprecht, L. Yu and V.A. Parsegian)) LSB/DCRT, OD/NIDDK, LCP/NIAMS, NIH, Bethesda, MD & Exxon Research and Engineering, NJ

The pressure-density phase diagram of long- (>10kbp), short-fragment (146bp) and supercoiled plasmid DNA was explored by the osmotic stress method. At high osmotic pressures (100atm <Π_{osm}< 10atm) long DNA fragments order in a columnar liquid crystal with short range positional and long range orientational bond order (line hexatic or N+6). This was inferred from a synchrotron (BNL) small angle x-ray study on oriented DNA samples, measuring the three dimensional structure factor $S(q_\perp, q_z)$. The line hexatic phase is the three dimensional analog to the hexatic phase in two dimensions. Its existence has been theoretically predicted but has never before seen.
At Π_{osm}=10atm DNA fragments show a phase transition to a cholesteric phase. Around the transition pressure we found a region where the N+6 and the cholesteric phase coexist, resulting in two distinct peaks in the x-ray structure factor. This is surprising because we hold all intrinsic variables (p,T,μ's) fixed and there should be no phase coexistence. That we see one might indicate that the transition is sensitive to the local base pair distribution along the DNA strands. The phase transition itself is of either higher order or weakly first order.
We also performed osmotic stress experiments with supercoiled plasmid DNA. Plasmid DNA is a closed loop of DNA which can be, because of the closed structure, under torsional stress. This stress leads to the formation of supercoils. Plasmids and circular DNA in E.coli are naturally supercoiled. Supercoiling is also believed to be a factor in gene regulation in E.coli. Therefore the question about packing of supercoils is of biological relevance and importance. We found that, compared to long DNA fragments, supercoils pack closer at the same applied osmotic pressure in the cholesteric pressure regime. This means that supercoils repel each other less than long DNA fragments, possibly because of the suppression of bending fluctuations.

W-Pos380

THE APPLICATION OF SYNCHROTRON X-RAY RADIATION TO THE DEVELOPMENT OF TIME RESOLVED METHODS FOR THE STUDY OF RNA FOLDING. ((Bianca Sclavi[†], Sarah Woodson[¥], Michael Sullivan[†], Mark Chance[†‡] and Michael Brenowitz[‡])) Departments of [†]Physiology and Biophysics and [‡]Biochemistry Albert Einstein College of Medicine, Bronx, NY, and [¥]Department of Biochemistry, University of Maryland, College Park, MD.

The radiolysis of water by high energy x-rays produces free electrons and hydroxyl radicals. Hydroxyl radicals, which can break the phosphodiester backbone of DNA and RNA, have proven to be valuable reagents in the study of nucleic acid structure and protein-nucleic acid interactions. Irradiation of solutions containing ^{32}P labeled RNA by a high flux "white light" x-ray beam at *the National Synchrotron Light Source* (*NSLS*) yields sufficient concentrations of hydroxyl radicals so that folding studies can be conducted with single basepair resolution at millisecond timescales. Preliminary studies of the Mg^{2+} dependent folding of the *Tetrahymena* Sca I ribozyme are presented. This synchrotron based technology is a novel method with which to examine the time-resolved structural changes of nucleic acid conformation and protein-nucleic acid complexes. *This work* was supported by NIH grants RR 01633, GM 39929 and 51506. GM46686

W-Pos381

STRUCTURAL AND STATISTICAL ANALYSIS OF THE RESIDUES IN THE IMMUNOGLOBULIN MOLECULES

A. Kister and I. Gelfand

Department of Mathematics. Rutgers University. New Brunswick, NJ 08904

In this work we performed the analysis of the relation between the sequence, and secondary and three-dimensional structures of immunoglobulin molecules. At the first step about the 5000 secondary structures of antibodies from Kabat data base were predicted. The statistical analysis reveals the 47 positions in strands and loops whose residues are identical or share a common feature in almost all of the chains. The calculation of residue-residue contacts for the residues in these positions resulted in almost identical contact maps for all Ig structures examined. The analysis of the "conservative" contacts showed that the positions can be divided into two groups:1) the 24 positions whose residues have contacts only with residues in antiparallel β strands; 2) the 23 positions in which residues have contacts with residues of another β sheet as well. It appears that these "conservative" contacts are, to a large extent, responsible for β sheet framework of immunoglobulin structures.

W-Pos382

VARIETIES OF THE KNOT SUBSTRUCTURES OF PROTEINS **Rufus Lumry, Chemistry Dept. University of Minnesota, Minneaplis, MN 55455**

Most proteins are constructed using a standard module consisting of a large, soft, slightly unstable part *(matrix), a surface* part for communication with other modules and a small, hard and very stable part *(knot)* responsible for folded stability, kinetic stability and genetic stability, which conserves the structural description of its protein familiy It appears to be general that knots are hydrogen-bond structures, often cyclic, buried in a cocoon of oily groups the whole so rigid that permanent polarization is minimized. In evolution the critical discovery for a new function is often a new knot and apparently only a relatively small number have so far been discovered but a given knot is often used in more than one module and thus for more than one protein family. If this stability device is the unique feature of the discovery of knots, knots might be expected to exist in a number of physical forms and have a wide variety of applications. These consequences are already clearly seen in the knots so far characterized. The examples include the knots of the two functional domains required for each enzymic catalytic function of which there are two general classes: 1. The two knots of homodomain enzymes; i.e. those formed by an early gene duplication, demonstrate a pattern of B-factor palindromy which characterizes an entire family even though only the knot residue patterns are conserved. 2. Heterodomain enzymes replace the palindromy with a more subtle construction design still able to effect catalysis mechanically. Cofactors have their own modules with some well-known patterns and some less familiar. Knots maintain the dynamics of matrices as required for tight binding to other proteins; BPTI seems to be a good example. The leucine zippers zipp knots of two proteins into a joint knot, an example of "completing the knot". Other examples include knot formation in substrate and inhibitor binding to provide positive free energy for the binding process. The HIV-1 protease is such an example but it also demonstrates knot formation in the "fireman's grip" device holding the two protein units together, a device also generally found in repressor proteins. (see Lumry in "Protein-solvent Interactions, Gregory, Dekker 1994 and Methods in Enzymology, 259. Chap. 29 1995). More recently characterized knots reveal additional novelties some to be discussed

W-Pos383

LOCATING DISCONTINUOUS COMPACT DOMAINS CONTAINING MORE THAN TWO PEPTIDE UNITS. ((M.H. Zehfus)) College of Pharmacy, The Ohio State University, Columbus, OH 43210.

Previously, compactness was used to locate both continuous and binary discontinuous domains in proteins. In these procedures the compactness of all peptides and pairs of peptides were exhaustively evaluated, so the most compact regions could be identified. This direct approach cannot be used for domains with more than two peptides, however, because the number of possible combinations of units becomes too large to evaluate and search.

Since compact units are close to spherical in shape, a three dimensional protein structure may be screened for potential compact units by moving spheres of varying sizes through a protein's interior to find sets of peptides that are potentially compact. This screening procedure quickly locates potential compact units with any number of disjoint peptides. Once a potential compact peptide is located, the compactness of that unit and other closely related units can then be evaluated rigorously to find the most compact discontinuous peptide in that region.

This procedure has been implemented to find discontinuous units containing 2, 3, and 4 disjoint peptides. The binary units agree well with units found using the exhaustive evaluation procedure. The higher order discontinuous units for several proteins are presented.

W-Pos384

A NOVEL ALGORITHM TO INVESTIGATE DOMAIN MOVEMENTS IN PROTEINS ((W. Wriggers and K. Schulten)) Beckman Institute and Department of Physics, UIUC, Urbana, IL 61801.

A new algorithm for the identification of domain movements in proteins is described. The method partitions a protein in domains of preserved packing by comparing two structures. It then characterizes the domain movements by hinge points and rotation axes. The algorithm has been implemented in X-PLOR script language (Brunger, 1992). The output files can be visualized by standard molecular graphics packages. The algorithm is applied to several known instances of domain movements in proteins for which there is crystallographic evidence for the movement. The compared structures exhibit a variety of hinge and shear motions depicted by the algorithm. The method should be a useful tool to analyze domain movements in crystallographic structures or structures from computer simulations.

CIRCULATION

W-Pos385

MECHANISMS OF α -THROMBIN, HISTAMINE AND BRADYKININ INDUCED ENDOTHELIAL PERMEABILITY William D. Ehringer*, Michael J. Edwards+, and Frederick N. Miller*#. Center for Applied Microcirculatory Research, Department of Surgery and Department of Physiology, University of Louisville, Lousville, KY 40292.

α -Thrombin (AT), bradykinin (BK) and histamine (HT) are endogenous mediators that can increase endothelial permebility. However it is not known if the mechanisms for the increased permeability induced by these compounds are similar, or if the compounds would have a synergistic effect with each other. Human umbilical vein endothelial cells (HUVEC) were grown to confluence on Transwell membranes and then tested for alterations in permeability to a flourescein isothiocyanate-labeled human serum albumin. Addition of 1 μM AT or BK initially increased the permeability coefficent of the HUVEC monolayer, but the coefficent declined over the course of the two hour experiment. In contrast, the HT permeability coefficents increased and then remained relatively constant compared to AT and BK. To determine a possible intracellular mechanism for the altered permeability coefficents, HUVEC were labeled with FURA-2 and intracellular calcium was monitored. AT, and to a lesser extent, HT increased HUVEC intracellular calcium but BK had no effect on intracellular calcium mobilzation. Surprisingly, pre-treatment of the HUVEC with 1 M BK or the BK antagonist (Na-adamantaneacetyl-bradykinin reduced the AT calcium response by 42% and 71.6% respectively. Pretreatment of the HUVEC with HT had no effect on AT induced intracellular calcium mobilization. Fluorescent photomicrographs of HUVEC stained with BODIPY-phalloidin, indicated that AT and HT affected HUVEC f-actin content by 30 minutes, while BK stimulated HUVEC f-actin was unaffected. Pretreatment of the HUVEC with BK for 30 minutes decreased the effects of AT on f-actin distribution. AT dependent fibrinogen to fibrin clotting assays had decreased clotting times in the presence of BK, suggesting that the inhibitory effects of BK occur by its interaction with AT in solution. The results of this study demonstrate that while permeability may be increased by the three agonists, the intracellular mechanisms by which the permeability arises are different. Furthermore, rather than being synergistic, these mediators may actually be inhibitory with each other.

W-Pos386

PORCINE CORONARY ARTERY REACTIVITY IS ATTENUATED BY GLYCATED ALBUMIN. ((G.M. Dick and M. Sturek)) Vascular Biology Laboratory, Dalton Cardiovascular Research Center, and Department of Physiology, University of Missouri, Columbia, MO 65211.

Glycated proteins accumulate in diabetes and have been implicated in the vascular complications associated with this disease. Vascular endothelial cells express a receptor for glycated albumin (*GA*); furthermore, we reported previously that *GA* impairs endothelial Ca^{2+} regulation. We have since hypothesized that *GA* would be damaging to vascular reactivity. Isometric tension techniques were used to assess reactivity of isolated coronary artery rings. Vessel segments (3 mm) were incubated one hour at 37 ° C in 40 mg/ml normal albumin or *GA* prior to determining effects on contractions elicited by 30 mM KCl, and relaxations elicited by bradykinin (10^{-11} to 10^{-6} M), sodium nitroprusside (10^{-10} to 10^{-4} M), and A23187 (10^{-9} to 10^{-5} M). Bradykinin relaxed KCl-contracted rings 52 ± 4 %, n = 6, whereas pretreatment with *GA* attenuated relaxation to 4 ± 6 %, n = 6. A23187-induced relaxations were similarly affected by *GA*. Smooth muscle defects were also elicited by *GA*, as nitroprusside relaxations were shifted to the right (EC_{50} 0.9 ± 0.1 vs. 5.3 ± 1.4 μM) and KCl contractions inhibited (10.5 ± 0.8 vs. 4.4 ± 0.4 g). Endothelium-dependent relaxations were abolished when coronary artery rings were denuded of endothelium prior to albumin treatment (n = 4 in each group); however, importantly, *GA* no longer impaired smooth muscle function. That is, nitroprusside relaxations were unaffected (EC_{50} 0.8 ± 0.3 vs. 1.1 ± 0.5 μM) and contractility was preserved (10.4 ± 0.4 vs. 9.7 ± 0.5 g). Our data indicate that *GA* impairs vascular reactivity in an endothelium-dependent manner. Support: American Diabetes Assoc., NIH HL02872, and AHA predoctoral fellowship.

W-Pos387

POTENTIATION OF MYOGENIC REACTIVITY BY EPIDERMAL GROWTH FACTOR (EGF): ROLE OF TYROSINE KINASE (TK). ((Adam Kirton, Rodger Loutzenhiser)), Smooth Muscle Research Group, Department of Pharmacology and Therapeutics, University of Calgary, Calgary, Alberta, Canada, T2N 4N1.

Evidence suggests that TK is not only involved in mitogen signalling but may also influence smooth muscle contractility. We investigated the latter by examining the effects of EGF on myogenic reactivity of renal afferent arterioles (AA), using the *in vitro* perfused hydronephrotic rat kidney model (Circ Res 74:861-9, 1994). 10 nM EGF elicited a transient vasoconstriction, reducing diameter from 18.0±0.7 to 12.6±1.1 μm, n=5, p=0.0003). A second EGF application was without effect, suggesting rapid inactivation of EGF receptors at this concentration. At 0.3 nM, EGF did not alter basal diameter (16.5±0.6 vs 16.1±0.7, control & EGF respectively p=0.67), but markedly augmented the myogenic reactivity of the AA (figure), shifting the response range to lower pressures and augmenting the maximal vasoconstriction (diameter reduced to 10.5±0.8 μm vs. 5.8±0.9 μm at 180 mm Hg, control and EGF respectively, p=0.002). These effects persisted for >90 minutes and were not prevented by 100 μM ibuprofen or 30 μM diadzein. However, 30 μM genistein completely abolished these effects of EGF, but did not alter basal reactivity of the AA to pressure (p>0.06) or to 30 mM KCl (p>0.5). These results suggest that TK is not involved in the normal response of the AA to pressure, but that myogenic reactivity is enhanced when TK is activated by EGF. TK may alter vascular reactivity by an alternate signalling pathway, interacting synergistically with other smooth muscle activating mechanisms.

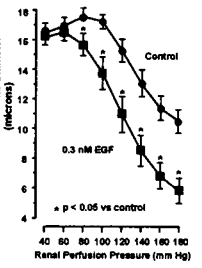

W-Pos388

STREPTOMYCIN INHIBITS MYOGENIC TONE IN RAT SMALL CEREBRAL ARTERIES (BUT ONLY AT CONCENTRATIONS WHICH BLOCK VOLTAGE-GATED Ca^{2+} CHANNELS). ((A.L. Miller & P.D. Langton)) Ion Channel Group, Dept. Cell Physiology and Pharmacology, University of Leicester, LE1 9HN, U.K.

Streptomycin has been used to block mechanosensitve ion channels in a wide variety of tissues including heart. Many small arteries are mechanosensitive and contract actively when subjected to approximately physiological transmural pressures, a phenomena called the ***myogenic response***. Associated with myogenic tone is a 20 to 30 mV depolarization of the smooth muscle which may reflect the induction of a mechanosensitive conductance. The effects of streptomycin on myogenic tone, K^+-induced force and voltage-gated Ca current in rat cerebral arterial smooth muscle have been examined. **Results:** Segments of middle cerebral artery were mounted in a Halpern pressure myograph and pressurized to 80 mmHg. Vessels subsequently developed myogenic tone, their diameter spontaneously decreasing by 102±5 μm from an initial diameter of 230±1.7 μm (n=3). Streptomycin in the range 10 - 100 μM, commonly used to block mechanosensitive channels, had little effect but concentration-dependently dilated the vessels at higher concentrations, the IC_{50} being 3.1. mM with a slope of 1.2. At such high concentrations it is possible that relaxation of tone reflects inhibition of voltage gated Ca^{2+} channels. In rat basilar artery, high (40 mM) K^+-induced isometric force is abolished in the absence of Ca_o and is blocked by the dihydropyridine (DHP) antagonist (-)202-791 (IC_{50} 2 nM). Streptomycin above 100 μM concentration-dependently inhibited K^+-induced force with IC_{50} of 1.14 mM and a slope of 1.4 (n=4). Whole-cell patch clamp recordings of caesium-dialysed rat isolated basilar arterial myocytes revealed voltage-gated inward current carried by 10 mM Ca^{2+} which exhibited DHP-sensitivity typical of L-type current. Streptomycin inhibited peak inward current with an IC_{50} of 2.14 mM and a slope of 1.07.

Thus, streptomycin relaxes myogenic tone in pressurized rat cerebral arteries but only at high (millimolar) concentrations. In the same concentration range streptomycin inhibits K^+-induced contraction and voltage-gated Ca^{2+} current. These data suggest that myogenic depolarization is not mediated by a streptomycin-sensitive conductance.

Supported by the British Heart Foundation. Grant PG95/101

W-Pos389

DESIGN AND DYNAMICS OF HEMOGLOBIN MULTI-LINKERS ((K. W. Olsen, L. Zhao, H. Huang, Q. Zhang, and S. Kondubhotla)) Department of Chemistry, Loyola University, 6525 N. Sheridan Rd., Chicago, IL 60626.

The synthesis of a series of crosslinking reagents, that were proposed by computer-aided molecular design to modify hemoglobin A, will be presented. These crosslinking reagents include the bifunctional aspirin analog, bis (3,5-dibromosalicyl) sebacate , and the tetrafunctional reagents, tetra(3,5-dibromosalicyl)-3,3',4,4'-benzophenone-tetracarboxylate and 3,3',5,5'-benzophenone tetra(sodium methyl phosphate). In addition, double crosslinked hemoglobin has been prepared by reacting the protein with bis (3,5-dibromosalicyl) fumarate sequentially under two different oxygenation states. The functional and structural properties of these crosslinked hemoglobins demonstrate that the desired properties of low oxygen affinity and high thermal stability can be achieved. Finally, the molecular dynamics simulations of both α99 and β82 fumarate crosslinked HbA's will be used to demonstrate the effects of crosslinking on the protein's flexibility.

W-Pos390

MULTILINKING OF HEMOGLOBIN FOR POTENTIAL BLOOD SUBSTITUTES AND BIOCONJUGATES. ((Y. ZHENG and K.W. OLSEN)) Dept of Chemistry, Loyola University of Chicago, 6525 N. Sheridan Rd., Chicago, IL, 60626.

The reactions of human hemoglobin A (HbA) with the trilinkers, tris(3,5-dibromosalicyl) tricarballylate (DBTA) and tris(3,5-dibromosalicyl) 5-acetate isophthalate ether (DBAIE), produce thermally stable proteins. The tetralinkers, tetra(3,5-dibromosalicyl) 5,5'-(1,3-propanedioxy) diisophthalate ether (DBPDE) or tetra(3,5-dibromosalicyl) 5,5'-triethyleneglycol diisophthalate ether (DBTDE), can react with HbA to crosslink between two tetramers forming an octamer, as demonstrated by SDS-PAGE and gel filtration chromatography. This product could be used to test the hypothesis that larger crosslinked Hb's remain longer in the circulation. All of these reagents are designed using molecular graphics to react with the β82 lysines in deoxy human HbA. Using the tetralinkers, some biochemical interesting compounds, such as dyes with absorption at particular wavelengths, could be conjugated to the proteins. The biophysical properties of the modified proteins will be presented.

W-Pos391

HEMOGLOBIN OCTAMERS: A POTENTIAL BLOOD SUBSTITUTE ((S. Kondubhotla and K. W. Olsen)) Department of Chemistry, Loyola University of Chicago, 6525 N. Sheridan Rd., Chicago, IL 60626

Hemoglobin octamers have the capacity to carry double the amount of oxygen per molecule at the same oncotic pressure. Oxy human hemoglobin is known to have a reactive cysteine residue at position β93. Maleimides react specifically with sulfhydryl groups at pH 6.5 to 7.5. A commercially available homobifunctional sulfhydryl specific crosslinking reagent, bismaleimidohexane, was reacted with oxy human HbA. The structural and functional properties of this modified hemoglobin have been studied. The molecular mass of the native product, as determined gel filtration chromatography, was twice the size of the normal protein. SDS-PAGE showed the presence of dimers. The thermal stability of the crosslinked species was increased by about 9°C over that of normal HbA. The autoxidation rate was faster than that of HbA. The oxygen affinity of the octamer was increased. To try to decrease the oxygen affinity, the reaction was repeated using α99 fumarate crosslinked hemoglobin, however the modification of β93 cysteine causes the resulting double crosslinked product to have high oxygen affinity.

W-Pos392

DIRECT MEASUREMENTS OF EXOCYTOSIS IN SINGLE RAT PLATELETS ((A.F. Oberhauser)) University of Chile and Centro de Estudios Cientificos de Santiago, Chile. (Spon. by O. Alvarez).

The activation of platelets by specific agonists is a tightly regulated mechanism that involves an increase in the $[Ca^{2+}]_i$ and leads to the secretion of dense granules (containing 5HT) and α granules (containing fibrinogen). The mechanism of exocytosis is poorly understood in platelets mainly because of the lack of techniques to directly study the exocytotic fusion of single secretory granules. Here I show that, exocytosis can be followed in single rat platelets by measuring the cell membrane capacitance (Cm) or the release of oxidizable substances with a carbon fiber in the amperometric mode. The secretory response induced by the external application of thrombin (5U/ml) was characterized by a burst of amperometric spikes (4 to 8, n=8) that, presumably, represented the release of 5HT from dense granules. The total charge of these spikes ranged from 0.3 to 4 pC (mean: 0.64±0.06, n=23). It was possible in a few cases (n=4) to obtain stable Cm recordings (using amphotericin-permeabilized patches). After application of thrombin, the Cm increased gradually (to about 100fF) with a few step increases in Cm of 3 to 10 fF. Thus, this approach may prove useful in the study of the signalling pathways that control dense and α granule exocytosis in rat platelets.

W-Pos393

THE INTERACTION OF HUMAN SERUM PROTEINS WITH METALS.

((R. Rosal and L. Claudio)) Departments of Community Medicine and Pathology, Mount Sinai Medical Center, New York, NY 10029.

Analyzing the role of serum proteins in modulating the transport of metals through the Blood Brain Barrier (BBB) will help elucidate the mechanism by which environmental metals (i.e. Mn, Pb) exert neurotoxic effects on human health. The interaction of purified human serum transferrin and albumin, with metal ligands: Fe, Mn, and Pb was analyzed with Circular Dichroism Spectroscopy (CD). We observed that proteins in solution without the addition of metals exhibited mostly alpha-helical configurations in 5.0 mM Na-phosphate buffer, pH 7.4 and 15 mM Na-Bicarbonate. We added 1.0 µl of 1.0 M solutions of $FeCl_3$, $MnCl_2$ and Pb-Acetate to constant concentrations of serum proteins (0.1 mole/1.5 ml volume). It was observed that Fe had the greatest effect on CD spectral change, followed by Mn. Lead, even at very high concentrations did not change the CD spectrum of transferrin or albumin. The binding curves obtained from the CD spectra show that albumin has twice the peak binding affinity (at 7.0 µM) with Fe as compared to transferrin. These proteins also bind Mn, but with half the affinity, compared to Fe. The CD spectra for transferrin exhibits a sigmoidal when Fe was added to the protein, suggesting a cooperative binding mechanism. These data suggest that transferrin and albumin have a higher affinity for Fe, followed by Mn, neither protein appeared to bind Pb with high affinity. These findings suggest that transferrin and albumin can interact and possibly transport Fe and Mn through the BBB, while Pb may be transported by some other mechanisms. Other human serum proteins such as α-macroglobulin and IGg will also be analyzed.

(Supported by NIEHS T35 ES07298 and Environmental Health Foundation).

SPECIALIZED FUNCTIONS - IMMUNE

W-Pos394

CORRELATED CHANGES IN CALCIUM SIGNALING AND PROLIFERATION RESPONSE IN THE COURSE OF HUMAN T LYMPHOCYTE ACTIVATION. ((J.A.H. Verheugen, V. Devignot, H. Korn)) Neurobiologie Cellulaire and Moleculaire, INSERM U261, Institut Pasteur, 75724 Paris, France.

Stimulation of the T cell receptor (TCR) of peripheral blood T lymphocytes initiates a series of intracellular events, eventually resulting in cell proliferation and differentiation into immuno-competent cells. Among the earliest responses are IP3 production, followed by Ca^{2+} release from intracellular stores and capacitative Ca^{2+} influx across the cell membrane. The resulting calcium signal varies between cells, ranging from transient to prolonged elevations with variable degrees of oscillation. We have used calcium-imaging of fura-2 loaded cells to study the mechanisms underlying this variability in relation with the final cellular response. We found that the percentage of responding cells and the average amplitude of the calcium signal upon TCR stimulation by PHA increases in the first 5 days of T cell activation (from <50% and −150 nM in resting cells to >90% and ~230 nM at the maximum level) and declines thereafter, with more pronounced $[Ca^{2+}]_i$ oscillations in later stages. The proliferative capacity, measured by thymidine incorporation and cell cycle analysis, gradually increases after activation (up to 3-6 fold at day 5 compared to resting cells) then decreases, paralleling the changes in the average Ca^{2+} signal. Buffering $[Ca^{2+}]_i$ by loading the cells with BAPTA or EGTA prevents TCR induced proliferation. While the response evoked by antibodies to the CD3 moiety of the TCR/CD3-complex shows a dependence on activation state similar to that seen with PHA, co-stimulation of CD3 and CD4 or CD8 accessory molecules always produces an enhanced Ca^{2+} response to the maximum level attained in the course of activation by anti-CD3 alone. This indicates that the magnitude of the rise in $[Ca^{2+}]_i$ is determined by the efficacy of TCR signaling. Additional modulation of the Ca^{2+} signal is provided by activity of K^+ channels, since the blocker charybdotoxin (CTX) either accentuates or damps the $[Ca^{2+}]_i$ oscillations, depending upon the activation state. The differential effects of CTX reflects the degree of expression of K(Ca) channels. However, CTX has only small effects on the average increase of $[Ca^{2+}]_i$ and fails to inhibit the subsequent proliferation to a large extent. Taken together, the results suggest that memory T cells could increase their proliferative capacity through amplification of their calcium response by increasing the efficacy of TCR signal transduction. More pronounced Ca^{2+} oscillations in later stages of activation may point to a role for K(Ca) channel mediated Ca^{2+} oscillations in the pathway towards final differentiation into effector cells.

W-Pos395

A NOVEL CLASS OF POTENT ORGANIC BLOCKERS OF THE T-CELL K CHANNEL, Kv1.3, THAT ARE SELECTIVE FOR HISTIDINE 404. A. Nguyen, J. Kath, D. Hanson, B. Dethlefs, G. Gutman, M.D. Cahalan, K.G. Chandy. Depts. of Physiol. & Biophys., and Microbiol. & Mol. Gen., Univ. California Irvine, CA., and Pfizer Central Research, Groton, CT.

Kv1.3 plays a major role in regulating T-cell function and is a potential target for therapeutic immunosuppressive agents. Recently, a novel and potent inhibitor of Kv1.3, WIN 17317-3, was shown to compete with charybdotoxin (ChTX) for its binding site at the external entrance to the pore, and suppress T-cell activation at nanomolar concentrations. We synthesized WIN 17317-3 and showed that it blocked Kv1.3 (Kd 81nM) with significantly greater potency than its closely related homologues, Kv1.1 (Kd 62µM), Kv1.2 (Kd 14µM), Kv1.5 (Kd 19µM) and Kv3.1 (Kd 17µM). We synthesized seven additional analogues to study their interactions with Kv1.3, and in particular with H404, a residue shown to be critical for ChTX binding. cRNA of the wild type Kv1.3 channel and five H404 mutants (H404T/V/L/R/Y) were injected into rat basophilic leukemic (RBL) cells with an Eppendorf microinjection system, and the cells patch clamped after 4-8 hours. Our results clearly indicate that H404 is critical for the binding of all 8 analogs and may be responsible for their Kv1.3-selectivity. How might H404 interact with these drugs? A histidine in the neurokinin-1 receptor has been shown to interact with a benzhydryl containing antagonist, CP96345, via an amino-aromatic interaction; such an interaction might play a role in the binding of WIN 17317-3 to Kv1.3. Modeling one of WIN 17317-3 analogs into the Kv1.3 pore with its aromatic rings interacting with the imidazole nitrogen of H404, allows the 5-6 carbon aliphatic chain of these drugs to be placed into a hydrophobic pocket made up of W389, W390 and V406; shortening or lengthening this chain had been shown to dramatically reduce the drug's potency in blocking the channel possibly via disruption of its association with the hydrophobic pocket. It might now be possible to rationally modify these compounds to develop more selective Kv1.3 blockers for use as therapeutic immunosuppressants.

W-Pos396

INTERACTIONS OF RABBIT NEUTROPHIL DEFENSINS WITH BILAYERS ((K.Hristova, M.E.Selsted and S.H.White)) Department of Physiology and Biophysics and Department of Pathology, University of California, Irvine, CA 92717

Defensins are small (M_W=3,500-4000) cationic β-sheet peptides that exhibit broad antimicrobial activity. They are stored in the cytoplasmic granules of mammalian neutrophils and Paneth cells of the small intestine. We examined the interactions of rabbit neutrophil defensins with lipid bilayers of different composition: POPG, POPG/POPE, POPG/POPC, and *E. coli* lipid extract. All rabbit defensins, as well as their naturally occurring mixture, caused graded release of the contents of POPG vesicles while the addition of neutral (zwitterionic) lipids to the POPG vesicles eliminates the defensin - induced leakage although it does not prevent defensins from binding to the bilayer. Rabbit neutrophil defensins, with the exception of NP-4 and NP-5, permeabilize *E. coli* bilayers. The individual rabbit neutrophil defensins NP-1, NP-2, NP-3A and NP-3B cause graded leakage of *E. coli* vesicles while the mixture of the six defensins causes release in all-or-none manner. We observed leakage of large dextrans from *E. coli* vesicles induced by not only the rabbit defensin mixture, but by the individual defensins as well. The results suggest that the rabbit defensins cause leakage of *E. coli* liposomes in both graded and all-or-none manner. The kinetics of leakage of two dextrans (MW 18,700 and 50,700) are very similar which indicates that leakage does not occur through a well defined pore that can be sized.

W-Pos397

THE TIME-RESOLVED FLUORESCENCE OF ACRYLODAN LABELED FK506 BINDING PROTEIN: EXPERIMENT AND MOLECULAR SIMULATIONS ((Norberto Silva, Jr., and Franklyn Prendergast)) Mayo Clinic, Guggenheim 14, 200 First St. SW, Rochester, MN 55905. Supported by GM34847 and the Damon Runyon-Walter Winchell Fellowship Foundation, DRG-1289.

The immunosuppressant drug FK506 has been effective in reducing the incidence of graft rejections in organ transplants. Immunosuppression results after FK506 is bound by a peptidyl-prolyl cis-trans isomerase called FK506 binding protein (FKBP12). We have previously reported that the side chain dynamics of W59, as monitored by its time-resolved fluorescence anisotropy, may be important in the association of FK506 to FKBP12. FKBP12 also offers another opportunity toward probing the effect of ligand binding on side chain dynamics through fluorescence studies of acrylodan labeled FKBP12. We have successfully labeled FKBP12 with acrylodan in a one-to-one stoichiometry at its single cysteine, C22. In addition, acrylodan labeled FKBP12 retains activity and binds to FK506. The labeling of FKBP12 by acrylodan is interesting since C22 is buried from solvent exposure as determined by the X-ray crystal structures of uncomplexed and FK506 complexed FKBP12. Yet, how does acrylodan label the buried C22 side chain? In other words, which surface residues occluding C22 stochastically open up access to C22 for acrylodan? We attempt to answer this question by monitoring the change in solvent exposure of C22 via stochastic boundary simulation of unlabeled FKBP12 in a region surrounding C22 using the CHARMM molecular dynamics program. Knowing the simulation generated protein structure that allows for acrylodan labeling may help us rationalize the observed time-resolved fluorescence anisotropy decay of acrylodan-labeled FKBP12 which shows a decrease in the recovered order parameter squared (S^2) for this moiety *upon* FK506 binding. This experimental result is consistent with the observed increase in the crystallographic B-factors of some surface side chain residues surrounding the C22 site.

W-Pos398

EXPRESSION AND FUNCTION OF VOLTAGE-DEPENDENT POTASSIUM CHANNEL GENES DURING THE RESPONSE OF CD4$^+$ VB8.1 TCR$^+$ LYMPHOCYTES TO MLS-1^a STIMULATION. ((Freedman, B.D., Fleischmann, B.K., Gaulton, G., Yui, K., and Kotlikoff, M.I.)) Departments of Pathology and Laboratory Medicine and Animal Biology, University of Pennsylvania, Philadelphia, PA. (Sponsored by B. Storey)

Voltage-dependent potassium channels are encoded by many different genes within a large gene superfamily. Blockade of potassium channels inhibits proliferation of T lymphocytes *in vitro*. We have used selective peptidyl blockers and patch clamp recordings to characterize the expression and function of voltage-dependent K^+ channels in murine CD4$^+$ VB8.1 TCR$^+$ transgenic lymphocytes after antigen-stimulation *in vivo*. RNA-PCR was used to confirm the molecular identity of the K^+ currents. Pharmacological separation allowed the identification of Kv1.1 and Kv1.3 currents in resting CD4$^+$ lymphocytes, and RNA-PCR indicated the presence of Kv1.1, Kv1.3, and Kv1.6 mRNA. Both the magnitude and composition of the aggregate K^+ current is modulated during the mls-1^a response *in vivo*. Potassium currents in resting CD4$^+$ VB8.1 TCR$^+$ lymphocytes are composed of charybdotoxin-sensitive and -resistant (dendrotoxin I-sensitive) components, whereas day 3 lymphocytes express a 3-4 fold higher current density, which is completely blocked by CTX. Anergic lymphocytes (day 14) like resting lymphocytes, express two current components, however the magnitude of the aggregate current and the charybdotoxin-sensitive component are larger (1.6 fold). To confirm a physiological role for these K^+ channels, we evaluated the effect of charybdotoxin (to block Kv1.3, Kv1.6) and dendrotoxin I (to block Kv1.1) on mls-1^a stimulated proliferation in culture. Each of the blockers inhibits proliferation and the combined effect is additive. K^+ blockers appear to inhibit IL2 production because exogenous rIL2 reverses their inhibitory effect.

W-Pos399

KINETICS OF PEPTIDE BINDING TO THE CLASS I MAJOR HISTOCOMPATIBILITY H2-K^d MOLECULE ((D.M. Gakamsky[1], P.J. Bjorkman[2] and I. Pecht[1])) [1]Immunology Dept., Weizmann Institute of Science, Rehovot, Israel; [2]Division of Biology 156-29, California Institute of Technology, Pasadena, CA 91125. (Spon. by Y. Palti)

The empty class I MHC heterodimer (H2-K^d) provides a unique system for direct monitoring in real-time antigenic peptide binding/dissociation kinetics. Interactions of a series of peptides synthesized on the basis of the influenza virus nucleoprotein NP1 (residues 147-155, TYQRTALV) was studied between -5 to 30°C. This series was produced by replacing a single residue (position 3 to 7) by a cystein. Dansyl was covalently bound to this cystein and fluorescence titrations revealed that this labeling practically does not affect the binding affinity. The peptide binding kinetics to the heterodimer is a second order activation controlled process. Externally added β_2-microglobulin (β_2m) affects both association and dissociation kinetics while peptide binding increases association constant of the heavy chain/β_2m heterodimer and a β_2m excess significantly slows down the peptide dissociation rate. Hence, the peptides' affinity is also a function of β_2m concentration. Coupling between the heterodimer and its interaction with the peptides is discussed On the basis of thermal stability profiles of H2-K^d heterodimer loaded with the peptides and Arrhenius plots of the dissociation rate constants we conclude that conformation of the peptide-heterodimer complex is also a function of a peptide structure.

W-Pos400

INTERFEROMETRIC FRINGE PATTERN PHOTOBLEACHING RECOVERY MEASUREMENTS INTERROGATE ENTIRE CELLS. ((H.M. Munnelly, W.F. Wade, D.A. Roess and B.G. Barisas.)) Departs. of Chem. and Physiol., Colorado State Univ., Ft. Collins, CO 80523 and Dept. of Microbiology, Dartmouth Medical School, Lebanon, NH 03756.

Lateral diffusion of cell surface proteins is commonly measured by spot fluorescence photobleaching recovery (FPR) methods where the $1/e^2$ radius of the interrogated spot is typically 0.5 μm. Results can thus reflect dynamics of 100 or fewer protein molecules. A new method for interferometric fringe pattern FPR permits simultaneous interrogation of the entire surface of round cells. Fringe or spot measurements can be performed interchangeably in a conventional microscope FPR system. Methods for interpreting recovery kinetics on round cells and for determining the fraction of mobile protein are presented. Fringe FPR data of wt murine I-A^k expressed on M12.C3.F6 cells show fluorescence signals improved 50-fold relative to spot FPR, with corresponding improvements in S/N ratios of recovery traces. Diffusion coefficients of 2.07 ± 0.37 and $1.79\pm0.97\times10^{-10}$ cm^2sec^{-1} were obtained by fringe and spot methods, respectively. The corresponding mobile fractions of I-A^k were $66.1\pm7.8\%$ and $63.4\pm 18.0\%$. Improved reproducibility of fringe over spot results is slightly less than signal improvements predict. There may thus be substantial variation from cell to cell in protein dynamics and this method may permit the assessment of such variation. Supported in part by NIH grant AI36306 to BGB.

W-Pos401

INTERACTION OF ANTIMICROBIAL PEPTIDE INDOLICIDIN WITH MEMBRANES. ((A. S. Ladokhin, M. E. Selsted and S. H. White)) Departments of Physiology/Biophysics and Pathology, University of California, Irvine, CA 92717-4560

Indolicidin is an antimicrobial peptide-amide isolated from the cytoplasmic granules of bovine neutrophils and its mechanism of action is believed to be cell membrane disruption. Its remarkably high tryptophan content (five of thirteen residues), indicative of a highly membrane-active peptide, is consistent with such a mechanism. We have characterized its interactions with large unilamellar vesicles formed from POPC and POPG in order to explore possible modes of interaction with cell membranes. We examined (1) membrane binding, (2) induction of leakage of vesicle contents, and (3) the conformation and tryptophan fluorescence of the free and bound peptide. Equilibrium dialysis measurements indicate that indolicidin binds strongly to both neutral and anionic vesicles: $\Delta G \approx$ -8.4 kcal/mol for partitioning into POPC LUVs and -10 kcal/mol or more for partitioning into POPG LUVs. Fluorescence requenching measurements on vesicles containing the fluorphore/quencher pair ANTS/DPX reveal that indolicidin induces lipid-dependent graded preferential leakage. An empirical kinetic model indicates that indolicidin causes a more rapid and more complete release of DPX and ANTS from POPG vesicles than from POPC vesicles. The structure-function relationships of indolicidin will be further explored with a set of analogs in which the tryptophans are selectively substituted. GM-46823 & AI-22931.

W-Pos402 ***(Presented at Tu-AM-A9)***

RECOVERY FROM C-TYPE INACTIVATION IS MODULATED BY EXTRACELLULAR POTASSIUM ((D.I. Levy and C. Deutsch)) Dept. of Physiology, University of Pennsylvania, Philadelphia, PA 19104-6085.

The T-lymphocyte K^+ channel, Kv1.3, undergoes C-type inactivation with a time constant of ~150ms and recovers with a time constant of about 10sec, in a physiological bath solution. The results of whole-cell patch clamp recordings of peripheral-blood T lymphocytes show that there is a linear increase in the rate of recovery from inactivation with increasing $[K^+]_o$. An increase from 5 to 150mM K^+_o causes a sixfold acceleration of recovery rate at a holding potential of -90mV. Our results suggest that 1) a low affinity K^+ binding site is involved in recovery, 2) this site is distinct from K^+ binding sites that influence macroscopic channel conductance or the inactivation rate, 3) the rate of recovery from inactivation is dependent on voltage and increases with hyperpolarization, 4) potassium must bind to the channel prior to inactivation in order to speed its recovery, and 5) recovery rate depends on external $[K^+]$ but not on internal $[K^+]$, magnitude of the driving force, nor direction of flux through open channels. We present a model in which a bound K^+ ion destabilizes the inactivated state to increase the rate of recovery of C-type inactivation, thereby providing a mechanism for autoregulation of K^+ channel activity. The ability of K^+ to regulate its own conductance may play a role in modulating voltage-dependent immune function. (Supp. GM41467 and GM52302).